Ecological Studies on the Cell Cycle of Freshwater Bacteria and its Role in Methane Cycling

Motoo UTSUMI

January, 1997

Submitted in partial fulfillment of the requirements for the degree of Doctor of Philosophy in Science, in the Doctoral Program in Biological Sciences, University of Tsukuba.

Plate 1. Matsumi-ike Bog during summer. The bog is occupied exclusively by a cattail.

Plate 3. The author and research vessel for the investigation at Lake Kasumigaura.

CONTENTS

SUMMARY

The structure and function of microbial communities in the freshwater environments were studied with special reference to ecological significance of the planktonic and attached stages in the cell cycle of bacteria. The research was made firstly on the fundamental structure of cell cycle of microbial communities in Matsumi-ike Bog, and secondly on its function in the methane cycle in Lake Nojiri and Lake Kasumigaura.

Effect of emergent vegetation on the population dynamics of microbial communities was studied in Matsumi-ike Bog, a typical bog at the climax stage of limnological succession. Population density of the predominant phytoplankton showed sinusoidal fluctuation regulated primarily by the water temperature, with various lag phases affected by other environmental factors. Shading by the emergent vegetation shifted the initiation of phytoplankton fluctuation earlier. This fluctuation pattern was most obvious among those phytoplankton contain chlorophyll-a and -b, but not -a and -c. The population density of phytoplankton with chlorophyll-b decreased but those with chlorophyll-c increased, due to the shading effect of the emergent vegetation with the limnological succession of the bog. At the climax stage of succession, the dynamics stage of phytoplankton community has become more stable.

The water temperature was shown to control primarily bacterioplankton dynamics as the limiting factor throughout the year. The second most profound factor on the dynamics was the concentration of dissolved organic carbon (DOC) when dead phytoplankton were the major DOC source in the bog, whereas phosphate concentration was most important during the periods when the dead emergent plants (*Typha latifolia*) were responsible for the DOC

supply. The density of attached bacteria was higher at the sediment boundary layer than in the water column, and it was low in the sediment ooze (< 10 mm at the bottom boundary layer) throughout the year. The density of attached bacteria was the highest during spring when the source of organic matter in the water column was mainly withered cattail, and it gradually decreased toward summer, while the phytoplankton became the dominant source of organic matter in the water column. The attachment and detachment rates of the epibacterial population in the water column and at the boundary showed almost the same seasonal fluctuation, but the growth rates did not show the evident seasonal fluctuation and the annual average growth rates were all lower than that of bacterioplankton in the water column.

Changes in the vertical distribution of dissolved methane were monitored during the autumnal lake overturn period in the mesotrophic lake of Nojiri. As a result of the lake overturn in mid-December, methane, which had accumulated in the hypolimnion during the stratification period, mixed rapidly throughout the water column. Increased methane in the epilimnion quickly disappeared after the overturn as a result of the rising of methane oxidation activity throughout the water column. During this period, the diffusive flux of methane across the air-water interface increased, but this was not the dominant sink (average rate: 0.83 mg CH_4 m^{-2} day^{-1}). Rather, methane oxidation in the water column was the dominant methane sink (average rate: 15.4 mg CH_4 m^{-2} day^{-1}) removing about 95% of the methane during the overturn period. A significant methane flux from the bottom sediments throughout the overturn period was confirmed, however, it decreased gradually as the overturn proceeded. Oxidation of methane in the water column by methanotrophs during the overturn period was comparable in extent to primary production at that time.

Long term seasonal variations in water column methane oxidation were studied at the shallow eutrophic lake of Kasumigaura, Japan. The entire water column was oxic throughout the year. The existence of methane oxidation activity in the oxic lake water was confirmed. Methane oxidation was distinctly seasonal, with low activity from January to April and high activity from August to November. Maximum methane oxidation was observed in late summer or early autumn, when the turnover time of dissolved methane was usually shorter than half a day. Methane oxidation activity does not depend on water temperature, dissolved methane concentration, dissolved oxygen or dissolved inorganic nitrogen. In freshwater lakes, methane oxidation is most active at interfaces between oxic and anoxic zones, where all necessary substrates for methanotrophs are available in sufficient quantities. An oxic-anoxic interface exists in the surface sediment in Lake Kasumigaura, so methane oxidation activity in this lake should be most active there. With the daily mixing of water, methanotrophs in the sediment are transported to the oxic water column and retain their activities in the planktonic state. The annual average methane consumption rate was 12.3 ± 15.5 mg CH_4 m^{-2} day^{-1}. Methane oxidation was the dominant methane sink, consuming an annual average of 74% of dissolved methane in the water column of Lake Kasumigaura.

Chapter 1

GENERAL INTRODUCTION

1.1. Bacteria in nature

The bacteria inhabit every where in the biosphere: Their habitats range from the favourable conditions such as rumen or sewage, to less comfortable habitats such as Antarctic ice (Sullivan and Palmisano, 1984), where other multicellular organisms can rarely live (Kushner, 1978). They can live in the vicinity of deep-sea hydrothermal vents (e.g., Karl, 1987; Jannasch, 1984; Utsumi et al., 1994) or hot springs (e.g., Brock, 1978; Sasa et al., 1996), and survive even in an artificial Mars condition (Imshenetskii et al., 1984).

In the biosphere, every biological element passes through a continuous cycle. In this cycle, bacteria have been shown to be greatly responsible for the decomposition of organic materials due to (e.g., Seki, 1982):

1) their omnipresence throughout the biosphere,

2) their versatile activity to decompose and utilize almost all kinds of organic compounds (including trace gasses such as methane),

3) their high rates in metabolism and growth.

However, little has been known of the structure and function in the microbial community as a whole. Each process of a certain group of microorganisms in a certain natural habitat has not been determined systematically.

Another important function of the bacteria is that they act as the producers of the detritus food chain (e.g., Seki, 1972; Azam et al., 1983). In the aquatic environment, organic materials are finally decomposed to carbon dioxide (Figure 1). It was demonstrated that bacteria constituted a significant proportion of the plankton biomass (Azam and Fuhrman, 1984), and that a significant part of the phytoplankton primary production was channelled

through bacteria. All natural, non-living organic materials, dissolved or particulate, are potentially substrates for bacteria, although obviously some compounds are more readily available than others. Even though bacteria transport and utilize only dissolved materials, they can solubilize particulate organic material with their exoenzymes, so that both particulate and dissolved materials can be potential bacterial substrates.

Generally, bacterial forms in the aquatic environments can be classified into two groups depending on the mode of life with special reference to the liquid-solid phases in natural waters; bacterioplankton with the free-living form in water, and epibacteria in the attached form on the solid substratum in water. Quantitative significance of each bacterial form has not been clarified in the heterotrophic processes in the geochemical cycles and in trophodynamics of the food webs. Some works show more important contribution of bacterioplankton in these processes (e.g., Fuhrman and Azam, 1980; Jordan and Likens, 1980; Zimmermann et al., 1978), the others emphasize greater contribution of attached bacteria (e.g., Harvey and Young, 1980; Pedros-Alio and Brock, 1982; Wilson and Stenvenson, 1980). However, it has not been studied ecological significance of planktonic and attached stages in the cell cycle (Brock and Madigan, 1991) of bacteria in Nature (Figure 2).

1.2. Role of methanotrophs in methane cycling

Methane is one of important atmospheric trace gases. Atmospheric methane levels, which have been increasing at an annual rate of approximately 1% for the last century (Blake and Rowland, 1988; Khalil et al., 1989), have caused concern because of the important roles of methane in atmospheric chemistry and the global climate system. Furthermore, methane is

the most stable carbon compound in anaerobic environments and is a very important intermediate in reactions that eventually lead to organic matter remineralization (Dagley, 1978).

Methane has been associated with aquatic environments since its discovery in 1776 by Volta (Sohngen, 1906) who described the formation of "combustible air" in the sediments of several lakes, ponds and streams. Since then pure bacterial cultures have been isolated, usually from aquatic sources, which either produce or oxidize methane. Until very recently, however, almost all of the research on these bacteria has been confined to the laboratory. Therefore, very little information has been generated concerning their activities in their native aquatic habitats (e.g., Rudd and Taylor, 1980).

Methane is produced by attached bacteria primarily in the anoxic sediments mainly from acetic acid, carbon dioxide and hydrogen (Figure 1). These substrates are the end products of a series of fermentative reactions which consume plant remains that have settled on to the sediment surface and are the known substrates of methanogenic bacteria (methanogens). The production of methane or any other hydrocarbon as a major catabolic product is unique to this group of microbes, which share many other characteristics that are not common among other microbes. Phylogenetically, methanogens are Domain Archaea (Woese, 1987), a group of microbes that are distinguished from Domain Bacteria by a number of characteristics, including the possession of membrane lipids composed of isoprenoids ether-linked to glycerol or other carbohydrates (de Rosa and Gambacorta, 1988; Jones et al., 1987; Langworthy, 1985), a lack of peptidoglycan containing muramic acid (Kandler and Hippe, 1977), and distinctive ribosomal RNA sequences (Balch et al., 1979; Woese, 1987).

This group also includes some extreme halophiles and some extremely thermophilic, sulfur-dependent microbes (Woese, 1987) and is phylogenetically distinct from Domain Eucarya and Domain Bacteria. Methanogens function in the global cycling of carbon; a large amount of methane are produced as an end product in the degradation of organic matter entering diverse anaerobic habitats. The methane is oxidized to carbon dioxide in aerobic zones or anaerobic zone by methanotrophs.

Methanotrophic bacteria (methanotrophs) are a subset of physiological group of bacteria known as methylotrophs that can grow using only one-carbon compounds such as methane, methanol, methylamine, formate, and so on (e.g., Anthony, 1986; Brock and Madigan, 1991). Many, but not all methylotrophs are also methanotrophs, and it is important to distinguish between methylotrophs and methanotrophs. A wide variety of bacteria are known which will grow on methanol, methylamine or formate, but not methane, and these bacteria are members of various genera of chemoorganotrophs: *Hyphomicrobium*, *Pseudomonas*, *Bacillus*, and *Vibrio*. In contrast, methanotrophs are unique in that they can grow not only some of those oxidized one-carbon compounds, but also on methane. The methane-oxidizing bacteria possess a specific enzyme system, methane monooxygenase for the introduction of an oxygen atom into the methane molecule, leading to the formation of methanol (e.g., Higgins et al., 1981). It should be noted that although the methanotrophs can also oxidize the oxidized one-carbon compounds such as methanol and formate, initial isolation from nature requires the use of methane as a sole electron donor. All methanotrophs appear to be obligate C-1 utilizers, unable to utilize compounds with carbon-carbon bonds.

By contrast, many nonmethanotrophic methylotrophs are able to utilize organic acids, ethanol, and sugars.

Methanotrophs are widespread both with free-living and attached forms in aquatic and terrestrial environments, being found wherever stable sources of methane are present. In freshwater most methane oxidation occurs aerobically by epibacteria at the oxic-anoxic interface either within the sediments or by bacterioplankton in the water column (Rudd and Hamilton, 1980; Hanson and Hanson, 1996). Most previous studies in lakes have been done at locations with permanently or seasonally anoxic hypolimnia, and the studies on methane oxidation in the water column have concentrated mainly on oxic-anoxic interfaces. Hence, the knowledge of methane oxidation in the oxic water column of the lake is still very poor.

1.3. Purpose of the present study

This study focuses on the structure and function of bacterial communities in the freshwater environment, with special reference to planktonic and attached stages in the cell cycle of bacteria. In chapter 2, I analyzed the contribution of the microbial communities to the trophodynamics structure in Matsumi-ike Bog, with reference to the seasonal alternation of organic nutrient sources. In chapter 3, I presented the result of surveys of methane oxidation rate in the water column at two distinct lake types, Lake Nojiri and Lake Kasumigaura. I also evaluated the relative importance of a diffusive flux across the air-water interface versus methane oxidation in the lake.

Chapter 2

MICROBIAL COMMUNITIES IN A SWAMPY BOG

2.1. Introduction

The aquatic environment can be viewed upon as a complex combination of interactions among its inorganic and organic components (Odum, 1971). In the natural environment, these numerous components fluctuate and interact each other. Each species as one of these components has a distinguished niche, in which it can survive and reproduce (Odum, 1971). As composed by these component complex, the aquatic ecosystem is known to have each ecological component oscillating within certain threshold values (Seki, 1982). The environment is far from being static in this sense, and for that reason, it may be favourable for one species at one time but unsuitable for the same species at the other time. Through these complex interactions, the overall production and decomposition of organic material should be remarkably well balanced.

The limnological succession of a bog is accelerated by filling the whole bog bottom with withered emergent vegetation, because the vegetation can gain a foothold throughout its basin. The bog is transformed soon into a moor as the final stage of successional phenomena of a water body. As the limnological succession of a water body progresses, predominant component of primary producers is displaced from the phytoplankton community in the vegetative matter of emergent plants such as reed or cattail (Hutchinson, 1975). Thus, in a bog at the climax stage of the limnological succession, either phytoplankters or withered emergent plants are the major nutrient source for bacterioplankton, if the influx of allochthonous organic matter into the bog is negligible. There is a lot of phytoplankton biomass during the period from spring to autumn but little during winter. The emergent plants

start to grow during spring, and fall into the water early in the winter thus supplying organic debris. Although phytoplankton supply their cytoplasm as the perfect organic nutrients for bacterioplankton (e.g., Bird and Kalff, 1984; Giorgio and Robert, 1993), emergent plants supply their cytoplasm within a short period after falling into the water, thereafter, the imperfect organic nutrients only rich in C and H (such as cellulose) remain as the nutrient source for bacterioplankton. Most bacterioplankton uptake some essential elements in the form of inorganic nutrients, when these elements are not available as the components of organic nutrients (Seki and Nakano, 1981; Seki, 1982; Benner et al, 1988; Kroer, 1993). The organic debris of dead emergent plants of this category are an important starting point of the detritus food chain in the bog ecosystem. Furthermore, the deposition of organic debris inputting the water column accelerates the progress of limnological succession.

The debris comprises dissolved and particulate organic matter in the water body. Characterization of the dissolved and particulate organic matter may help to elucidate the transformation pathway of this organic matter in the cycling of biological elements in a natural water body. Optical characterization of dissolved organic matter has been studied in both freshwater (e.g., Davis-Colley and Vant, 1987) and seawater (e.g., Blough et al., 1993; Bricaud et al., 1981; Prieur and Sathyendranath, 1981) environments, using optical absorption or fluorescence (e.g., Ferrari and Tassan, 1991; Green and Blough, 1994; Hoge et al., 1993) with special relation to yellow substances or humic substances.

The concentrations of dissolved organic carbon (DOC) in sea water has been measured optically at wavelengths of 280 nm (e.g., Krom and Sholkovitz, 1977; Naganuma and Seki, 1993) and 250 nm (e.g., Stewart and Wetzel, 1981) to determine DOC. The same method

was also applied to the measurement and characterization of DOC in inland water (e.g., Rostan and Cellot, 1995; Zumstein and Buffle, 1989).

Those former studies have been mainly dealing with the fraction of humic substances in DOC which are highly resistant to biodegradation and hence have slow turnover rates (Seki, 1982). In this study, I focused on these particular organic substances which are moderately resistant to biodegradation either with a more rapid turnover rate or rapid turnover rates (Seki, 1982). I used UV absorption spectra to characterize and quantify DOC, particulate organic carbon (POC) and particulate organic nitrogen (PON). The seasonal fluctuation of particulate organic matter is also discussed.

Matsumi-ike Bog, which is located in the campus of the University of Tsukuba, is a bog that has attained the final stage of maturation of a natural water body. As a characteristic of a water body at the climax stage of maturing process, Matsumi-ike Bog must have the highest biological productivity among all types of water body. Hence its trophodynamic structure represents symbolically a highly efficient energy flow for an aquatic ecosystem. In this study, I analyzed trophodynamics structure of the microbial communities over the progress of limnological succession in Matsumi-ike Bog, with special reference to the seasonal alternation of organic nutrient sources.

The aquatic bacteria associated with a solid surface utilize the nutrients concentrated on the solid surface (ZoBell and Anderson, 1936), establish microcolonies (Bott and Brock, 1970a; Marshall et al., 1971; Caldwell et al., 1981) and ultimately form a biofilm community (Wolfaardt et al., 1994). A swampy bog has the largest interface area between water and solid surface because of its shallowness and the abundant particulate organic materials (POM)

in the water column among the hydrosphere. The epibacterial population is important for the ecosystem, especially at the boundary layer between water and sediment ooze. In the previous studies (Aida et al., 1988; Batomalaque et al., 1992), the dynamics study of the epibacterial population focused on those in the water column. Hence dynamics of the epibacterial population at the bottom boundary has not been studied. I report here the dynamics of epibacterial population at the boundary layer of bog bottom.

2.2. Materials and Methods

2.2.1. Study site

Matsumi-ike Bog

Matsumi-ike Bog (Figure 3), which is located in the campus of the University of Tsukuba, Tsukuba City (140°6'40"E, 36°5'20"N), is a bog that has attained the final stage of maturation of a natural water body. The bog was originally a paddy field. Total area of the bog is 1.5 ha; Kami-ike has 0.7 ha and Shimo-ike 0.8 ha. The maximum depth is less than 0.5 meter. Matsumi-ike Bog has been artificially separated in 1976 into these two basins of Kami-ike and Shimo-ike. The bog water can flow from Kami-ike to Shimo-ike through earthend pipes, then flows out into neighbouring the River Hanamuro, which flows in to Lake Kasumigaura at Tsuchiurairi Inlet. Kami-ike has been embanked and surrounded by university buildings and lawns since 1976; Shimo-ike has been left natural as a wildlife sanctuary since the establishment of the university in 1976. Matsumi-ike Bog receives water inputs of rain-fall and rain drainage. No river or stream flows into the bog. Hence, the bog and its watershed have been free from the direct perturbations of domestic and industrial pollution.

2.2.2. Sampling

***In situ* procedures**

The field investigation at the matured stage of Matsumi-ike bog has been performed weekly at Station 2 (Naganuma and Seki, 1985; Miyamoto and Seki, 1992) from April 1991

until March 1992 for bacterioplankton and phytoplankton study, and after 1992 for the particulate organic matter (POM) and the epibacterial population study.

The water temperature, the ooze temperature (only during the study period of attached bacteria) and the solar radiation were measured electrically *in situ* at 9:00 am every sampling day. The optical transmittance through the emergent vegetation over the bog was calculated by the radiation ratio above and below the vegetation leaves over the bog surface, in order to determine the shading efficiency by the plants. The pH and Eh were measured electrically (Horiba pH Meter, Hitachi) at the sampling time in the laboratory. The dissolved oxygen (DO) was measured by the Winkler's method (Strickland and Parsons, 1968). Water samples were collected aseptically at several cm below the water surface with a sterilized Hyroht sampling bottle (2,000 ml) for bacterioplankton and phytoplankton study, and polythene bags (10 l) for chemical analyses (Seki, 1976).

Chemical Analyses

A part of the bog water samples was filtered through Whatman GF/C glass fiber filters which were treated at 450°C for more 2 hours to burn out organic substances prior to the filtration (Parsons et al., 1984). The GF/C filter can collect particles larger than 1 μm; materials passing through the filter were regarded as "dissolved". Particles collected on the filters were analyzed for particulate organic carbon (POC) and particulate organic nitrogen (PON), chlorophylls. Other filtered samples were obtained for each water samples to extract particulate organic matter (POM) by an acid treatment described below.

The POC and PON (only for samples after 1992) were measured by combustion method and gas chromatography with thermal conductivity detection using a CHN Analyzer (SUMIGRAPH NC-90A, Sumika Analysis Center Co., Tokyo) or by using the Yanagimoto CHN Analyzer (Kyoto).

The DOC in filtrates was measured as difference of total carbon and inorganic carbon with a combustion-infrared method using a TOC Analyzer (TOC-5000, Shimazu, Kyoto). The optical spectra of filtrates were measured with a UV-VIS spectrometer (UV-200, Shimazu, Kyoto) using quartz glass cells with 10 cm path length.

The concentration of chlorophyll-a, -b, and -c were determined by the method of Jeffrey and Humphrey (1975). Pigments on each filter were extracted with 10 ml of 90 % (v/v) acetone in one day and centrifuged at 2,500g for 10 min to separate filters. Optical absorbance of the supernatant at 750, 664, 647 and 630 nm was measured with the UV-VIS spectrometer. Chlorophyll concentrations were calculated according to equations of Jeffrey and Humphrey (1975), because these equations give more accurate values for mixed phytoplankton populations in the freshwater environments than the SCOR/UNESCO equations (1966).

The nutrients (nitrate, nitrite, ammonium, total N, phosphate and total P) were colorimetrically determined by the methods in Golterman (1969). Both the samples on the filters and the filtrates were frozen at -20°C until chemical analyses.

Acid treatment for POM

Acid extraction of POM from the GF/C filters were used for spectrometry. The filters were soaked in 25 ml of 1 N HCl for 3 days. The extracts were centrifuged and decanted to separate the acid soluble fraction from the glass fiber and insoluble fraction. The optical absorption of supernatant was measured with the UV-VIS spectrometer.

Adjusting the pH of these extractions to higher than 3 by adding 1 N NaOH aggregated and precipitated basic components. These aggregates were separated by centrifugation (2,500g, 10 min). The absorption spectra of the supernatant were also measured with the UV-VIS spectrometer.

Extraction ratio of POM by acid treatment was determined as follows. A water sample was filtered on 20 GF/C filters as described above. Ten of these filters were used to determine POC and PON before acid extraction with the CHN Analyzer. The other 10 of those filters were treated by acid extraction as described above. After decantation, each extracted filter was re-suspended in 1 N HCl and filtered on GF/C filter pre-acidified by 1 N HCl in a filtering apparatus. These filters were washed on the filtering apparatus with 12 ml of 1 N HCl to eliminate residual extracts on filters. Optical absorbance of washing filtrate at 335 nm were monitored with the UV-VIS spectrometer to ensure elimination of extracts. Acid washed filters were washed again with 60 ml of distilled water to eliminate chloride and neutralize the filters. The pH of filtrate was monitored to confirm neutralization (pH > 5). These washed filters were used to determine the unextracted fraction of POC and PON using the CHN Analyzer.

Biological Analyses

Phytoplankton and vegetation flora

Another part of each bog water sample was used for identification and enumeration of phytoplankters. A 0.025 ml of water sample fixed by glutaldehyde (5%) was pipetted onto a phytoplankton counting chamber ruled with slits for microscopic examination (Rigosha Co., Tokyo). Every count made from plural subsamples of 0.025 ml required more than 100 cells of phytoplankters, in order to reliably record the density of predominant species. Identification of phytoplankton species was made according to Mizuno (1971), Prescott (1973) and Smith (1933).

The vegetation flora in the bog were occupied exclusively by a cattail (*Typha latifolia*). Each part of the vegetations (root, stem and leaf) was collected from the 1/2 square meter area. The collection was made from spaces of the atmosphere (leaf), the water column (stem) and bottom sediment (root) of the bog. The cattail samples were dried at 60 °C, and then determined their biomass.

Bacterioplankton

Another portion of bog water sample was fixed with 5% glutaraldehyde immediately after sampling, and the bacterioplankton population density was determined using an epifluorescent microscope (Hobbie et al., 1977; Zimmerman et al., 1978; Naganuma et al., 1989). A certain volume of the sample water was filtered on a Nuclepore filter (diameter of 25 mm, pore size of 0.2 μm) pre-stained with Sudan black (6 mg dissolved in 100 ml of 50% ethanol). Bacterial cells on the filter were stained with acridine orange solution (1:10,000 in

6.6 mM of pH 6.6 phosphate buffer) and counted under an epifluorescent microscope (Nikon OPTIPHOT, EFD2, Tokyo). The filtered volume was determined so that the counts were more than 20 bacterial cells in each microscopic field, and counts of more than 500 cells were made for further statistical analysis. This range is within the limit of reasonable counts suggested by Kirchman et al. (1982).

The growth rate of the natural bacterioplankton was measured by a simulated *in situ* method using a chemostat (Naganuma and Seki, 1985; 1988; Miyamoto and Seki, 1992). The culture medium for this method was the bog water collected from Matsumi-ike Bog one day before each sampling day, in order to simulate the bog environment as precisely as possible. The bog water for culture medium was filtered with glass fiber filters (Whatman GF/D and GF/C) and then autoclaved. The chemostat culture was made immediately after the sampling at *in situ* water temperature. At each sampling time 1.5 l of the bog water was put into culture continuous with a medium input of 40 ml hr^{-1}; i.e., the dilution rate was 0.027 hr^{-1}. This dilution rate was appropriate to simulate the bacterioplankton community of the bog (Miyamoto and Seki, 1992). Subsamples collected during the chemostat culture of 1, 2, 4 and 6 hr, were used for the bacterioplankton counting. Wash-out rate was obtained from the least-square method of the logarithmic plots of bacterial density against culture time (Jannasch, 1969). The bacterioplankton growth rate (R) was calculated from the equation of $R = D - A$, where D is the dilution rate and A is the washout rate.

Attached bacteria

Model of epibacterial population dynamics

The population dynamics of microcolonies on the substratum are affected by three processes; attachment, detachment and growth (Ytow and Seki, 1996; Figure 4).

The attachment rate was assumed to be proportional to both the concentration of bacterial particles (F_i) drifting in the water column, and the attachment rate coefficient a_i of each bacterial particle. Since the transformation of attached cells to irreversibly attached cells modifies only the attachment rate coefficient (Mueller et al., 1992), the effect of the transformation is already introduced in the coefficient a_i. This coefficient could be variable depending on the size of the bacterial particle because the interaction could depend on the number of cells interacting with solid surface. The coefficient should be also variable with the quality of the solid surface including the effect of conditioning by organic molecules.

The microcolony of i cells of attached bacteria would have its own growth rate coefficient g_i. The growth rate of the density of i cell microcolonies, C_i, would depend on both the growth rate coefficient and the density itself as their yield, g_iC_i. The growth of a single cell in an (i-1) cell microcolony increases the density of the i cell microcolony by one, and decreases the density of the (i-1) cell microcolony, C_{i-1}, also by one. Hence, the contribution of the growth in microcolonies to the density of i cell microcolonies would be $g_{i-1}C_{i-1} - g_iC_i$, or a difference of growth in the one cell smaller microcolonies (size of i-1) and the given microcolonies (size of i).

The colony density of attached bacteria does not increase to infinity but rather to a saturated level (Millsap et al., 1994). This indicates that there must be detachment of cells

(Peyton and Characklis, 1993) after 'irreversible' attachment though it is termed as 'irreversible'. The i cell microcolony would have its own rate coefficient of bacterial detachment b_i. The detachment rate of density of i cell microcolonies would depend on both the coefficient and the density itself as its yield b_iC_i. The detachment of a single cell from the (i+1) cell microcolony decreases the density of the (i+1) cell microcolonies by one, and increases the density of the i cell microcolonies also by one. Hence, the contribution of the detachment in microcolonies to the density of i cell microcolonies would be $-b_iC_i + b_{i+1}C_{i+1}$, or difference of detachment from the one cell larger microcolonies (size of i+1) and the given microcolonies (size of i).

The population dynamics are, therefore, expressed as

$$\frac{dC_i}{dt} = -g_iC_i + g_{i-1}C_{i-1} - b_iC_i + b_{i+1}C_{i+1} + a_iF_i \tag{1}$$

Within a regular investigation period, the growth rate coefficient g_i, the detachment rate coefficient b_i and concentration of the drifting bacterial particle F_i can be regarded as constants.

Summing up the equation (1) for i to any integer $j \geq \bar{i}$

$$\frac{d\sum_{i=1}^{j} C_i}{dt} = -b_1C_1 + \sum_{i=1}^{j} a_iF_i - g_{\bar{i}}C_{\bar{i}} + b_{\bar{i}+1}C_{\bar{i}+1} \tag{2}$$

because $g_0C_0 = 0$.

Since each cell has finite volume and colony density is finite, there must be an integer i witch satisfies for any integer $j > \bar{i}$

$$\sum_{i=1}^{j>\bar{i}} C_i = \sum_{i=1}^{\bar{i}} C_i. \tag{3}$$

Hence, with j large enough, it can be described total density of microcolonies as

$$\sum C_i = \sum_{i=1}^{i>\bar{i}} C_i, \tag{4}$$

without ambiguity and losing generality. A practical value of $\bar{i}$ is the cell number of the largest microcolony observed.

The total density of microcolonies is increased by the attachment and decreased by the detachment of single-cell microcolonies, but is not affected by the bacterial growth: The growth of a microcolony causes an increase of the cell number in the microcolony, whereas it has no effect on the number of microcolonies. Hence, the total density of microcolonies, ΣC_i, is expressed as another equation as

$$\frac{d\sum C_i}{dt} = -b_1 C_1 + \Sigma a_i F_i. \tag{5}$$

These two equations (2) and (5) give the condition of

$$-g_{\bar{i}} C_{\bar{i}} + b_{\bar{i}+1} C_{\bar{i}+1} = 0. \tag{6}$$

This equation indicates that the growth must be balanced by detachment for the microcolonies of maximum cells, or, no growth in microcolonies of maximum cells ($g_{\bar{i}} = 0$) and hence no microcolonies larger than maximum cells ($C_{\bar{i}+1} = 0$).

In most cases, the bacterial particles that newly attach are composed of a single cell, $F_i = 0$ for $i \neq 1$, and hence $\Sigma a_i F_i$ can be regarded as $a_i F_i$. Under this condition, dynamics of the total microcolony densities can be simplified as

$$\frac{d\sum C_i}{dt} = -b_1 C_1 + a_i F_i \tag{7}$$

When the coefficient of attachment rate a_1 is constant, the plot of C_1 versus $d\Sigma C_i/dt$ gives an regression line with the intercept of a_1 and the slope of $-b_1$, respectively. In this case, the density of microcolonies would increase asymptotically to a steady-state $d\Sigma C_i/dt = 0$, or

$$b_1\bar{C}_1 = a_1\bar{F}_1 \tag{8}$$

where $\bar{C}_1$ and $\bar{F}_1$ are values at the steady-state. The time course of total microcolony density is an exponential curve.

The attachment rate coefficient depends on the quality of the substratum surface which is conditioned by adsorption of organic molecules. In the case where this conditioning and microbial attachment occur simultaneously, the attachment rate coefficient should be considered time dependent. The adsorption of dissolved matter by the surface can modify the attachment rate coefficient as

$$a_1 = A_0 + A_1[1 - \exp(-t/\tau)], \tag{9}$$

where A_0, A_1 and τ are constants. In this case the density of microcolonies increases to the steady state with S-shaped time course.

Although the coefficients, a_1, g_i and b_i, can be determined by the least square regression, each coefficient g_i or b_i appears twice in the right side of successive equation (1) and makes determination of these coefficients unstable. Here the regression is readily proceeded with the following modification equation (1),

$$\frac{d\sum_{j=i} C_j}{dt} = \begin{cases} -b_1C_1 + a_1F_1 & \text{for } i = 1 \\ -b_iC_i + g_{i-1}C_{i-1} & \text{for } i = 2, 3, \ldots \end{cases} \tag{10}$$

because the parameters g_i and b_i appear only once in the right side of the equations. Thus these parameters can be determined practically by applying each equation independently.

At the later stage of bacterial attachment, when bacteria have covered a nontrivial extent of the substratum, only bacteria attached to the free surface of substratum increase their number of colonies upon attachment (Fletcher, 1977). The bacteria newly attached to the indigenous bacterial colonies do not increase the number of microcolonies but the cell number of the microcolonies. The population dynamics of the later stage is, therefore, expressed as

$$\frac{d\sum C_i}{dt} = -b_1 C_1 + (1 - \sum \sigma_i C_i)\sum a_i F_i, \tag{11}$$

and

$$\frac{dC_i}{dt} = -g_i C_i + g_{i-1} C_{i-1} - b_i C_i + b_{i+1} C_{i+1} + (1 - \sum \sigma_i C_i) a_i F_i + \sum_{j=1}^{i-1} (\sigma_j C_j a_{i-j} F_{i-j}). \tag{12}$$

where each σ_i is a probability of interaction between indigenous i cell microcolony and newly attached bacterial cell. This probability has dimension of area and is so-called the cross section of microcolonies. Assuming the cross section is proportional to the cell number in a microcolony $(\sigma_i = i\sigma_1)$, and no detachment $(b_1 = 0)$, equation (11) is the same as the adsorption equation of Fletcher (1977) because $\sum \sigma_i C_i = \sigma_1 \sum i C_i = \sigma N$, where N is number of bactrial cells. The σ gives a criteria of the later stage: The σ_1 would be the order of the geometrical cross section of single bacterial cell.

Total number of cells

The total cell density, $N \equiv \sum i C_i$, is governed by an equation

$$\frac{dN}{dt} \equiv \frac{d\sum iC_i}{dt}$$

$$= \sum i a_i F_i + \sum g_i C_i - \sum b_i C_i \tag{13}$$

which is the sum of a series of equation (1) as multiplied by i.

In a particular case where both coefficients of the growth rate and the detachment rate are proportional to microcolony size i as $g_i = iG$ and $b_i = iB$, equation (13) is simplified as

$$\frac{dN}{dt} = \Sigma a_i F_i + G\Sigma iC_i - B\Sigma iC_i, \tag{14}$$

$$= \Sigma a_i F_i + GN - BN. \tag{15}$$

Equation (15) is same as the model proposed by Aida et al. (1988) with the assumption that $F_i = 0$ for $i \neq 1$, i.e., all bacterial particles are comprised of a single cell. It is also the same as the model proposed by Caldwell et al. (1983) with the assumption of $F_i = 0$ for any $i \neq 1$, and a substitution of $B = 0$.

In the case where all aF, G and B are constant, equation (15) can be solved analytically as

$$N = \frac{A}{B-G}[1 - \exp\{-(B-G)t\}], \tag{16}$$

where $A = \Sigma a_i F_i$. In this case, the coefficients must be $B>G$, or, bacterial cells must detach faster than grow, as the number of bacterial cells becomes a steady value as observed previously (Bott and Brock, 1970b; Fletcher, 1977). There must be some modification of coefficients in equation (15) as shown by Aida et al. (1988).

Epibacterial population in Matsumi-ike Bog

The attachment, detachment and growth kinetics of the epibacterial population at the boundary between the water column and the ooze sediment were studied at Matsumi-ike Bog (Naganuma and Seki, 1985; Miyamoto and Seki, 1992) throughout the year.

The glass slides (non-fluoressence) were submerged at the boundary between the water column and the ooze sediment for 3 days to examine the vertical distribution of bacterial attachment on the slide (Figure 5). Before being submerged, the slides were washed carefully in distilled water, and made free of organic materials by combustion in a muffle furnace at a temperature of 500°C for 24 hr.

Each slide was recovered one by one every 24 hr, after the first and second slide were recovered at 6 hr and 12 hr from the start of the *in situ* experiment. The recovered slides were washed in filtered water with 100 times reciprocation to remove non-attached materials and bacteria. It has been confirmed previously that washing between 50 and 150 times is needed to isolate only the irreversible attached bacteria on the slide (Aida et al., 1988). The washed slides were fixed in 4% neutral formaldehyde solution for several hours, and then stained for 5 min with acridine orange solution (1:10,000 in 6.6 mM of pH 6.6 phosphate buffer). Then the slide was washed by distilled water and dried for examination under an epifluorescent microscope (Nikon, Tokyo). Enumeration was performed to determine the density of bacterial microcolonies on the slide and the cell number in each microcolony.

The attached bacteria were counted at a magnification of 1,200. Vertical profiles of bacteria attached on the slide during each 24 hr were examined with 1 mm interval. In order to get the attachment, detachment and growth rates of attached bacterial community on every glass slide, monthly investigation was conducted at the three locations; 1) in the water column, 2) at the bottom boundary, 3) in the sediment ooze. Usually, the locations to be examined in

the water column and in the sediment ooze were selected to be above or below 20 mm from the bottom boundary on every glass slide. In order to obtain accurate estimates of attachment, detachment and growth rates, the cells of more than 50 colonies were counted on every slide, and more than 10 fields at each location.

The examination of these glass slides gave a periodical series of bacterial microcolony development on the solid surface as a set of time series of microcolony density with different numbers of cells in each microcolony, $C_i(t)$. Linear and non-linear least square methods were used to determine the parameters of the population dynamics of attached bacteria, A_0, A_1, g_i, b_i and τ. Since the dynamics are expressed by a set of differential equations, it is necessary to apply a non-linear least square method with numerical integration of these differential equations for determination of the parameters. The result of non-linear least square method with numerical integration firmly depends on the initial value of these parameters. Here the initial values were determined by applying the linear (for $i > 2$ in equation (10)) and non-linear (for $i = 1$ in equation (10)) least square method with the differential equations (10) with approximation of the differentiation by central difference, the difference of microcolony density and previous microcolony density divided by time increment. The parameters determined by these least square methods were used as initial values in the non-linear least square method for numerical integration to determine precise parameters without approximation of differentiation.

The modified Gram-Shumidt method (Bjorck, 1967) was used for the linear least square regression, which gives the parameters by linear matrix operation to the time series of measured microcolony density. The modified Marquardt method (Marquardt, 1963; More, 1978) was used for the non-linear least square regression repeating the modified Gram-Shumidt method until the minimized. Using the parameters estimated by these methods as initial value, the parameters were determined by the hybrid method (Powell, 1970a, b) which can be applied to least square method with numerical integration.

Other environmental factors (water temperature, ooze temperature, nutrients, POC and PON, chlorophylls and DOC) were also measured at the sampling time.

2.3. Results

2.3.1. Characteristics of Matsumi-ike Bog

Water temperature and ooze temperature

The water temperature of the bog surface fluctuated in a typical temperate pattern throughout the year (Figure 6). The water temperature T (° C) could be expressed in a sinusoidal regression statistically with a high significance level,

$$T = 10.2 \sin[2\pi(t\text{-}21.0)/366] + 15.9$$

$$(F=959,\ F_{0.01[1,49]}=7.18)$$

where t is number of days since 1 April 1991. It fluctuated with a lag of 30 days behind that of solar radiation. The temperature was usually lower in the ooze than in the water column, and the difference of the temperature in water and ooze was the greatest during winter (Figure 7).

Dissolved oxygen

The dissolved oxygen (DO) concentration at the surface of the bog was between 3 and 15 mg O_2 l^{-1} throughout the year, showing a significant negative correlation with the water temperature (Figure 8). It seems that the DO fluctuation in this range affects little on aquatic bacterial metabolism in the bog, because critical concentration for bacterial respiration was estimated to be as low as 0.43 mg O_2 l^{-1} for natural bacterial community (Pamatmat, 1971; Seki et al., 1984) as well as for a pure strain of marine bacterium (ZoBell, 1940). It has been

also suggested that the multiplication and respiration of lake bacteria are independent of DO throughout the range from 0.30 to 36 mg O_2 l^{-1} (ZoBell, 1946).

Inorganic nutrients

Nitrate and ammonium were the major components of inorganic nitrogen in the bog water (Figures 7 and 9). From 1991 to 1992, the concentration of nitrate plus nitrite was the lowest during the period of spring and summer, the greatest during the period of autumn, but decreased to the moderate level in winter (Figure 9). From 1992 to 1993, the concentration of nitrate plus nitrite was the lowest at May, and increased at the beginning of June and maintained higher level until end of October. Thereafter the concentration decreased and maintained lower level during winter (Figure 7). The ammonium concentration was kept at a low level with occasional high pulses (Figures 7 and 9).

The concentration of phosphate (Figure 9) increased drastically end of January, because the cattails fall into the water column for a heavy snowfall on January 28 1992. Thereafter the concentration decreased rapidly to a moderate level (about 1.0 μg atom P l^{-1}) and increased gradually in March. The moderate level was maintained from April to January except the early summer phytoplankton bloom (Figure 9). From 1992 to 1993, the concentration of phosphate showed almost same fluctuation as 1991-1992 observation, except decreased drastically in October and December (Figure 7).

DOC

From 1991 to 1992, the DOC (dissolved organic carbon) concentration was the greatest from June to August, thereafter the concentration decreased gradually to October, and maintained lower level in winter (Figure 8). The greatest DOC concentration from June to August was evidently produced by the summer bloom of phytoplankton in the water column. The concentration of DOC became higher again in February because of cattails collapsed into the water column. From 1992 to 1993, the DOC concentration was decreased gradually from April to end of June (Figure 10). The concentration increased drastically at the middle of August, when the summer phytoplankton bloom was finished, and maintained high level until the middle of October. Thereafter the concentration drastically decreased and maintained lower level during winter (there was no DOC data after January 1993).

An optical density spectrum of the filtrate is shown in Figure 11. The optical density OD_λ at wavelength λ was proportional to λ^4 , expressed by the following regression (r^2 = 0.963 ± 0.038);

$$OD_\lambda = a/\lambda^4$$

where the value of a varied with samples. The residue to the λ^{-4} fitting is also shown in Figure 11. It has a small peak at the wavelength of 280 nm and a shoulder at 320 nm.

The optical density at λ = 280 nm was proportional to the DOC concentration throughout the year as shown in Figure 12. It is expressed by the following regression;

$$OD_{280} = 0.172\ \mathrm{DOC} + 0.131 \qquad r^2 = 0.898\ (n = 47).$$

POC and PON

The POC (particulate organic carbon) concentration from 1991 to 1992 was the greatest during the summer phytoplankton bloom, thereafter the concentration became lower progressively toward the early winter, and became higher progressively toward the spring (Figure 8). The primary constituents of particles from late spring to summer were possibly living phytoplankters and phytodetritus (Brown and Parsons, 1972).

The POC and PON (particulate organic nitrogen) concentrations after 1992 fluctuated with almost the same profiles during the period from spring to autumn, when the dominant constituents of particles were living phytoplankton and phytodetritus (Figure 10). Actually, each pulse of the particles corresponded to a chlorophyll-a pulse. During winter, however, different fluctuation profiles were observed between POC and PON, because the primary source of particle constituents changed from phytoplankton to dead cattails (*Typha latifolia*) that fall down into the water column in winter.

The dominant substances comprising POM (particulate organic matter) in the Matsumi-ike Bog were manifold during two different periods, i.e., one is from April to October or November while the phytoplankton biomass comprised the predominant POM components because most of the cattail grew to stand above the bog water column. Another is during winter while the phytoplankton biomass was low while the withered cattail became the primary POM source in the water column. The correlations between POC and PON concentrations in each period are shown in Figure 13. Each relationship could be expressed as highly significant regression;

From April to October: $POC = 0.115 + 6.04 \times PON$ $r^2 = 0.752$ ($n = 27$),

From November to March: $POC = -0.641 + 9.94 \times PON$ $r^2 = 0.661$ ($n = 21$).

The regression slopes of POC vs PON plot were different during each period ($t = 11.755 > t_{[44, 0.05]} = 2.015$). This indicates the difference of dominant components comprising POM in different periods. During the period from November to March while withered cattail was the dominant POM source, POM had less nitrogen elements than that in the other period while the phytoplankton was the dominant POM source.

Acid extract of POM

The absorption spectrum of an acid extract is shown in Figure 14. There were two absorbance peaks at 220 nm and 335 nm. The absorption spectrum (A_λ at wavelength of λ) was expressed by the sum of two Lorentz functions ($r^2 = 0.996 \pm 0.003$);

$$A_\lambda = b + c_{223} /(1 + (\lambda - \lambda_{223})^2 /w^2_{223}) + c_{340} /(1 + (\lambda - \lambda_{340})^2 /w^2_{340}),$$

where each λ is the central wavelength of absorption, w is the half width at half maximum, c is the absorption intensity and b is a constant. Suffixes indicate the central wavelength, $\lambda_{223} = 22.6 \pm 1.0$ nm and $\lambda_{334} = 339.5 \pm 0.5$ nm, respectively. The value of b and c varied according to the sample.

Making the pH of the extracts to be higher than pH 3, resulted in the formation of brown flocculates. The absorption spectra of supernatants had no peaks at wavelengths of 220 nm and 335 nm (data are not shown). These absorption maxima in the acid extract were due to the precipitates. The flocculates were re-solubilized by acidification and the re-solubilized samples formed flocculates again by neutralization. This repetitive flocculation and re-solubilization indicate that the flocculates are basic substances, since the re-solubilized sample had the same absorption as that of the origin acid extraction.

The absorption at several wavelengths exponentially increased depending on the duration of acid treatment as shown in Figure 15. The time constant of extraction was 0.5 days. With 3 days extraction, the absorption reached a plateau. Hence we used 3 days extraction as analytical procedure. During 3 days extraction, POC and POM on the filter decreased 24 ± 8 % and 21 ± 7 %, respectively.

In the following comparison of optical absorption of POM acid extraction and PON/POC ratio, I measure absorption at 280 nm and 335 nm since these absorption bands are more stable than that at 220 nm in the time course of extraction. Absorption at 280 nm was selected since it is used in DOC measurement and it is near the bottom of the POM extraction spectrum.

Absorption at the wavelengths of 280 nm (A_{280}) was almost proportional to absorption at 335 nm (A_{335}) (Figure 16). There was a tendency that the A_{280}/A_{335} ratio was smaller than 0.7 for higher A_{335}. Although the absorptions ratio was independent from the particulate organic carbon concentration (r^2 = 0.0002, data are not shown), it was dependent on the nitrogen/carbon (N/C) ratio (Figure 17). The ratio increased above a value of 0.14 which approximately corresponds to one nitrogen atom to 7 carbon atoms. The increase of the nitrogen fraction in acid extractable/hydrolysable proportion of POM was obvious at a A_{280}/A_{335} ratio greater than 0.7. The frequency distribution of the absorption ratios was divided into two groups around the ratio of 0.7 (Figure 18). The ratios fluctuated throughout the year, as shown in Figure 19, with two periods of lower and higher A_{280}/A_{335} ratios. Two pronounced high ratios on April and June corresponded to the phytoplankton bloom.

The correlations between POC and chlorophyll concentrations are shown in Figure 20. The dependency of chlorophyll-a and -b on POC was different during the seasons, and could be estimated by high and low A_{280}/A_{335} ratios. In the season with the lower ratio, the fraction of chlorophyll-a and -b in POC was smaller and vice versa. For chlorophyll-c, on the other hand, no obvious difference in regression was found.

The optical density at $\lambda = 280$ nm was proportional to POC concentration as shown in Figure 21. The regression depends on the A280/A335 ratio, as

$$POC = 9.15\, A_{280} - 7.06 \times 10^{-2},$$

for samples with $A_{280}/A_{335} \geq 0.7$ ($r^2 = 0.627$) and

$$POC = 12.35\, A_{280} - 2.96 \times 10^{-2},$$

for samples with $A_{280}/A_{335} < 0.7$ ($r^2 = 0.689$), respectively. There was no significant difference in the slopes ($t = 1.671 < t_{[60,\ 0.05]} = 2.000$) but in intercept ($t = 11.25 > t_{[60,\ 0.001]} = 3.460$).

Emergent vegetation and optical transmittance

The biomass of emergent vegetation increased logistically (Figure 6). In its growing phase (April - August), the total biomass LV_{total} (kg m^{-2}) and the leaf biomass above the water column LV_{leaf} (kg m^{-2}) could be expressed in highly significant regression as:

$$LV_{total} = 7.7 / (5.0 + 56.1\exp(-(t\text{-}50.3)/16.4))$$

$$(F = 65.7,\ F_{0.01[1,4]} = 21.2),$$

$$LV_{leaf} = 6.8 / (4.7 + 51.0\exp(-(t\text{-}50.4)/17.9))$$

$$(F = 139.9,\ F_{0.01[1,4]} = 21.2).$$

Both leaf part and whole part of the plants sustained its maximal biomass, 1.45 kg m^{-2} and 1.54 kg m^{-2}, respectively. The biomass above the bog water decreased from December to the end of January, when cattails collapsed into the water column due to a heavy snowfall. Most of the cattail biomass was immersed completely in water within these two months.

The optical transmittance below the emergent vegetation decreased as the vegetation biomass increased (Figure 6). The transmittance increased from August to November, though the vegetation biomass was constant. The optical transmittance was different vegetating structures even with the same vegetation biomass.

Chlorophylls

The amounts of chlorophylls -a, -b and -c fluctuated seasonally in the range of 4.0×10^0 to 2.0×10^2 μg l^{-1}, 0.3 to 30 μg l^{-1} and 0.03 to 5×10^2 μg l^{-1}, respectively (Figure 6 and 22).

Chlorophyll-a

The best regression for annual fluctuation of chlorophyll -a concentration, $C_{chl\text{-}a}$ (μg l^{-1}), could be expressed as a highly significant sinusoidal equation (Figure 6) as:

$$\log C_{chl\text{-}a} = 1.20 + 0.26 \sin[2\pi(t\text{-}5.1)/366]$$

$$(F = 23.58, F_{0.01[1,49]} = 7.18).$$

The chlorophyll-a concentration showed a similar annual fluctuation to water temperature with a time lag of 16 days. There were eight periods distinguished, however, based on the amplitude and inter peak interval (IPI) of its fluctuation as follows: Period I, April 5 - June 5

(IPI = 21.7 ± 5.8 days); Period II, June 12 - June 16 (IPI = 14.8 ± 2.0 days); Period III, June 16 - September 18 (IPI = 22.0 ± 4.5 days); Period IV, September 25 - October 29 (IPI = 23.1 ± 19.8 days); Period V, November 6 - November 19 (IPI = 48.8 days); Period VI, November 26 - January 14 (IPI = 20.59 ± 3.8 days); Period VII, January 21 - February 11 (IPI = 64.5 days); and Period VIII, February 18 - March 23 (IPI = 13.6 ± 0.6 days). The periods are indicated in Figure 6 by the Roman number.

Chlorophyll-b

The chlorophyll-b concentration, $C_{chl\text{-}b}$ (μ g l^{-1}), could be expressed in a highly significant sinusoidal regression (Figure 22) as:

$$\log C_{chl\text{-}b} = 0.12 + 0.24 \sin[2\pi(t\text{-}32.2)/366]$$

$$(F = 10.7, F_{0.01[1,49]} = 7.18).$$

The annual fluctuation of chlorophyll-b concentration related to that of water temperature with a time lag of 11.2 days. Five distinguished periods were evident, according to the IPI and amplitude of the fluctuation: Period I, April 5 - June 12 (IPI = 39.0 ± 11.0 days); Period II, June 18 - July 10 (IPI = 15.4 ± 4.4 days); Period III, July 16 - September 25 (IPI = 27.90 ± 4.9 days); Period IV, October 2 - October 29 (IPI = 19.1 ± 2.1 days) and Period V, November 6 - March 23 (IPI = 26.0 ± 14.4 days).

Chlorophyll-c

The chlorophyll-c concentration fluctuated seasonally without giving significant sinusoidal regression ($F = 0.15$, $F_{0.05[1.49]} = 4.04$) (Figure 22). There were five periods

distinguished, based on the amplitude and the IPI of the fluctuations: Period I, April 5 - June 12 (IPI = 43.1 ± 7.1 days); Period II, June 18 - September 18 (IPI = 17.3 ± 3.7 days); Period III, September 25 - December 17 (IPI = 36.7 ± 5.6 days); Period IV, December 17 - February 25 (IPI = 16.6 ± 3.3 days) and Period V, March 3 - March 23 (IPI = 17.2 ± 3.0 days).

Phytoplankton

The dominant phytoplankton in Matsumi-ike Bog were classified into the genera *Chlamydomonas*, *Scenedesmus*, *Navicula*, *Melosira* and *Chroococcus*. Species of the genera *Chlamydomonas* and *Scenedesmus* belong to chlorophyll-b group; those of the genera *Navicula* and *Melosira* belong to chlorophyll-c group; and those of the genera *Chroococcus* belong to the cyanobacteria group (Seki and Takahashi, 1983). These phytoplankton had population densities of more than 1.0 cell ml^{-1} throughout the year, except *Scenedesmus* spp. which was lower than 1.0 cell ml^{-1} during winter.

Total phytoplankton

The population density of total phytoplankton fluctuated seasonally within the range of 2.0×10^1 (in January) and 3.5×10^4 (in August) cells ml^{-1}, and the population density, P_{total} (cells ml^{-1}), could be expressed as a highly significant regression as:

$$\log P_{total} = 2.78 + 0.42 \sin[2\pi(t\text{-}32.6)/366]$$

$$(F = 35.8, F_{0.01[1,49]} = 7.18)$$

with short pulses of phytoplankton bloom (Figure 6). There was a time lag of 11.6 days between their population density and the water temperature. There were eight periods

distinguished, based on the IPI and amplitude of fluctuation: Period I, April 5 - June 5 (IPI = 18.5 ± 4.8 days); Period II, June 12 - July 31 (IPI = 22.3 ± 12.2 days); Period III, August 6 - September 25 (IPI = 20.1 ± 4.7 days); Period IV, October 2 - November 12 (IPI = 16.0 ± 2.7 days); Period V, November 19 - December 3 (IPI = 14.4 days); Period VI, December 10 - December 27 (IPI = 24.2 days); Period VII, January 6 - January 14 (IPI = 19.9 days); and Period VIII, January 21 - March 23 (IPI = 30.8 ± 0.2 days).

Chroococcus

The population density of *Chroococcus* fluctuated seasonally within the range of 1.0 (in June and January) and 1.8×10^3 (in August) cells ml^{-1}, and *Chroococcus* density, $P_{Chroococcus}$ (cells ml^{-1}), could be expressed as a significant regression as:

$$\log P_{Chroococcus} = 1.81 + 0.28 \sin[2\pi(t+8.6)/366]$$

$$(F = 5.11, F_{0.05[1,49]} = 4.04)$$

with short pulses of *Chroococcus* bloom (Figure 22). There was a time lag of -29.6 days between its population density and the water temperature. There were six periods distinguished, based on the IPI and amplitude of fluctuation: Period I, April 5 - June 12 (IPI = 18.8 ± 4.6 days); Period II, June 12 - July 10 (IPI = 11.1 days); Period III, July 16 - September 25 (IPI = 17.5 ± 5.2 days); Period IV, October 2 - October 29 (IPI = 12.9 ± 1.8 days); Period V, November 6 - January 14 (IPI = 18.4 ± 3.5 days); and Period VI, January 14 - March 23 (IPI = 15.4 ± 3.8 days).

Scenedesmus

The population density of *Scenedesmus* fluctuated within the range of 40 and 10^3 cells ml^{-1} from April to mid November, and *Scenedesmus* density, $P_{Scenedesmus}$ (cells ml^{-1}), could be expressed as a highly significant regression as:

$$\log P_{Scenedesmus} = 1.25 + 1.24 \sin[2\pi(t\text{-}25.38.6)/366]$$

$$(F = 58.0, F_{0.01[1,49]} = 7.18)$$

with short pulses of *Scenedesmus* bloom (Figure 22). There was a time lag of 4.3 days between its population density and the water temperature. The magnitude of fluctuation was greater during spring and autumn than during summer. There were six periods distinguished, based on the IPI and amplitude of fluctuation: Period I, April 5 - June 12 (IPI = 21.6 ± 7.6 days); Period II, June 18 - July 31 (IPI = 19.2 ± 1.4 days); Period III, August 6 - September 25 (IPI = 24.5 ± 5.2 days); Period IV, October 2 - October 29 (IPI = 13.8 ± 2.1 days); Period V, November 6 - November 19 (IPI = 19.7 ± 5.7 days); and Period VI, November 26 - March 23.

Chlamydomonas

The population density of *Chlamydomonas* fluctuated seasonally within the range of 2.0×10^1 (in January) and 3.5×10^4 (in August) cells ml^{-1}, and *Chlamydomonas* density, $P_{Chlamydomonas}$ (cells ml^{-1}), could be expressed as a highly significant regression as:

$$\log P_{Chlamydomonas} = 2.13 + 0.41 \sin[2\pi(t\text{-}41.2)/366]$$

$$(F = 14.7, F_{0.01[1,49]} = 7.18)$$

with short pulses of *Chlamydomonas* bloom (Figure 22). There was a time lag of 20.2 days between its population density and the water temperature. There were six periods

distinguished, based on the IPI and amplitude of fluctuation: Period I, April 5 - May 21 (IPI = 16.5 ± 2.9 days); Period II, May 28 - June 16 (IPI = 17.9 ± 2.7 days); Period III, June 23 - September 25 (IPI = 19.0 ± 3.2 days); Period IV, October 2 - November 12 (IPI = 15.1 ± 2.9 days); Period V, November 19 - January 6 (IPI = 15.1 ± 2.9 days); and Period VI, January 6 - March 23 (IPI = 39.2 ± 1.5 days).

Melosira

The population density of *Melosira* fluctuated seasonally within the range of 1.0 (in June, October, January and February) and 3.0×10^3 (in September) cells ml^{-1}, and *Melosira* density, $P_{Melosira}$ (cells ml^{-1}), could be expressed as a significant regression as:

$$\log P_{Melosira} = 1.76 + 0.43 \sin[2\pi(t\text{-}33.8)/366]$$

$$(F = 10.2, F_{0.01[1,49]} = 7.18)$$

with short pulses of *Melosira* bloom (Figure 22). There was a time lag of 12.8 days between its population density and the water temperature. There were four periods distinguished, based on the IPI and amplitude of fluctuation: Period I, April 5 - June 25 (IPI = 17.7 ± 0.3 days); Period II, June 25 - October 14 (IPI = 22.0 ± 6.7 days); Period III, October 14 - January 14 (IPI = 29.5 ± 7.7 days); and Period IV, January 14 - March 23 (IPI = 31.9 ± 3.9 days).

Navicula

The population density of *Navicula* fluctuated seasonally within the range of 1.0 (in April, November and February) and 2.0×10^3 (in August) cells ml^{-1}, and *Navicula* density, $P_{Navicula}$ (cells ml^{-1}), could be expressed as a significant regression as:

$$\log P_{Navicula} = 1.78 + 0.34 \sin[2\pi(t\text{-}47.4)/366]$$

$$(F = 8.2, F_{0.01[1,49]} = 7.18)$$

with short pulses of *Navicula* bloom (Figure 22). There was a time lag of 26.4 days between its population density and the water temperature. There were five periods distinguished, based on the IPI and amplitude of fluctuation: Period I, April 5 - June 18 (IPI = 17.5 ± 3.8 days); Period II, June 25 - September 25 (IPI = 24.0 ± 1.8 days); Period III, October 2 - November 26 (IPI = 17.4 ± 2.3 days); Period IV, November 26 - December 27 (IPI = 28.2 ± 1.1 days); and Period V, January 6 - March 23 (IPI = 15.3 ± 2.4 days).

Microbial communities at the different stages of limnological succession

At the first stage of the limnological succession of a bog progresses, Matsumi-ike Bog has no littoral vegetation. Matsumi-ike Bog at this stage (e.g., 1983-1984; Naganuma and Seki, 1985; Shiraishi et al., 1985) was flat with the depth of up to 1 m, and emergent plants were not observed. The chlorophyll a concentration which indicates the phytoplankton density increased from winter to summer, and decreased from summer to winter. The bacterioplankton density increased from spring to autumn and decreased from autumn to spring, with steady-state fluctuations of a small amplitude between 10^9 and 10^{10} cells l^{-1}. These annual fluctuations can be regressed as sinusoidal curves with highly significant levels as follows:

$$Bac = 4.6 \times 10^9 \sin[2\pi(t\text{-}139)/366] + 8.5 \times 10^9$$

$$(F=95.2,\ F_{0.01[1,49]}=7.18),$$

$$Chl\text{-}a = 17 \sin[2\pi(t\text{-}17)/366] + 19$$

$$(F = 39.4,\ F_{0.01[1,49]} = 7.18),$$

where *Bac* is the bacterioplankton density (cells l^{-1}), *Chl-a* is the concentration of chlorophyll a ($\mu g\ l^{-1}$), and t is the number of days elapsed since 1 April 1983 (Naganuma and Seki, 1985: Figure 23).

The chlorophyll fluctuated seasonally without a time lag behind the water temperature ($T = 9.0 \sin[2\pi(t\text{-}41)/366] + 288$, where T is the water temperature (K); Naganuma and Seki, 1985). However, the bacterioplankton density fluctuated with a time lag of about 4 months behind the water temperature.

At the second stage of limnological succession, a bog has littoral vegetation on most shorelines, and the vegetation starts to expand towards the bog center. In Matsumi-ike Bog of this stage (e.g., 1988-1989; Miyamoto and Seki, 1992), the water column was reduced to a depth between 30 and 60 cm because of the ooze sedimentation with debris originated from the dead emergent plants of a cattail (*Typha latifolia*). The seasonal fluctuation of phytoplankton density was characterized by two phytoplankton blooms; one during spring and the other during autumn. During winter the chlorophyll concentration at the second stage was higher than that of the other stages of limnological succession. The pattern of annual fluctuation of chlorophyll concentration showed no similarity with that of the water temperature:

$$Chl\text{-}a = 2.2 \sin[2\pi(t+18)/365] + 23$$

$(F = 0.730,\ F_{0.05[1,46]} = 4.05)$

where t is the number of days elapsed since 1 April 1988 (Miyamoto and Seki, 1992: Figure 23).

The annual fluctuation of bacterioplankton at the second stage showed transitional characteristics of the limnological succession from a stable system of the first stage to the next stage stable system. The bacterioplankton at this stage fluctuated between the population densities of 10^9 and 10^{12} cells l^{-1} with greater amplitude and period than those of the other stages. It multiplied remarkably up to such a high density as about 10^{12} cells l^{-1} during summer. Such unstable fluctuation of the bacterioplankton density must induce instability of the trophodynamics of bog ecosystem.

At the third stage; i.e., the final stage of limnological succession, the bog has littoral vegetation throughout the whole bog basin. At this stage, Matsumi-ike Bog (e.g., 1991-1992) was less than 50 cm deep, because of accelerated sedimentation of ooze by withering of emergent plants. The emergent plants, covering whole bog basin during the period from spring to autumn, fell down into the water column during winter. The phytoplankton biomass increased from winter to summer, and decreased from summer to winter. The bacterioplankton increased from winter to summer, and decreased from summer to winter with the annual fluctuation of a small amplitude between 10^8 and 10^9 cells l^{-1}. Annual fluctuations could be regressed as high significant regressions as:

$$Bac = 7.3 \times 10^8 \sin[2\pi(t\text{-}17)/366] + 1.9 \times 10^9$$

$$(F = 22.9,\ F_{0.01[1,48]} = 7.19),$$

$$Chl\text{-}a = 18 \sin[2\pi(t\text{-}19)/366] + 22$$

$(F = 12.3,\ F_{0.01[1,49]} = 7.18)$,

where t is the number of days elapsed since 1 April 1991 (Figure 23).

Bacterioplankton growth during 1991-1992

The seasonal fluctuation of bacterioplankton growth rate showed a pattern as high from spring to summer and low from autumn to winter (Figure 24). The highest growth rate was 0.181 hr^{-1} (generation time of 3.8 hr) on 12 June 1991, and the growth rates were occasionally negative in autumn.

The function of environmental factors on the growth rate of bacterioplankton throughout the year was analyzed based on the theories of Liebig (1840), Blackman (1905) and Ohle (1965). For this analysis, the relationship between the growth rate of bacterioplankton and temperature was examined using the equation of Arrhenius (Johnson et al., 1954), and the relationship between the bacterial growth rate and the concentrations of DOC or inorganic nutrients (nitrate, nitrite, ammonium, TIN and phosphate) was examined using the equation of Monod (1949).

The effect of temperature on the bacterial growth rate could be expressed as a highly significant regression:

$$\log R = -1350\ T^{-1} + 3.52$$

$$(F = 24.6,\ F_{0.01[1,44]} = 7.25)$$

where T is absolute temperature of the bog water (Figure 25).

The effect of nutrients was not primarily important as; phosphate ($F = 7.88$, $F_{0.01[1,47]} = 7.21$); DOC ($F = 3.92$, $F_{0.05[1.48]} = 4.04$); nitrite ($F = 2.91$, $F_{0.05[1,47]} = 4.05$); nitrate ($F = 1.95$,

$F_{0.05[1,48]}$ = 4.04); ammonium (F = 1.40, $F_{0.05[1,43]}$ = 4.07); TIN (F = 0.189, $F_{0.05[1,42]}$ = 4.07). Therefore, the temperature was shown to be the limiting factor for the growth rate of bacterioplankton.

In order to analyze the nutrient effect on the bacterial growth, the growth rate (R) was substituted with the standardized growth rate (R') at 20°C to eliminate temperature effect by the following formula, $R' = R_{20}\ \alpha^{-1}\ R$, where R_{20} and α are the growth rate at 20°C and the calculated rate at the *in situ* temperature, respectively (Shiraishi et al., 1985).

From spring to autumn, the phytoplankton biomass was the predominant organic nutrient source because the cattail kept growing and standing above the bog water column. During winter, on the other hand, the phytoplankton biomass was small, and the withered cattail became the primarily organic nutrient source in the water column. Hence, I should distinguish two periods in a year based on the supply of organic nutrients for bacterioplankton nutrient, i.e., (I) Period while the nutrients were phytoplankton originated debris and (II) Period while the nutrients were debris originating from emergent plants.

Period I: 19 April 1991 - 12 November 1991

This period was initiated by the nutrient supply from the spring phytoplankton bloom and was terminated by the break down of withered emergent plants in the water column. There was a greater amount of phytoplankton in the water column during this period than the other period (the average chlorophyll-a concentration was 29.5 $\mu g\ l^{-1}$).

The effect of DOC concentration as the nutrient source for bacterioplankton was primarily significant and could be expressed as a highly significant regression:

$$R' = 0.089(d\text{-}0.0096)\exp[1\text{-}0.83(d\text{-}0.0096)]$$

$$(F = 8.67,\ F_{0.01[1,28]} = 7.64)$$

where d is the DOC concentration (mg C l^{-1}) in the bog water (Figure 26).

The relationship between the bacterial growth rate and the concentration of inorganic nutrients (nitrate, nitrite, ammonium, TIN and phosphate) were also analyzed, and it was shown that phosphate had the second most profound effect among nutrients on the growth rate of bacterioplankton as follows:

$$R' = 0.074(p\text{-}0.050)\exp[1\text{-}0.61(p\text{-}0.050)]$$

$$(F = 6.20,\ F_{0.025[1,27]} = 5.63)$$

where p (μg atom l^{-1}) is the phosphate concentration (Figure 26). The statistical significance of the effect of other nutrients on the bacterial growth were; nitrite ($F = 1.70$, $F_{0.05[1,28]} = 4.20$), ammonium ($F = 1.24$, $F_{0.05[1,25]} = 4.24$), TIN ($F = 0.0660$, $F_{0.05[1,25]} = 4.24$), and nitrate ($F = 0.0320$, $F_{0.05[1,28]} = 4.20$), in that order.

Period II: 5 April 1991 - 12 April 1991, 19 November 1991 - 23 March 1992

This period was characterized by the organic nutrient supply primarily from the withered cattail falling into the water column. The period was terminated at the spring phytoplankton bloom in the next year. There was small phytoplankton biomass at less than half the level during Period I (the average chlorophyll-a concentration was 12.1 μg l^{-1}).

The effect of DOC concentration as an organic energy source on the growth rate of bacterioplankton could not be expressed as a significant regression, so that DOC did not primarily affect the bacterial growth. The best regression curve was as follows:

$$R' = 0.048d\exp[1\text{-}0.83d]$$

$$(F = 0.81,\ F_{0.05[1,18]} = 4.35)$$

where d is the DOC concentration (mg C l^{-1}) in the bog water (Figure 27).

When the effect of other nutrients (nitrate, nitrite, ammonium, TIN and phosphate) on the bacterial growth was analyzed using the equation of Monod (1949), phosphate was shown to have the primary effect on the growth rate of bacterioplankton among all nutrients. The relationship between the bacterial growth and the phosphate concentration was highly significant as follows:

$$R' = 0.048(p\text{-}0.32)\exp[1\text{-}0.76(p\text{-}0.32)]$$

$$(F = 20.5,\ F_{0.01[1,18]} = 8.29)$$

where p (μg atom l^{-1}) is the phosphate concentration (Figure 27). The statistical significance of the effect of other nutrients on the bacterial growth were; nitrate ($F = 5.56$, $F_{0.05[1,18]} = 4.41$), TIN ($F = 1.95$, $F_{0.05[1,15]} = 4.54$), ammonium ($F = 0.493$, $F_{0.05[1,16]} = 4.49$), and nitrite ($F = 0.116$, $F_{0.05[1,17]} = 4.45$), in that order.

Attached bacteria

Monthly change of vertical profiles of attached bacteria on the glass slide submerged for 24 hours is shown in Figure 28. The dominant epibacterial forms in Matsumi-ike Bog were rods or bacilli in the water column and at the boundary (same as Batomalaque et al., 1992), but they were cocci in the sediment ooze. At the bottom boundary layer, the density of attached bacteria was always higher than other locations (in the water column and in the sediment ooze) at Matsumi-ike Bog throughout the year. There was usually very low

bacterial density in the sediment ooze deeper than 10 mm below the boundary, and every volume of the attached bacteria in the sediment ooze was smaller than that of other locations. In the water column, the density of attached bacteria was uniform throughout glass slide, but it showed high value at a particular area where the slide was evidently coated with the mucus of other organisms (*Euconjugatineae spirogyra* in spring, *Tubificina* from spring to summer).

In the water column and at the boundary, seasonal fluctuations of the epibacterial density were observed; the maximum bacterial density was maintained during the period from April to May, and it gradually decreased toward summer. The low density was common during the period from autumn to winter, with the minimum density in October or November. The bacterial density increased gradually during the period from December to March (Figure 28).

In the water column, seasonal fluctuations were obvious in the attachment and detachment rates of the epibacterial community onto glass slides submerged in Matsumi-ike Bog (Figure 29); showing their peaks in early summer, late summer, and winter. These two rates fluctuated almost simultaneously throughout the year. The maximum rates of attachment and detachment were 7.8×10^2 cells mm^{-2} hr^{-1} (January) and 0.317 hr^{-1} (January), respectively. The growth rate of epibacterial population showed the maximum in December (0.075 hr^{-1}), but the annual average of growth rate was lower than that of bacterioplankton in the water column (Naganuma and Seki, 1985; Miyamoto and Seki, 1992).

The rates of attachment and detachment at the bottom boundary showed the same seasonal fluctuation as that in the water column (Figure 29); their peaks were observed in early summer, late summer, and winter. The maximum rates of attachment and detachment

were 10×10^2 cells mm^{-2} hr^{-1} (May) and 0.285 hr^{-1} (May), respectively. The maximum growth rate of the epibacterial population was observed in May as 0.041 hr^{-1}.

In the sediment ooze, the fluctuation range of attachment rate was about one order magnitude lower than that of other two location observed (Figure 29). The maximum rates of attachment and detachment were 2.9×10^2 cells mm^{-2} hr^{-1} (September) and 0.822 hr^{-1} (May), respectively. The maximum growth rate of the epibacterial population was observed in May as 0.235 hr^{-1}.

2.4. Discussion

2.4.1. DOM and acid extract of POM in the bog

The optical density spectrum of DOM was dependent on the wavelength λ as λ^{-4}, rather than the exponential dependency reported for yellow substances (e.g., Bricaud et al., 1981). This spectrum dependency indicates that the optical density is based primarily on scattering by dissolved molecules, since intensity of Rayleigh scattering by molecules varies with λ^{-4} in the wavelength (e.g., Jenkins and White, 1981). Hence, DOM of the bog water seems to be composed mostly of small organic molecules without complex structures such as aromatic rings containing nitrogen. There were also small absorption maxima at wavelengths of 280 nm (peak) and 320 nm (shoulder). The intensities of these small absorption peaks were on the order of one tenth of that of scattering. The absorption at 280 nm suggests the existence of aromatic compounds such as phenol, benzene or amino acids. Those absorption maxima have been shown to correspond to peaks in excitation spectra of fluorescence of acidified sea water from different depths (Coble et al., 1990). This spectral similarity suggests chemical similarity of dissolved organic matter in the bog and the sea water.

As the optical density (OD) of sea water at the wavelengths of 280 nm linearly depends on dissolved organic carbon for estuary samples (e.g., Krom and Sholkovitz, 1977; Naganuma and Seki, 1993), the OD was shown to be dependent linearly on the DOC of the bog water. The dependency was constant throughout years. It indicates that the composition of DOM varies only in the optically undetectable range.

The optical spectrum of the POM acid extract shows specific absorption at wavelength of 220 nm and 335 nm. These absorption maxima were not found in the supernatant of acid extractions at pH 3 or above. These absorption peaks belong to the flocculates and precipitates for water samples with higher pH treatment, as confirmed by spectrometry of the re-solubilized sample of these flocculates. The absorption spectrum of acid extraction corresponds to basic substances that flocculate at pH 3 or above. These substances would be solubilized not only by protonation but also by possible hydrolysis and fragmentation during acid treatment. In natural waters with pH higher than 3, these substances could exist as suspended particles since these substances would be deprotonated and exist as larger molecular without the possible fragmentation by the acid treatment.

Although the optical absorption of acid extracts at 280 nm (A_{280}) and 335 nm (A_{335}) was proportional to each other, the ratio A_{280}/A_{335} varied with the N/C ratio of POM and of the chlorophyll fraction in POC. A correlation between A_{280}/A_{335} and the N/C ratio was observed for values of $A_{280}/A_{335} > 0.7$ and N/C > 0.14 (C/N < 7), indicating that the A_{280} component corresponds to the nitrogen-rich fraction of POM. It could be reasoned that the A_{280} component corresponds to amino acids, protein or nucleic acid. Three amino acids and protein show optical absorption maxima at 280 nm and their N/C ratio range from 0.1 to 0.5. Nucleic acids show optical absorption at 260 nm and their N/C ratio ranges from 0.2 to 0.6. The A_{280}/A_{335} ratio correlates with the composition of particulate organic substances.

The slopes of regression in POC vs chlorophyll plot were different for different A_{280}/A_{335} ratios. These slopes indicate ratio of chlorophyll fraction in POC. Hence, the A_{280}/A_{335} ratio indicates chlorophyll fraction in POC: The higher A_{280}/A_{335} ratio indicates the

greater chlorophyll fraction in POC. The absorption bands at 220 nm and 335 nm correspond to the non-chlorophyll fraction of particulate organic substances. Since phytoplankton and littoral vegetations are two dominant sources of POC in the bog, the A_{280}/A_{335} ratio also indicates the contribution from these sources to POC.

The A_{280}/A_{335} ratio showed a minimum during autumn. During this season, the littoral vegetations are under gradual degradation. Therefore, the optical absorptions at wavelength of 220 nm and 335 nm should correspond to the microbial degradation products of littoral vegetations. The basic nature of the absorption component (or flocculate) and dependency on N/C ratio suggest the incorporation of disintegration products from dead plants into microbial cell components such as peptide glycans or the direct release of alkaloids from littoral vegetations. The C/N ratio of decomposing phytoplankton (Otsuki and Hanya, 1967) which increased from 5 to 7 during progress of decomposition and sustained the ratio of 7 suggests the incorporation into microbial cell components.

2.4.2. Phytoplankton in the bog

At the final stage of limnological succession, the population density of every dominant phytoplankton showed seasonal sinusoidal fluctuation with therefrom small deviating pulses of various amplitudes and phases. As a rule, dynamics of the phytoplankton population should be governed primarily by biochemical reactions. Hence, in Matsumi-ike Bog, the dynamics were regulated primarily by temperature, with the secondary modification by the nutrient factor.

During the third stage, the phytoplankton dynamics became stable as exclusively controlled by the water temperature. Seasonal vicissitude of dominant phytoplankton was not apparent, although predominancy alternated among several dominant phytoplankton species. The earliest appearance among them in the year was *Chroococcus*, that fluctuated prior to the temperature fluctuation. Since the temperature phase was behind that of solar radiation with the lag of 30 days, and the phase of *Chroococcus* dynamics was behind that of solar radiation with the lag of only 0.4 days. Hence, *Chroococcus* is apparently regulated by solar radiation rather than the water temperature. The population density of *Scenedesmus*, *Melosira*, *Chlamydomonas* and *Navicula*, on the other hand, fluctuated with the time lag of 4.3, 12.8, 20.2 and 26.4 days, respectively, behind the temperature fluctuation. The time lag of the fluctuation phase of total phytoplankton was 11.6 days behind water temperature, which corresponded to the lag of the predominant phytoplankton, *Chlamydomonas*.

The seasonal alternation of dominant genera during the third stage, *Chlamydomonas* was predominant among the phytoplankton of chlorophyll-b group. During the transitional period to the most matured stage of Matsumi-ike Bog from 1991 to 1992, *Chlamydomonas* was predominant among all phytoplankton throughout the year. During this period *Navicula* took over the predominancy of *Melosira* among the chlorophyll-c group according to the progress of seasons.

The periods with small IPI were commonly observed in the chlorophyll fluctuations; Periods II, IV, VI and VIII for chlorophyll-a, Periods II and IV for chlorophyll-b and IV for chlorophyll-c. The quick alternation in these fluctuations could not be explained only by temperature, because of its quickness is more than that explained by Q_{10}.

The minima and maxima of the *Melosira* pulse resembled that of *Chroococcus*, though they showed different thermal responses. This similarity among *Melosira* and *Chroococcus* could be caused by efficient nutrient uptake orientated to the oligotrophic conditions, thereby both could co-exist in the mesotrophic conditions of Matsumi-ike Bog. The same profile was shown among *Navicula* and *Scenedesmus*, suggesting co-existence by the same mechanism. Among all inorganic nutrients, the nitrate concentration showed negative correlation to the phytoplankton dynamics, even if nitrate was not the limiting factor. All these nutrients showed only a minor effect on phytoplankton in any period.

The emergent vegetation affected the population density of phytoplankton community by shading the solar radiation. The amplitude of *Chroococcus* dynamics increased with the light transmittance, as was observed for *Chroococcus*. The base-line of population dynamics of both *Navicula* and *Melosira* lowered significantly by the decrease of light transmittance, showing the significant response of chlorophyll-c group to the change of the light spectra.

2.4.3. Bacterioplankton in the bog

The growth rate of the bacterioplankton at the third stage was shown to be controlled by the water temperature as the limiting factor. The growth of bacterioplankton was controlled secondly by nutrients during each period. During Period I, it was the DOC originating from phytoplankton that was the organic nutrient source for bacterioplankton. Thereby the DOC contained all essential elements. Hence, the DOC had the major effect on the growth rate of bacterioplankton during Period I.

At Period II, on the other hand, phosphate was the main determining factor on the growth rate of bacterioplankton. There were excess amounts of organic C and H but limiting amounts of P in the organic debris originating from the withered emergent plants. Thus these organic matter during Period II were not the complete organic nutrients used for the bacterial growth. The bacterioplankton must have found supplemental elements from the inorganic nutrients in the bog water for their growth.

2.4.4. Attached bacteria in the bog

During the study period, the size of the attached bacteria in the water column and at the bottom boundary were always larger than that of bacterioplankton in the water column. Bacterioplankton increased during the period from winter to summer, and decreased during another period from summer to winter with the annual fluctuation of a small amplitude between 10^8 and 10^9 cells l^{-1}, having small and almost constant volumes. The average growth rate of attached bacteria was lower than that of bacterioplankton in the water column and at the bottom boundary. It has been reported that almost all of the attached bacteria were derived from bacterioplankton (Kang and Seki, 1983; Batomalaque et al., 1992; Costerton and Lewandowski, 1995), these results indicate that each attached bacterium utilized its increased cell material to make their larger cell volume rather than to divide into two cells.

A higher density of the attached bacteria occurred on a biofilm which had a coat of extracellular mucus from plant or animals on the glass slide. Microbial growth on the biofilm contributed to the deposition and promotion of more adherence of inorganic and organic suspended solids from the water column onto the biofilm. The biofilms with greater amount

of the inorganic and organic nutrients promote the availability of nutrients for microbial growth on the biofilm (Batomalaque et al., 1992). At the boundary between the water column and the sediment ooze, the greater accumulation of organic matter must have occurred on the submerged glass slide, because the highest density of attached bacteria was observed at the bottom boundary layer throughout the year.

While the period of high epibacterial density, i.e., from spring to early summer, the withered cattail was still the primary source of POM and DOM (dissolved organic matter) in the water column. There were excess amounts of organic C and H with a shortage of other nutrient elements in the organic debris originating from the withered cattails. Thus these organic matter were not complete organic nutrients for the bacterial growth. The bacterial community in the water column must have found supplementary elements from the inorganic nutrients in the bog water for their growth. This was the main reason why a high density of the attached bacteria was observed in the water column and at the boundary during this period.

During summer, the density of attached bacteria gradually decreased when the main organic matter source changed from the withered cattail to the phytoplankton. The POM and DOM originating from phytoplankton were complete organic nutrients for the bacterial growth. Thereby, there was no need to attach onto a solid surface for getting nutrients efficiently from the interface. Hence, the rates of attachment and detachment in the water column and at the boundary were high, as was favoured by higher water temperature and greater supply of organic matter.

During the period from autumn to early winter, the density of attached bacteria was the minimum for the year, because the supply of organic nutrients from phytoplankton and the nutrient concentration in the water was minimal during this period. When the new supply of dead cattail in the water column started in December or January, the rate of bacterial attachment increased again in the water column and at the bottom boundary. The density of attached bacteria in the water column (including the boundary) increased gradually toward spring.

Chapter 3

METHANE OXIDATION IN THE LAKE WATER

3.1. Introduction

Methane is the most stable carbon compound in anaerobic environments and is a very important intermediate in reactions that eventually lead to organic matter remineralization (Dagley, 1978). In addition, methane is one of the most important atmospheric trace gases involved in global warming because of its strong radiative forcing and rapid tropospheric increase since the Industrial Revolution. During the 1980s, methane increased in the atmosphere at a rate of about 0.8% $year^{-1}$ (IPCC, 1994). The release of methane to the atmosphere results in an increased rate of global warming (Ehalt, 1974; Ehalt and Schmidt, 1978; Lelieveld et al., 1993).

Methane escapes from anaerobic environments to the atmosphere when it is not oxidized by methanotrophs. The oxidation of methane is now known to occur in both aerobic and anaerobic environments (Rudd and Taylor, 1980; Higgins et al., 1981; Hanson and Hanson, 1996). Previous study has suggested that terrestrial environments (freshwater wetlands, lakes, rivers, rice paddies and enteric fermentation) are much more important as sources of methane to the atmosphere than are marine environments (cf. Cicerone and Oremland, 1988). In contrast to our knowledge of methane production in freshwater, information on methane oxidation in such environments is limited. The distribution of methane oxidation activity has been studied in several eutrophic lakes (e.g., Jannasch, 1975; Rudd et al., 1974; Rudd and Hamilton, 1978; Harrits and Hanson, 1980; Iversen et al., 1987), but most previous studies in lakes have been done at locations with permanently or seasonally anoxic hypolimnia, and the

studies on methane oxidation in the water column have concentrated mainly on oxic-anoxic interfaces.

Aerobic methane oxidation is often at a maximum where methane and oxygen coexist in the oxic/anoxic transition zone, and it is thought this serves to remove most of the methane diffusing from deep anoxic layers before it is transported to the atmosphere (e.g., Rudd and Hamilton, 1975; Ward et al., 1987). If the lake has an anoxic hypolimnion, methane produced in the anoxic sediment diffuses directly into the anoxic hypolimnion without aerobic methane oxidation. It is then consumed by methanotrophs at the oxic-anoxic interface in the water column (Jannasch, 1975; Rudd and Hamilton, 1975; Harrits and Hanson, 1980; Scranton et al., 1993). On the other hand, if the lake does not have an anoxic hypolimnion, methane diffuses into oxic surface sediment, and is partially consumed by methanotrophs in the sediment (Kuivila et al., 1988; Frenzel et al., 1990; King et al., 1990). Only the residual portion of methane, then, can diffuse into the oxic hypolimnion. Because much attention has not been directed to methanotrophs in the oxic water column, the knowledge about this type of pass way in methane consumption is still very poor.

The observations of methane oxidation are rare in winter, when lake overturn is driven by cooling in cold climates. The lack of precise studies of the dynamics of methane and methane oxidation rates in lakes during the overturn period leads to uncertainty in estimates of methane budgets for fresh water lakes. I present the results of a survey of methane concentrations and methane oxidation rates in Lake Nojiri, a dimictic and mesotrophic lake in Japan. I have evaluated the relative importance of diffusive flux across the air-water interface versus methane oxidation in the lake during the overturn period.

In the case of large, shallow lakes, anaerobic bottom water is rarely observed because of wind-driven water mixing throughout the year. Although this type of lake is common, methane cycling in such environments has not been studied. I present the results of surveys of methane oxidation activity in the water column of Lake Kasumigaura, a eutrophic, shallow lake in Japan. Along with long term observation of methane concentrations in the lake (Nakamura et al., submitted), I investigated various processes related to methane production, transport and consumption in the lake. Measured methane oxidation rates were used to identify the factors controlling methane turnover in the water column. Finally, I evaluated the relative importance of a diffusive flux across the air-water interface versus methane oxidation in the lake.

3.2. Materials and Methods

3.2.1. Study site

Lake Nojiri

Lake Nojiri (Figure 30 and Table 1) is located in central Japan (36°49'N, 138°13'E; 645 m above sea level). It is a mesotrophic, dimictic freshwater lake, 4.4 km^2 in area, with a maximum depth of 38.5 m. This is a dammed lake formed by the debris ejected from the volcano Mt. Kurohime located to the west of the lake. The lake has no large inflowing stream, lake water flows out through the R. Ikejiri, which has been a source of irrigation water since the 17th century. Aside from water supply, fishery and recreation, power generation are also an important use of the lake water. The fossils of Naumann elephant, known to have lived some 20,000 years ago, are excavated frequently from the lake's shallow bottom. The residence time of water is estimated to be 2.0 years. Stratification begins in April or May and continues into December. In winter, the lake surface did not completely freeze for the previous ten years, but did freeze in the winter of 1995-1996.

Lake Kasumigaura

Lake Kasumigaura (Figure 31 and Table 2) is the second largest lake (surface area, 168 km^2) of Japan located about 60 km northeast of Tokyo (35°52'-36°09'N, 140°38'E). The lake has 2 large bays, which are called Takahamairi and Tsuchiurairi. The lake basin is smooth and shallow, with a surface area of 168 km^{-2}, a mean depth is 4.0 m and maximum depth of only 7.4 m near the mouth of Takahamairi Bay. Mean water renewal rate is 0.6 year (Otsuki

et al., 1993). The level of lake water surface is only 1 m above the sea level and the level of lake is controlled to within ± 0.5 m.

Water temperature at the lake center, which is approximated as a sinewave from January, was the lowest at 2 to 5 °C in February and the highest at 26 to 32 °C in August. Differences in water temperature between the surface and bottom are minimal (less than 2°C, except for a few calm days in summer) because winds are usually sufficient to cause daily turnover. Consequently, the lake water is always well oxygenated. The pH of the surface layer was 7.2-8.2 in winter and 8.4-9.8 in summer. Secchi disk transparency at Station 1, (most eutrophic by inflow of polluted rivers) was 0.2-1.0 m and that at Station 9 was 0.8-3.0 m throughout the years. Heavy blooms of *Microcystis* were observed every summer from the early 1970s to 1986 (e.g., Takamura et al., 1985). They suddenly disappeared in 1987 and have not been observed since then. Instead, *Planktothrix* (*Oscillatoria*) *agardhii* has tended to occur abundantly in summer and autumn (e.g., Takamura et al., 1992).

Eutrophication of the lake has created problems in the utilization of lake water by municipal waterworks. The National Institute for Environmental Studies has conducted monthly samplings of Lake Kasumigaura since April 1977 without interruption; physical, chemical and biological parameters including nutrients, primary production and phytoplankton species composition have been measured (e.g., Takamura et al. 1992).

3.2.2. Sampling

Analysis of dissolved methane concentration

The dissolved methane concentration was measured with an automatic system consisting of a purge and trap apparatus and a gas chromatograph with a flame ionization detector (GC-FID) as shown in Figure 32 (Nojiri, 1991; Nakamura et al., 1994). The operating conditions of this analytical system are shown in Table 3. With this system, automatic analysis of one sample bottle takes about 34 minutes. A standard gas mixture of methane and air was used for calibration with correlation of gas volume in the GC sampling loop by temperature. Analytical precision, expressed as the coefficient of variation for repeated measurements of standards and lake water samples, was 0.2% or 0.6% respectively.

Lake Nojiri

From May to December in 1992, It was conducted an ecological time series study with water samples collected monthly at a station (Sta. 1) near the center of Lake Nojiri (Figure 30), mainly from the epilimnion. Samples were also collected in the winters from December 1993 to January 1994, and from December 1994 to January 1995 at Station 53, the deepest point in the lake. The position of the boat on station for every sampling time in 1993 and later was confirmed with a Global Positioning System (GPS; Panasonic, KX-G 5500). Additional samplings were performed to reveal horizontal distribution. Maximum addition was 6 stations and minimum was 1 station from the points indicated in Figure 30.

Water samples were collected from different depths with Go-Flo samplers (Figure 33). Samples were drawn from the sampler into 50 ml glass bottles allowing several bottle volumes to overflow. Samples were then immediately poisoned with 0.5 ml of a 3.5% $HgCl_2$ solution. Each bottle was capped immediately with an isoprene rubber stopper, which had been pierced

with a hypodermic needle to ensure that all entrapped air bubbles were displaced as the stopper was seated. After the hypodermic needle was removed, the bottles were further sealed with an aluminum crip. Samples were transported back to the laboratory in a cool bag at 2°C, and stored in a refrigerator until analysis described below. Samples collected and stored in this manner showed no detectable change in methane concentration for at least several days.

Profiles of dissolved oxygen (DO) concentration and water temperature were determined with an oxygen/temperature meter (Yellow Springs Instruments Co., model 58) during every survey. Other water samples were also taken with the same Go-Flo sampler for dissolved nutrients (nitrate, nitrite, ammonium, phosphate, total phosphorus and total nitrogen) and pH. The pH was measured on the boat with a pH meter (Yokogawa Electric Co., model PH82) as soon as possible after collection. The nutrient concentrations were measured in the laboratory with a Technicon Autoanalyzer (AA2).

Methane oxidation measurement

During the 1994-1995 winter sampling, specific methane oxidation rates were measured by incubating Station 53 water from 0.5, 20 and 36 m depths (Figure 33). For each depth, 10 to 12 replicate 50 ml glass bottles were used. These glass bottles had been soaked in 3 N HNO_3, to avoid contamination by metallic elements, washed with distilled water and then sterilized. The water samples from each depth were collected with Go-Flo samplers and immediately transferred to the incubation bottles. Bottles were overflowed with several volumes of water and sealed with no headspace. This procedure prevents the contamination

of anaerobic deep water samples with oxygen. After sealing, incubations were started as soon as possible at *in situ* water temperature in the dark. Methane oxidation was determined at three or four different time points ranging from 3 to 24 hours after the start of incubations. At the end of each incubation period, 2 bottles were sacrificed and methane oxidation was stopped by addition of $HgCl_2$. Controls consisted of samples to which $HgCl_2$ was added immediately after bottling. The concentrations of dissolved methane after mercury poisoning were measured as described above. The calculation method of specific methane oxidation rate also describes below (see "Methane oxidation measurement" in Lake Kasumigaura).

Lake Kasumigaura

Methane oxidation rate measurement

Methane oxidation rates were measured at 2 stations, Station 3 in Takahamairi Bay and Station 9 in the lake's center (Figure 31). The depths of Station 3 and Station 9 are 3.7 m and 5.8 m, respectively. Water samples for methane oxidation measurements were taken at about 0.5 m depth with 10 l Go-Flo sampler (Figure 33). Preliminary measurements of oxidation rate began in August 1990. From July 1991 to March 1996, measurements were taken at least monthly for both stations. For each station, ten to sixteen 50 ml glass serum bottles were used for measuring methane oxidation rate. These glass bottles had been soaked in 3 N HNO_3, to avoid contamination by metals, thoroughly washed with distilled water and then sterilized. The water samples were immediately transferred to the incubation bottles on board. Bottles were slowly overflowed with several volumes of water and sealed with no headspace. Each glass bottle was stoppered with an isoprene rubber septum and sealed with

an aluminium crimp seal. After sealing, incubations were started on board at *in situ* water temperature in the dark. Because neither dilution nor addition of any nutrients was done, there was no reason to expect any time lag in the activity of the enclosed bacterial populations. The rates observed at the beginning of the incubation period could therefore be expected to mimic those occurring naturally.

Methane oxidation was determined at 3 or 4 different time points, ranging from 2 to 24 hours after the start of incubation. At each point, 2 bottles were sacrificed and methane oxidation was stopped by addition of 0.5 ml of 3.5% $HgCl_2$ solution, which completely inhibited methane consumption in the bottle. Controls consisted of samples to which $HgCl_2$ was added immediately after bottling on board. The concentrations of dissolved methane after mercury poisoning were measured as described above.

The specific rate of methane oxidation was calculated by linear regression of the natural log of methane concentration against time; the specific rate of methane oxidation is equivalent to the slope in such a regression line. Only samples in the period when the methane decrease was linear were used to determine methane oxidation rates. The specific oxidation rate is the first order rate constant for methane oxidation (in units of hr^{-1}). This rate is useful for comparing relative methane oxidation activities among samples with large differences in methane concentration because it is independent of methane concentration. The turnover time for methane is the inverse of the specific oxidation rate. Actual rates of methane oxidation (methane consumption rate; in units of nM CH_4 hr^{-1}) can be calculated by multiplying the specific oxidation rate at any station by the measured ambient methane concentration.

Other environmental factors measurement

. Water samples for dissolved methane analysis were also collected with a Go-Flo sampler from 7 stations in Lake Kasumigaura, and variations in dissolved methane concentrations within the lake have been reported elsewhere (Nakamura et al., submitted). The method for sampling of lake water is described above (see 3.2.2. Sampling "Lake Nojiri").

Profiles of dissolved oxygen (DO) concentration and water temperature were measured by oxygen temperature sensor at every survey. Other water samples were taken with an acrylic tube column sampler of 2 m long or a Go-Flo sampler, for dissolved nutrients (nitrate, nitrite, ammonium, dissolved total nitrogen, total nitrogen phosphate, dissolved total phosphorus and total phosphorus) (e.g., Otsuki et al., 1993). The nutrients concentrations were measured at laboratory by a Technicon Autoanalyzer (AA2).

3.3. Results

3.3.1. Lake Nojiri

Monthly sampling in 1992

The position of the boat during sampling in 1992 varied slightly since GPS had not been available to us at that time. The deepest sample was collected just above the bottom at the station. The methane maximum (97 nM), observed more distinctly at other times at about 10 m depth, was not obvious in June (Figure 34). Also, the range of concentrations with depth in June was smaller than that observed in other months (Figure 34). By August, a significant sub-surface methane maximum (290 nM) at 7.5 m depth had accumulated, and a rapid concentration decline with depth was observed. The depth and concentration of the sub-surface methane maximum were shallower and higher than those in June. The surface methane concentration in August was 3 times that measured in June. By October, the sub-surface methane maximum had deepened to 15 m, and its concentration had declined to 150 nM. Also, the surface methane concentration had decreased to 94 nM. The concentration of methane at the near-bottom depth was a minimum in late autumn. Methane accumulation in the bottom layer below 30 m had never been observed in July (data not shown) but had started by August.

A weak sub-surface methane maximum was already present in May at 15 m depth (Figure 35). The methane concentration in the sub-surface maximum increased with time, peaking in August. The sub-surface maximum shoaled with time, reaching its shallowest in July and August. The surface methane concentration increased from May to August roughly

in proportion to the increases in the sub-surface methane maximum concentration. After August, the sub-surface maximum weakened and descended, disappearing altogether by November. The decrease in surface and sub-surface methane concentrations during the period can be explained by surface water cooling and deepening of the surface mixed layer. By the middle of December (21 Dec. 1992), when lake overturn had begun, the surface methane concentration had increased to a level higher than that of the summer maximum.

This increase in surface methane concentration may result in an unexpectedly large flux from the lake. It was carried out frequent measurements during the overturn periods of the following two winters to correctly estimate winter methane fluxes.

1993-1994 winter sampling

On 4 December, just before overturn, the surface water temperature was 9.1°C and a thermocline was observed around 20 m (Figure 36a). At that time, the epilimnion methane concentration was uniform (about 70 nM; Figure 36c) and supersaturated relative to methane in the atmosphere (1.7 ppmv; equivalent to 3.6 nM at that water temperature (Yamamoto et al., 1976)). Below 20 m, the depth of the oxycline, methane decreased to about 25 nM and DO (Figure 36b) decreased with depth to 35 m, where the observed concentration was close to the limit of detection. A great deal of dissolved methane accumulated in the waters below 30 m, reaching a maximum concentration of 1.93×10^4 nM at 37 m depth. The concentration of methane in the anoxic layer below 35 m depth was higher than that in the microaerobic waters above that depth.

By 22 December, the surface water temperature had declined to 6.5° C and the thermocline had disappeared (Figure 36a). The distribution of DO was uniform (8.6 mg O_2 l^{-1}) to 30 m, however, the anoxic layer still remained below 35 m (Figure 36b). The mixing of the oxygen depleted bottom water with the aerobic surface water decreased the surface DO concentration. The supply of oxygen to the deep oxygen depleted layer increased the DO content of the waters between 30 and 35 m depth. These profiles reflect the progression of water circulation from the surface to 30 m by that time. The methane concentration of the surface mixed layer increased to 360 nM, 5-fold higher than the level before overturn, but the hypolimnetic concentration decreased significantly. The large increase in surface methane was supplied by the mixing of a large amount of hypolimnetic methane into the epilimnion by water circulation. With the completion of lake overturn by 6 January 1994, the distributions of water temperature (5.0° C), DO (9.5 mg O_2 l^{-1}) and methane concentration (150 nM) were completely homogeneous from the surface to the bottom (Figure 36).

On 26 January, a weak inverse stratification was observed (Figure 36a) and the DO concentration had increased to 11.0 mg O_2 l^{-1}. The methane concentration was 110 nM near the surface, and increased with depth, reaching 217 nM at 35 m. This concentration gradient indicates that the bottom sediments were a source of methane to the water column during this period. The methane which had accumulated in the hypolimnion, was mixed into the whole water column quickly during overturn, and had disappeared completely within a month.

By the early March sampling (4 March 1994), the DO concentration had recovered to 12.0 mg O_2 l^{-1}, which is slightly lower than the saturation concentration (12.6 mg O_2 l^{-1}) for water at that temperature and standard air pressure at the altitude. The methane concentration

in the epilimnion was 120 nM, almost the same as that observed on 20 January. However methane increased in the hypolimnion; the maximum concentration (386 nM at 35 m) was 1.8 times higher than that measured on 20 January.

1994-1995 winter sampling

Profiles in the water column

The first winter survey was conducted on 10 December 1994, before the lake overturn period. A weak thermocline was observed at around 20 m (Figure 37a). The DO concentration was uniform to 15 m and then decreased gradually toward to the bottom (Figure 37b). However, oxygen depletion in the hypolimnion was not complete at that time. The methane profile (Figure 37c) from the surface to mid-depth was similar to that observed the previous year (4 Dec. 1993). However, about four times more methane had accumulated in the hypolimnion (>30 m depth; maximum concentration 6.98×10^4 nM at 36 m) than in the previous year.

Lake overturn started between 10 and 19 December and proceeded between 19 and 23 December, with the mixed layer deepening from about 25 to 35 m depth (Figure 37). The results of a strong mixing event due to effective surface cooling on the night of 19 December are reflected in the change in profiles collected on the preceding and following days. This process mixed a large amount of oxygen into the deep layer between 27 and 34 m. Simultaneously, the methane concentration gradient weakened as high methane water from between 27 and 34 m mixed with low methane water from shallower than 20 m. However, the DO and methane concentrations in the deepest samples, from 36 m, remained unchanged over

this one day period. With further mixing, the surface methane concentration increased from 152 nM (19 Dec.) to 329 nM (23 Dec.), the maximum surface concentration measured during this winter sampling campaign, while the hypolimnetic methane concentration maximum at 36 m decreased from 7.40×10^3 nM (19 Dec.) to 1.02×10^3 nM (23 Dec.).

The isothermal profile measured on 29 December suggests that the lake had by then completely mixed from surface to bottom. Surface cooling in excess of the subsequent 4°C decline in bottom temperatures resulted in the formation of a weak inverse thermocline between 3 and 20 January 1995. As the methane which had accumulated in the hypolimnion mixed upward into the upper water column, it began to disappear from the water column rapidly after 23 December. The water column methane distribution had approached uniformity by 29 December. The surface concentration of methane in the water column had decreased to 70 nM by 20 January 1995, the same surface methane concentration measured at the end of the stratified period on 10 Dec. 1994. Thus, the methane which had accumulated in the hypolimnion during the stratified period had been completely lost within a month of the onset of lake overturn.

Methane oxidation in the water column

On 10 December 1994, just before overturn, the specific methane oxidation rates were 0.0042, 0.0076 and 0.0118 hr^{-1}, corresponding to 0.32, 0.58 and 824 nM hr^{-1} at depths of 0.5, 20 and 36 m, respectively (Figure 38). The very high consumption rate measured at 36 m was mainly due to the high methane concentration at that depth.

On 19 December, I measured methane profiles, but not oxidation rates. On 20 December, after a strong mixing event had occurred during the previous night, the specific oxidation rate at 0.5 m had risen to 0.0087 hr^{-1} (twice as fast as that measured on 10 Dec.), but the rate at 20 m had declined slightly. The maximum specific rate measured during the entire sampling campaign was on 20 December at 36 m.

The specific rates at 0.5 and 20 m peaked on 23 December. By that time, the specific oxidation rate in the deep layer had already begun to decline with the deepening of the mixed layer. The methane consumption rate at 36 m had decreased markedly from the rate measured 3 days earlier due to the decreasing ambient methane concentration.

By 29 December when lake overturn was complete, methane oxidation activities had declined throughout the water column. Similar specific and absolute methane oxidation rates were observed at the three measured depths.

On 3 January 1995, specific methane oxidation rates were uniform throughout the water column and had not changed from those measured on 29 December 1994 (Figure 38a). Consumption rates, however, had decreased during this period, in parallel with the decline in methane concentrations in the water column (Figure 38b).

By 20 January, the specific and absolute methane oxidation rates in the water column had dropped to the lowest values measured. The rates at 36 m were somewhat higher than those measured at 0.5 and 20 m. This higher rate indicates supply of methane from the sediments to the water column which slightly elevates the methane concentration in the bottom water and produces the concentration gradient with depth. This methane supply may enhance

methane oxidation activity in the deep layer under the inverse stratification which followed lake overturn.

3.3.2. Lake Kasumigaura

Dissolved methane concentration

Seasonal changes of dissolved methane concentration in Lake Kasumigaura were measured monthly over a 6 year period from April 1990 to March 1996 to evaluate methane emissions to the atmosphere (Nakamura et al., submitted). Methane concentrations varied from 13.3 to 3,500 nM in the water column of the lake. The averaged and standard deviation was 248 ± 274 nM (n = 1010). The equilibrium methane concentration in water, with respect to an atmospheric methane concentration of 1.7 ppmv, is 2.2 nM at 30°C or 4.1 nM at 2°C (Wiesenburg and Guinasso, 1979). Hence the surface methane concentration in every Lake Kasumigaura sample was higher than the equilibrium concentration.

Whole lake averages of methane concentration were calculated with the morphological parameters of Lake Kasumigaura (Table 4). The boxes are separated by considering the geographical features and similarities in water quality (nutrients and salts). The average methane value for the whole lake during the 6 years of observations varied from 36.9 to 1,020 nM and the whole term average was 196 nM. There was a seasonal pattern; it was observed low concentrations from April to June, high concentrations from August to September, the minimum annual concentration in November or December, and relatively high concentrations in winter.

Methane oxidation in the oxic water column

In this study, I used a method for measuring methane oxidation rate different from radiotracer methods (e.g., Rudd et al., 1974; Harrits and Hanson, 1980; Griffiths et al., 1982; Ward et al., 1987; de Angelis and Scranton, 1993; Scranton et al., 1993). The method is an improvement on that of Jannasch (1975) or Sansone and Martens (1978) in that I measured methane oxidation rate by monitoring decreases in methane concentration with time for natural lake water samples incubated in glass bottles under near *in situ* conditions. Because of the high reproducibility of the GC-FID measurements with the purge and trap system, it was able to use short incubation periods with little consumption of dissolved methane, typically less than 20 to 30% of that initially present. These short incubation periods (maximum about a day, usually less than 10 hours) minimized both bottle effects and the change in methane and oxygen concentrations in the bottles during incubations. Using this method, it was thus possible to measure the rate close to the actual *in situ* methane oxidation activity in the water column without any extra operations or time lag.

The time course of dissolved methane concentration changes in the glass bottles (e.g., Figure 39) can be described as exponential decay. The relationship between the decrease in methane concentration and incubation time from 0 (start) to 9 hours can be expressed as a highly significant regression:

$$\ln(C) = -0.102t + 5.17 \qquad (n = 3,\ r^2 = 0.9997)$$

where C is methane concentration (nM) and t is time (hours) elapsed after the start of incubation. The relationship between dissolved methane concentration decrease and elapsed time was expressed with high linearity (Table 5). The specific methane oxidation rate can be

determined within a day of incubation. No time lag in methane oxidation activity of the bacterial populations (methanotrophs) was observed in any bottle samples at the start of incubation, so the calculated specific rate would be expected to mimic those occurring naturally in the lake water. Furthermore, dissolved methane concentration was never observed to increase in the bottles during any of my incubations. Thus, in the water column of Lake Kasumigaura, methane production might not occur because production of methane is strictly an anaerobic process (e.g., Rudd and Taylor, 1980; Daniels et al., 1984).

The measured specific oxidation rates in Lake Kasumigaura ranged from 0.0006 (10 February 1993; turnover time of 75 days) to 0.272 hr^{-1} (27 October 1992; turnover time of 3.7 hours) at Station 3 (Figure 40a), and from 0.0003 (8 June 1993; turnover time of 134 days) to 0.204 hr^{-1} (8 November 1995; turnover time of 4.9 hours) at Station 9 (Figure 40b). The dissolved methane depth profile was generally uniform (Nakamura et al., submitted), because of the lake's shallowness. Profiles of methane oxidation activity were correspondingly uniform, as confirmed by incubation of samples from several depths on several occasions.

Water column methane oxidation activity had not previously been reported in shallow and non-stratified lakes like Lake Kasumigaura. Most previous studies have been done in locations with permanently or seasonally anoxic hypolimnia, and studies on methane oxidation in the water column have concentrated mainly on oxic-anoxic interfaces. Here, I evaluated the seasonal change in methane oxidation activity in oxic lake water for 5 years, confirming the existence of methane oxidation activity in oxic water columns. It should be noted that this activity varied by as much as 3 orders of magnitude. Differences in activity between sampling times less than a month apart were sometimes as large as 2 orders of magnitude.

Methane oxidation activity was distinctly seasonal, with low activity from January to April and high activity from August to November at both stations (Figure 41a and b). The period from May to July was characterized by a shift in water column methane oxidation activity from low to high, while in December, it shifted from high to low. Inter-annual variability (displayed as bars in Figure 41) was very high in summer and autumn.

Methane consumption rates in the water column also fluctuated (Figure 41c and d). Minimum and maximum average monthly methane consumption rates for the 5 years of observation were: 0.7 ± 0.6 (March) and 45.6 ± 36.5 nM CH_4 hr^{-1} (September) at Station 3, 0.3 ± 0.2 (April) and 14.5 ± 8.3 nM CH_4 hr^{-1} (September) at Station 9. Methane consumption rates were at a minimum during spring, and a maximum in September. The minimal consumption rates at Station 3 and Station 9 were almost the same, however, the maximal consumption rate at Station 3 was about 3-fold that at Station 9.

3.4. Discussion

3.4.1. Lake Nojiri

Comparison between emission and oxidation during the 1994-1995 survey

One important mechanism for loss of water column methane is diffusive flux to the atmosphere across the air-water interface. The other important mechanism is methane oxidation by methanotrophs. The relative contributions of these two sinks for dissolved methane from Lake Nojiri were compared in units of kg CH_4 day^{-1} from the whole lake or mg CH_4 m^{-2} day^{-1} (Table 6). The diffusive loss of methane across a water surface to the atmosphere is a function of the difference between surface aqueous and atmospheric concentrations, wind velocity across the surface, and surface water temperature. I calculated the gas flux across the air-water interface from the wind velocity and surface supersaturation with the gas exchange model described by Liss and Slater (1974) and the relationship between wind velocity and gas exchange presented by Sebacher et al. (1983), with equations corrected for lake water temperature. Daily average of wind speeds at 8.3 m height were corrected to 0.02 m above the water surface to apply to the equation by Sebacher et al. (1983). The total mass of methane in Lake Nojiri was calculated by multiplying the methane concentration over a depth interval by the depth interval volume of the lake (Figure 30) and integrating over depth. Whole lake rates of methane consumption were calculated by multiplying the estimated methane consumption over a depth interval by the depth interval volume of the lake and integrating over depth. The corresponding areal values were calculated by dividing the totals by the surface area of the lake.

The calculated diffusive fluxes (Table 6) were not proportional to the variations in surface methane concentration, because of the large variation of the wind velocity during this period. The maximum and minimum diffusive methane fluxes were 1.71 and 0.144 mg CH_4 m^{-2} day^{-1} on 29 December and 20 January, respectively, and the average diffusive flux during the study period was 0.83 mg CH_4 m^{-2} day^{-1}.

Oxidation, the other major sink for water column methane, varied to a much greater extent than did the diffusive flux. The maximum calculated methane oxidation rate was 334 mg CH_4 m^{-2} day^{-1} on 10 December, but this calculation may be an overestimate due to the extrapolation of the specific rate of methane oxidation observed at 36 m depth, to the whole water column below 30 m. It was true that a large amount of methane oxidation occurred in the hypolimnion during the stratified period, however, specific methane oxidation rates depend strongly on the degree of oxygen depletion (e.g., Lilley et al., 1988). Methane oxidation rates usually peak at transition zones between aerobic and anaerobic condition. The loss of methane by oxidation in the water column from the surface to 30 m depth accounted for only 3.7 mg CH_4 m^{-2} day^{-1}. The average methane oxidation rate during the overturn period after 20 December, was 15.4 mg CH_4 m^{-2} day^{-1}. Diffusive flux across the air-water interface was not the dominant methane removal process for Lake Nojiri during the lake overturn period; rather, oxidation of methane was the dominant sink in the lake, consuming an average of 95% of dissolved methane during the period of the survey. The total amount of methane in the lake declined from 5960 to 116 kg during the period of the observations. Wind driven diffusive flux can not explain such a rapid decline. Microbial oxidation of methane is an important process,

destroying methane during the overturn period and thus reducing the transport of methane from the aquatic environment to the atmosphere.

The integrated amount of loss by diffusion and oxidation for each period between sequential samplings was always larger than the decrease of methane in the water column. This discrepancy suggests the existence of a source of methane from the lake sediments. I estimated the rate of methane release from the sediments from a mass balance budget for methane, as the difference between the change of water column methane minus the sum of the oxidative and diffusive sinks (Figure 42). Methane fluxes from the bottom sediments estimated in this way were between 4.1 and 79 mg CH_4 m^{-2} day^{-1} during the period of the survey. The sediment methane fluxes declined gradually as lake overturn proceeded. Rudd and Hamilton (1978) reported the benthic flux of methane from a similar calculation for Lake 227, in the Canadian experimental lakes area. The maximum flux of 79 mg CH_4 m^{-2} day^{-1} was smaller than that estimated for anoxic Lake 227 sediments (170 mg CH_4 m^{-2} day^{-1}) but larger than that estimated for oxic Lake 227 sediments (13 mg CH_4 m^{-2} day^{-1}). The fluxes calculated for the period between 29 December 1994 and 20 January 1995, after the overturn, were similar to those measured in oxic sediments in Lake 227 (Rudd and Hamilton, 1978) and in Lake Washington (3.4-5.0 mg CH_4 m^{-2} day^{-1}; Kuivila et al., 1988). During the earlier portion of the observation period, the sediment surface is expected to have been anoxic beneath the anoxic hypolimnion. Due to the absence of oxygen in the surface sediments, a large methane flux would be expected. With the progress of lake overturn and the penetration of oxygen to the sediment surface, the rate of methane oxidation at the sediment surface may decrease, thus reducing the benthic flux.

Assuming that 50% of the methane carbon oxidized by methanotrophs was converted to organic matter (bacterial cell materials) and the remainder to CO_2 (Rudd and Hamilton, 1978; Rudd and Taylor, 1980; Buchholz et al., 1995), the amount of methane carbon converted to bacterial cell material was from 0.45 (20 Jan. 1995) to 125 mg C m^{-2} day^{-1} (10 Dec. 1994). Unfortunately, the primary production was not measured since 1992. I expect that on 21 December 1992, a day on which we did measure primary production, the lake was in the midst of overturn, because the dissolved methane concentration observed (Figure 34) was close to the maximum concentrations measured during the following two winters. The primary production measured on that day was 170 mg C m^{-2} day^{-1}. Thus, the production powered by methane oxidation in the water column by methanotrophs was comparable in extent to the primary production in Lake Nojiri at the time of lake overturn.

3.4.2. Lake Kasumigaura

Methane oxidation activity in the oxic water column

Rudd and Hamilton (1978) reported annual changes in methane oxidation rates for dimictic Lake 227, in which an anaerobic hypolimnion was present during summer stratification. Methane oxidation activity strongly stratified and peaked at the oxic-anoxic interface during summer, and high rates of methane oxidation occurred throughout the water column during autumnal overturn. Seasonal changes in methane oxidation in monomictic Lake Washington (in which an aerobic hypolimnion is maintained throughout the year) was studied by Lidstrom and Somers (1984). They concluded that methane oxidation activity was negligible throughout the entire water column. It was observed high methane oxidation

activity in the oxic water column of shallow and non-stratified Lake Kasumigaura. Furthermore, this methane oxidation activity in the lake water was highly variable and seasonal.

The annual changes in dissolved methane concentrations at several stations in Lake Kasumigaura measured for 6 years by Nakamura et al. (see 3.2.1. Dissolved methane concentration in Lake Kasumigaura) followed a clear seasonal pattern with low concentrations from April to June, high concentrations from August to September, a minimum in November or December, and relatively high concentrations from January to March. The annual average dissolved methane concentration at the station in Takahamairi Bay (Sta. 3; 298 nM) was higher than that at the lake center station (Sta. 9; 179 nM), and the largest concentration differences between the 2 stations occurred in summer and autumn. The large differences in methane consumption rates for summer and autumn are partially due to the large differences in dissolved methane concentrations and partially due to the differences in specific methane oxidation rates (Figure 41c and d). The consumption rates from January to April were identical for both stations (Table 7).

Factors controlling methane oxidation activity in the water column

Various factors appear to control the activity of methanotrophs in different environments. As one would suspect in a biologically mediated process, temperature significantly affects biological reactions. Comparison, however, of pairs of the average specific oxidation rates at equivalent water temperature, e.g. April and November, or May and October, indicated significantly higher oxidation rates in autumn than those in spring at both stations (Table 7). The seemingly minor role of temperature as a regulatory factor for

methane oxidation activity differs substantially from the usually critical role it plays for other microbial processes. Seasonal variations in methane oxidation activity, therefore, can not be resolved by invoking temperature effects.

Methane oxidation activity in the water column is dependent, in part, on the existence of 2 primary substrates, dissolved methane and oxygen. There was a distinct seasonal pattern of dissolved methane concentrations in Lake Kasumigaura (Figure 41c and d). There was no statistically significant relationship, however, between dissolved methane concentration and specific oxidation rate for data from all seasons.

In Lake Kasumigaura, dissolved oxygen concentration was near saturation throughout the water column (6-12 mg O_2 l^{-1}) due to this lake's shallowness and the prevailing wind-driven mixing. The dissolved oxygen concentration was significantly above the range of the estimated half-saturation constant for methane oxidation, K_m (0.5-0.8 mg O_2 l^{-1}: Lidstrom and Somers, 1984), or the reported optimum range 0.1-1.0 mg O_2 l^{-1} (Rudd and Hamilton, 1975) for microbial methane oxidation in the water column. In my observations, on the other hand, high methane oxidation activity was observed in the water column when dissolved oxygen concentrations were high from late summer to autumn. The dissolved oxygen concentration, then, should not be the major factor limiting methane oxidation activity.

Methane oxidation activity depends, in part, on dissolved inorganic nitrogen. Rudd and Hamilton (1978, 1979) concluded that the combination of requirements for fixed nitrogen and oxygen constrained methane oxidation in Lake 227. According to their observations, methanotrophs fix nitrogen under low dissolved inorganic nitrogen conditions (<3 μ M). Because nitrogen fixation is disrupted by high concentrations of dissolved oxygen, methane

oxidation is confined to within a narrow zone at the oxycline. Methane oxidation activity in Lake 227 was thus limited during the period of lake stratification, and was widespread only during autumnal overturn under nitrogen limited conditions. I observed similar phenomena in stratified Lake Nojiri, Japan, where extensive methane oxidation occurs during the autumnal overturn period.

In the non-stratified, shallow Lake Kasumigaura, dissolved inorganic nitrogen concentrations are sometimes lower than 3 μM between mid-spring and autumn. Such low nitrogen concentrations there are mainly due to phytoplankton uptake, dominated by *Oscillatoria* (Takamura et al., 1992; Otsuki et al., 1993). Dissolved inorganic nitrogen usually increases in late autumn after the end of the summer phytoplankton bloom. Even under low dissolved inorganic nitrogen and high dissolved oxygen conditions from summer to early autumn, methane oxidation activity increased in the water column (Figure 43). Therefore the dissolved inorganic nitrogen concentration did not affect the methane oxidation activity in the water column of Lake Kasumigaura, similar to the situation in Lake Mendota sediments (Harrits and Hanson, 1980).

Methane dynamics in Lake Kasumigaura

Microbial oxidation is the only consumption process occurring within the water column that can prevent the eventual loss of methane to the atmosphere. Whole lake rates of methane consumption were calculated by dividing the lake into boxes (Table 4), multiplying the estimated methane consumption in each box by box volume and integrating the

consumption of all the boxes. The corresponding areal values were calculated by dividing the box-integrated totals by the surface area of the lake (168 km^2). The minimum and maximum monthly average methane consumption rates were 0.6 (April) and 48 mg CH_4 m^{-2} day^{-1} (August), and the annual average and standard deviation during the 5 years of the study were 12 ± 16 mg CH_4 m^{-2} day^{-1} (n = 12; Figure 44 and Table 8).

The other important mechanism for methane loss from the water column is diffusive flux to the atmosphere across the air-water interface. The calculated diffusive fluxes of methane across the air-water interface correlated primarily with the seasonal change in dissolved methane concentrations (Nakamura et al., submitted). The minimum and maximum monthly average fluxes were 1.1 (November) and 12 mg CH_4 m^{-2} day^{-1} (September), and the annual average and standard deviation was 4.2 ± 3.5 mg CH_4 m^{-2} day^{-1} (n = 12). From February to May, when methane oxidation activity in the water column was low, methane consumption in the lake was lower than the diffusive flux to the atmosphere, but in other seasons consumption rates were higher than the diffusive flux. Especially from late summer to autumn when the highest methane oxidation activity was observed, microbial oxidation of methane was an important methane consumption process in the water column, destroying methane and thus reducing the transport of methane from the lake to the atmosphere. Hence, oxidation of methane by methanotrophs rather than diffusive fluxes across the air-water interface was the dominant methane removal process for Lake Kasumigaura. Microbial oxidation is the dominant sink in the lake, consuming an annual average of 74% of the dissolved methane in the water column.

The turnover time of dissolved methane in an average water column for the entire lake (Table 8) was calculated by dividing the methane concentration by the total methane sink (consumption rate plus diffusive flux) in the water column. The shortest and longest turnover times of dissolved methane were 0.3 (in November) and 3.7 days (in February), and the annual average turnover time was 1.6 days. The turnover time of dissolved methane is very short relative to the renewal time of the lake water (0.6 year; Otsuki et al., 1993). Hence, the concentration of dissolved methane in the water column was not controlled by the water budget of the lake.

When comparing all measured consumption rates with methane concentrations (Figure 45a and b), the data for periods with shorter turnover times (< 1.5 days) can be clearly distinguished from those with longer turnover times (> 1.5 days) for both stations. The slopes of linear regressions of methane consumption rates on concentration for each of these groups of data points (Figure 45a and b) represent average specific oxidation rates. The slopes for the shorter turnover times are close to the maximum monthly average specific oxidation rates for the respective stations (Table 8). Variation in the slopes may indicate that different types of methanotrophs dominate during different seasons in Lake Kasumigaura.

The monthly average plots for the same data sets reveal a systematic seasonality, which can explain the seasonal change in dissolved methane in Lake Kasumigaura (Figure 45c and d). During the period from January to April, when methane consumption rates were lower than the diffusive flux (Table 8), methane concentrations decreased substantially with only a small decline in consumption rates, indicating decreasing methane supply from the bottom

sediment. Diffusive flux was the dominant methane sink during this season. Thus, the spring concentration minimum appears throughout the entire basin.

From May to September, the trends in methane concentration and consumption rates at the 2 stations differed. At Station 3 from May to July, methane concentration increased markedly with very little concomitant rise in consumption rates, essentially reversing the January to April shift. This trend was due to an increase in methane supply from the bottom sediment while methane oxidation activity remained low, resulting in high summer methane concentrations occurring earlier in the season at Station 3 than at other stations (Figure 45c). In contrast, the summer increase in methane concentrations at Station 9 did not begin until July (Figure 45d). The August point for Station 3 (Figure 45c) is based on the average of data for occasions with shorter and longer turnover times, both of which occurred in August over the 5 years of measurement. In September, high methane concentrations remained despite the higher methane oxidation activity which usually prevailed at that time, evidence for the largest methane supply from the bottom sediment in the year. The average turnover time of dissolved methane in September was 0.4 day (Table 8). The methane supply from the sediment in September seems to have been more than double the daily water column methane consumption at that time. The transition from the spring minimum concentration (April) to the summer maximum (August and September) at Station 9 (Figure 45d) proceeded more smoothly than that at Station 3 (Figure 45c), as the methane consumption rate increased concomitantly with methane concentration. The June or July concentration increase observed at Station 3 was rarely observed at Station 9 due to the more rapid increase in methane oxidation activity at the lake center.

From September to November, methane concentrations decrease until reaching the November minimum at both stations. Declining, but still high methane oxidation activity remains during this period, so I attribute the concentration minimum to gradually decreasing methane supply from the sediment.

I attribute the methane concentration increases in the December to January period to rapidly decreasing methane oxidation activity and slowly decreasing methane supply from the sediment. These conditions lead to high methane concentrations in Lake Kasumigaura in January.

Chapter 4

GENERAL DISCUSSION

In Matsumi-ike Bog, the dominant organic nutrients were manifold during two different periods, one is from April to October while the phytoplankton biomass comprised the predominant POM components. The other is during winter while the phytoplankton biomass was low while the withered cattail became the primary POM source in the water column of the bog. In this period, the POM had less nitrogen fraction than that in the other period while the phytoplankton was dominant POM source.

The bacterioplankton growth was shown to be controlled by the water temperature as the limiting factor. The growth was controlled secondly by nutrients during each period. From April to October, it was the DOC originating from phytoplankton. This is because the DOC contained all essential elements for growth of bacterioplankton. In winter, on the other hand, phosphate was the secondary limiting factor on the growth rate of bacterioplankton. This is because the DOC originating from the withered cattail did not contain all elements for growth of bacterioplankton. These DOC were not complete organic nutrients for bacterial growth, so the bacterioplankton must have obtained supplemental elements from the inorganic nutrients in the bog water for their growth.

The size of the attached bacteria in the water column and at the bottom boundary were always larger than that of bacterioplankton, and the average growth rate of attached bacteria was lower than that of bacterioplankton throughout the year. The highest density of attached bacteria was observed at the bottom boundary layer throughout the year, because the greater accumulation of organic matter must have occurred at this layer.

From April to May, it was observed high epibacterial density on the glass slide. This is because the bacterial community in the bog must have found supplementary elements from the bog water for their growth. The aquatic bacteria associated with a solid surface can utilize the nutrients concentrated on the solid surface (ZoBell and Anderson, 1936; Costerton and Lewandowski, 1995). During summer, the density of attached bacteria gradually decreased and the density of bacterioplankton increased. The organic debris from phytoplankton comprise complete nutrient elements for the bacterial growth, so that there was no need to attach onto a solid surface for getting nutrients efficiently from the interface. From autumn to early winter, the density of attached bacteria was the minimum for the year, because the supply of organic nutrients from phytoplankton and the nutrient concentration in the water was minimal. In this period, the density of bacterioplankton was also minimal and its growth rates were occasionally negative. When the new supply of dead cattail started, the rate of bacterial attachment increased again, and the density of attached bacteria in the water column (including the boundary) increased gradually toward spring.

These investigation results indicate that major components of the bacterioplankton and the attached bacteria in Matsumi-ike Bog form a single community, with the bacteria attached to a solid surface being recruited from the bacterioplankton, and the epibacterial community acting as a potential seeding source of bacterioplankton in the water column (e.g., Kang and Seki, 1983). Furthermore, in such an aquatic ecosystem as Matsumi-ike Bog, where it has attained the final stage of maturation of a natural water body and thereby greater interface area between water and solid surface due to the bog's shallowness and the abundant particulate organic materials in the water column, the bacterial community in the attached phase especially

at the boundary must play a significant role in the nutrient cycling of the bog ecosystem and in the progress of limnological succession.

I have confirmed methane oxidation activity in the oxic water column of the shallow eutrophic lake of Kasumigaura. This activity was distinctly seasonal, with low specific rates from January to April and high specific rates from August to November. The level of activity, however, fluctuated greatly from year to year. As the average turnover time of dissolved methane (1.6 days) is much shorter than that of the lake water (220 days), the concentration of dissolved methane was not controlled by the water budget, but rather by the methane supply from the sediment, oxidation in the water column and diffusion to the atmosphere.

A clear relationship between methane oxidation activity in the water column and routinely measured environmental factors was not observed. In freshwater lakes, methane oxidation is most active by methanotrophs at interfaces between oxic and anoxic zones, where all necessary substrates for methane oxidation are available in sufficient quantities. An oxic-anoxic interface exists at the surface layer of sediment in Lake Kasumigaura, so methane oxidation activity in this lake should be most active there by both bacterioplankton and epibacteria. With the daily mixing of water, attached methanotrophs in the sediment are transported to the oxic water column and retain their activities in the planktonic state.

This phenomenon is similar to that observed during the overturn period at Lake Nojiri, a deep and stratified lake. Before the autumnal overturn period, active methane oxidation was observed within a limited depth zone in the hypolimnion at the oxic-anoxic interface. As lake overturn proceeded, methane stored in the anoxic hypolimnion during summer stratification was oxidized by methanotrophs throughout the water column, as a result of oxygenated water

mixing with anoxic water containing high concentrations of methane. Methane oxidation activity in the surface layer was significantly increased by the water mixing. Microbial oxidation of methane is an important process (consume an average of 95% of dissolved methane during the period of the survey), destroying methane during the overturn period and thus reducing the transport of methane from the aquatic environment to the atmosphere.

The daily mixing of water in non-stratified Lake Kasumigaura transports methanotrophs to the water column, resulting in a phenomenon similar to that which occurs during the overturn period in stratified lakes. An increase in methane oxidation is observed, accompanied by maximum methane production in late summer. The relationship between concentration and consumption rate suggests a certain time lag in the decline of oxidation activity with decreasing methane production in early autumn. The high oxidation activity continues through the end of autumn, by when production of methane should have already decreased. Methane oxidation is the dominant methane sink in Lake Kasumigaura, consuming an annual average of 74% of dissolved methane in the water column. Methane oxidation in the water column is an important methane sink in shallow, non-stratified lakes.

For the methane cycling in the freshwater environment, methane oxidation by planktonic methanotrophs is one of the important pathways, which remove methane from the water column. These planktonic methanotrophs would be mainly supplied from attached methanotrophs at the surface sediment. Methanotrophs in the sediment are the seeding source of planktonic methanotrophs in the water column. As the results from a cooperative work of methane cycling experiment in Lake Kasumigaura, all the pathways of methane cycling in the lake, including methanogenesis in the sediment, sediment surface methane oxidation, water

column methane oxidation, diffusion from water surface and ebullition, were estimated from the observation in 1993. The methane concentration gradient in the bottom sediment revealed the intensity of methane generation in the sediment. Significant part of the methane generated was oxidized at the surface sediment. The activity of methane oxidation in the water column was generally paralleled with the methane oxidation at the surface sediment and also with the methanogenesis in the sediment. Assumption of the supply of methanotrophs from the surface sediment to the water column is consistent with the results of the analysis of methane balance in Lake Kasumigaura including the sediment, the water column and the atmosphere. The cycles of planktonic and attached stages of methanotrophs have significant role in the methane cycling in Lake Kasumigaura, same as the cycle of matter in Matsumi-ike Bog.

Considering the methane cycling in the world, it is important to clear the methane sink in each freshwater environment, especially freshwater bogs and mires which think the largest methane source. Because previous studies about freshwater bogs and mires have only considered the source of methane to the atmosphere (e.g., Asselman and Crutzen, 1989; Bartlett and Harriss, 1993), it will be necessary to study the methane cycling in the bogs and mires considering not only methanogenesis but also methane oxidation. I want to study the methane cycling in more detail using the new methods such as *in situ* PCR for methanogen and methanotroph or stable isotope analysis.

ACKNOWLEDGMENTS

The author wishes to express his sincere appreciation to Dr. Yukihiro Nojiri of National Institute for Environmental Studies (Associate Professor of the University Tsukuba) and Professor Humitake Seki of the University Tsukuba, for their guidance and constructive criticism throughout the course of his research and the preparation of the manuscript. The author is indebted to Professor Makoto Watanabe of National Institute for Environmental Studies, for his valuable suggestion and criticism.

A special debt of gratitude goes to Professor Morihiro Aizaki of Shimane University, Professor Takehiko Fukushima of Hiroshima University, and Drs. Nozomi Ytow of the University of Tsukuba, Shigeaki Kojima of the University of Tokyo, Kazuo Matsushige and Seiichi Kasuga of National Institute for Environmental Studies, who gave me much support and encouragement. The author wishes to express their gratitude to Messrs. Takeshi Nakanura of Tokyo University of Fisheries and Takeshi Nozawa of Tokyo University of Fisheries for generous assistance in carrying out the experiments. The author must thank Professor D. Macer of the University of Tsukuba and Dr. R. Weisburd of National Institute for Environmental Studies for their kind criticism and English correction. Special thanks must be accorded to all members of the laboratory and National Institute for Environmental Studies Lake Kasumigaura Water Research Station for technical assistance and useful discussion on the results.

REFERENCES

Aida, W., T. Muraoka, and H. Seki. 1988. Effect of rapid oligotrophication by an aquatic treatment pilot plant on the microbial community of a mesotrophic bog V. attachment and growth kinetics of epibacteria. *Water Air and Soil Pollut.* **42:** 433-438.

Anthony, C. 1986. Bacterial oxidation of methane and methanol. *Adv. Microb. Physiol.* **27:** 113-210.

Asselman, I., and P. J. Crutzen. 1989. Global distribution of natural freshwater wetlands and rice paddies, their net primary productivity, seasonality and possible methane emissions. *J. Atmos. Chem.* **8:** 307-358.

Azam, F., T. Fenchel, J. G. Field, J. S. Gray, L. A. Meyer-Reil, and F. Thingstad. 1983. The ecological role of water-column microbes in the sea. *Mar. Ecol. Prog. Ser.* **10:** 257-263.

Azam, F., and J. A. Fuhrman. 1984. Measurements of bacterioplankton growth in the sea and its regulation by environmental conditions, p. 179-196. *In* Hobbie, J. E., and P. J. LeB. Williams, (eds.), Heterotrophic Activity in the Sea. New York, Plenum Press.

Balch, W. E., G. E. Fox, L. J. Magrum, C. R. Woese, and R. S. Wolfe. 1979. Methanogens: Reevaluation of a unique biological group. *Microbiol. Rev.* **40:** 260-296.

Bartlett, K. B., and R. C. Harriss. 1993. Review and assessment of methane emissions from wetlands. *Chemosphere* **26:** 261-320.

Batomalaque, A. E., M. Kikuma, and H. Seki. 1992. Population dynamics of attached bacteria in a mesotrophic swampy bog of Japan. *Water Air and Soil Pollut.* **63:** 371-378.

Benner, R., L. E. K'nees, and R. E. Hodson. 1988. Carbon conversion efficiency for bacterial growth on lignocellulose: Implications for detritus-based food webs. *Limnol. Oceanogr.* **33:** 1514-1526.

Bird, D., and J. Kalff. 1984. The empirical relationships between bacterial abundance and chlorophyll concentrations in aquatic systems. *Can. J. Fish. Aquat. Sci.* **41:** 1015-1023.

Bjorck, Å. 1967. Solving linear least-squares problems by Gram-Schmidt orthogonalization. *BIT.* **7:** 1-21.

Blackman, F. F. 1905. Optima and limiting factors. *Ann. Bot.* **19:** 281-295.

Blake D. R., and F. S. Rowland. 1988. Continuing worldwide increase in tropospheric methane. *Science* **239:** 1129-1131.

Blough, N. V., O. C. Zafiriou, and J. Bonilla. 1993. Optical absorption spectra of waters from the Orinoco River outflow : Terrestrial input of colored organic matter to the Caribbean. *J. Geophys. Res.* **98:** 2271-2278.

Bott, T. L., and T. D. Brock. 1970(a). Growth and metabolism of periphytic bacteria: Methodology. *Limnol. Oceanogr.* **15:** 333-342.

Bott, T. L., and T. D. Brock. 1970(b). Growth rate of Sphaerotilus in a thermally polluted environment. *Appl. Environ. Microbiol.* 19: 100-102.

Bricaud, A., A. Morel, and L. Priour. 1981. Absorption by dissolved organic matter of the sea (yellow substance) in the UV and visible domains. *Limnol. Oceanogr.* **26:** 43-53.

Brock, T. D. 1978. Thermophilic Microorganisms and Life at High Temperatures. Springer-Verlag, New York. 465pp.

Brock, T. D., and M. T. Madigan. 1991. Biology of Microorganisms (6th ed.). Prentice Hall, New Jersey. 874pp.

Brown, P. S., and T. R. Parsons. 1972. The effect of simulated upwelling on the maximization of primary productivity and the formation of phytodetritus. *Mem. Ist. Ital. Idrobiol.* **29** Suppl: 169-183.

Buchholz, L. A., J. V. Klump, M. L. P. Collins, C. A. Brantner, and C. C. Remsen. 1995. Activity of methanotrophic bacteria in Green Bay sediments. *FEMS Microbiol. Ecol.* **16:** 1-8.

Caldwell, D. E., D. K. Brannan, M. E. Moriis, and M. R. Betlach. 1981. Quantitation of Microbial growth on surfaces. *Microb. Ecol.* **7:** 1-11.

Caldwell, D. E., J. A. Malone, and T. L. Kieft. 1983. Derivation of a growth rate equation describing microbial surface colonization. *Microb. Ecol.* **9:** 1-6.

Cicerone, R. J., and R. S. Oremland. 1988. Biogeochemical aspects of atmospheric methane. *Global Biogeochem. Cycles* **2:** 299-327.

Coble, P. G., S. A. Green, N. C. Blog, and R. B. Gagosian. 1990. Characterization of dissolved organic matter in the Black Sea by fluorescences spectroscopy. *Nature* **48:** 432-435.

Costerton, J. W., and Z. Lewandowski. 1995. Microbial biofilms. *Annu. Rev. Microbiol.* **49:** 711-745.

Dagley, S. 1978. Determinants of biodegradability. *Q. Rev. Biophys.* **11:** 577-602.

Daniels, L., R. Sparling, and G. D. Sprott. 1984. The bioenergetics of metanogenesis. *Biochim. Biophys. Acta* **768:** 113-163.

Davis-Colley, R. R., and W. N. Vant. 1987. Absorption of light by yellow substance in freshwater lakes. *Limnol. Oceanogr.* **32:** 416-425

de Angelis, M. A., and M. I. Scranton. 1993. Fate of methane in the Hudson River and estuary. *Global Biogeochem. Cycles* **7:** 509-523.

de Rosa, M., and A. Gambacorta. 1988. The lipids of archaebacteria. *Prog. Lipid Res.* **27:** 153-175.

Ehalt, D. H. 1974. The atmospheric cycle of methane. *Tellus* **26:** 58-70.

Ehalt, D. H., and U. Schmidt. 1978. Sources and sinks of atmospheric methane. *Pure Appl. Geophys.* **116:** 452-464.

Ferrari, G. M., and S. Tassan. 1991. On the accuracy of determining light absorption by "yellow substance" through measurements of induced fluorescence. *Limnol. Oceanogr.* **36:** 777-786.

Fletcher, M. 1977. The effects of culture concentration and age, time, and temperature on bacterial attachment to polystyrene. *Can. J. Microbiol.* **23:** 1-6.

Frenzel, P., B. Thebrath, and R. Conrad. 1990. Oxidation of methane in the oxic surface layer of a deep lake sediment (Lake Constance). *FEMS Microbiol. Ecol.* **73:** 149-158.

Fuhrman, J. A., and F. Azam. 1980. Bacterioplankton secondary production estimates for coastal waters of British Columbia, Antarctic, and California. *Appl. Environ. Microbiol.* **39:** 1085-1095.

Giorgio, P. A. D., and H. P. Robert. 1993. The influence DOC on the bacteria-chlorophyll relationship in lakes. *Verh. Internat. Verein. Limnol.* **25:** 359-362.

Golterman, H. L. 1969. Methods for Chemical Analysis of Freshwater. Int. Biol. Program Handbook 8, Blackwell Science Publications, Oxford. 172pp.

Green, S. A., and N. V. Blough. 1994. Optical absorption and fluorescence properties of chromophoric dissolved organic matter in natural waters. *Limnol. Oceanogr.* **39:** 1903-1916.

Griffiths, R. P., B. A. Caldwell, J. D. Cline, W. A. Broich, and R. Y. Morita. 1982. Field observations of methane concentrations and oxidation rates in the Southeastern Bering Sea. *Appl. Environ. Microbiol.* **44:** 435-446.

Hanson, R. S., and T. E. Hanson. 1996. Methanotrophic bacteria. *Microbiol. Rev.* **60:** 439-471.

Harrits, S. M., and R. S. Hanson. 1980. Stratification of aerobic methane-oxidizing organisms in Lake Mendota, Madison, Wisconsin. *Limnol. Oceanogr.* **25:** 412-421.

Harvey, W., and L. Y. Young. 1980. Enumeration of particle-bound and unattached respiring bacteria in the salt marsh environment. *Appl. Environ. Microbiol.* **40:** 156-160.

Higgins, I. J., D. J. Best, R. C. Hammond, and D. Scott. 1981. Methane-oxidizing microorganisms. *Microbiol. Rev.* **45:** 556-590.

Hobbie, J. E., R. J. Daley, and S. Jasper. 1977. Use of Nuclepore filters for counting bacteria by fluorescence microscopy. *Appl. Environ. Microbiol.* **33:** 1225-1228.

Hoge, F. E., A. Vodacek, and N. V. Blough. 1993. Inherent optical properties of the ocean: Retrieval of the absorption coefficient of chromophoric dissolved organic matter from fluorescence measurements. *Limnol. Oceanogr.* **38:** 1394-1402.

Hutchinson, G. E. 1975. A Treatise on Limnology; Limnological Botany (Vol. 3.). John Wiley and Sons, New York.

Imshenetskii, A. A., B. G. Murzakov, M. D. Evdokimova, and I. K. Drofeeva. 1984. Survival of bacteria in the "artificial Mars" apparatus. *Microbiology* **53:** 594-600.

IPCC (Intergovernmental Panel on Climate Change). 1994. Climate Change: the IPCC Scientific Assessment. Cambridge Univ. Press.

Iversen, N., R. S. Oremland, and M. J. Klug. 1987. Big Soda Lake (Nevada). 3. Pelagic methanogenesis and anaerobic methane oxidation. *Limnol. Oceanogr.* **32:** 804-814.

Jannasch, H. W. 1969. Estimations of bacterial growth rates in natural waters. *J. Bacteriol.* **99:** 156-160.

Jannasch, H. W. 1975. Methane oxidation in Lake Kivu. *Limnol. Oceanogr.* **20:** 860-864.

Jannasch, H. W. 1984. Microbes in the oceanic environment, p. 97-122. *In* Kelly, D. P., and N. G. Carr, (eds.), The Microbe 1984, Part II, Symposium 36, The Society for General Microbiology. Cambridge University Press.

Jeffrey, R. W., and G. F. Humprey. 1975. New spectrophotometric equations for determining chlorophyll-a, b, c1 and c2 in higher plants, algae and natural phytoplankton. *Biochem. Physiol. Pflanzen.* **167:** 191-193.

Jenkins, F. A., and H. E. White. 1981. Fundamentals of Optics (4th ed.). McGraw-Hill. London. 746pp.

Johnson, F. H., H. Eyring, and M. J. Polissar. 1954. The Kinetic Basis of Molecular Biology. John Wiley and Sons, New York. 874pp.

Jones, W. J., D. P. Nagel, Jr., and W. B. Whitman. 1987. Methanogens and the diversity of archaebacteria. *Microbiol. Rev.* **51:** 135-177.

Jordan, M. J., and G. E. Likens. 1980. Measurement of planktonic bacterial production in an oligotrophic lake. *Limnol. Oceanogr.* **25:** 719-732.

Kandler, O., and H. Hippe. 1977. Lack of peptidoglycan in the cell walls of *Methanosarcina barkeri*. *Arch. Microbiol.* **113:** 57-60.

Kang, H., and H. Seki. 1983. The gram-stain characteristics of the bacterial community as a function of the dynamics of organic debris in a mesotrophic irrigation pond. *Arch. Hydrobiol.* **98:** 39-58.

Karl, D. M. 1987. Bacterial production at deep-sea hydrothermal vents and cold seeps: Evidence for chemosynthetic primary production, p. 319-360. *In* Fletcher, M., T. R. G. Gray, and J. Jones, (eds.), Ecology of Microbial Communities, Symposium 41, The Society for General Microbiology. Cambrifge University Press.

Khalil, M. A. K., R. A. Rusmussen, and J. J. Shearer. 1989. Trends of atmospheric methane during the 1960s and 1970s. *J. Geophys. Res.* **94:** 18279-18288.

King, G. M., P. Roslev, and H. Skovgaard. 1990. Distribution and rate of methane oxidation in sediments of the Florida everglades. *Appl. Environ. Microbiol.* **56:** 2902-2911.

Kirchman, D., J. Sigda, R. Kapuscinski, and R. Mitchell. 1982. Statistical analysis of the direct count method for enumerating bacteria. *Appl. Environ. Microbiol.* **44:** 376-382.

Kroer, N. 1993. Bacterial growth efficiency on natural dissolved organic matter. *Limnol. Oceanogr.* **38:** 1282-1290.

Krom, M. D., and E. R. Sholkovitz. 1977. Nature and reactions of dissolved organic matter in the interstitial waters of marine sediments. *Geochim. Cosmochim. Acta* **41:** 1565-1573.

Kuivila, K. M., J. W. Murray, A. H. Devol, M. E. Lidstrom, and C. E. Reimers. 1988. Methane cycling in the sediments of Lake Washington. *Limnol. Oceanogr.* **33:** 571-581.

Kushner, D. J. (ed.) 1978. Microbial Life in Extreme Environments. Academic Press, London. 465pp.

Langworthy, T. A. 1985. Lipids of archaebacteria, p. 459-497. *In* Woese C. R., and R. S. Wolfe, (eds.), The Bacteria, vol. 8. Academic Press, New York.

Lelieveld, J., P. J. Crutzen, and C. Bruhl. 1993. Climate effects of atmospheric methane. *Chemosphere* **26:** 739-768.

Lidstrom, M. E., and L. Somers. 1984. Seasonal study of methane oxidation in Lake Washington. *Appl. Environ. Microbiol.* **47:** 1255-1260.

Liebig, J. 1840. Chemistry in Its Application to Agriculture and Physiology. Taylor and Walton, London. 352pp.

Lilley, M. D., J. A. Baross, and C. N. Dahm. 1988. Methane production and oxidation in lakes impacted by the May 18, 1980 eruption of Mount St. Helens. *Global Biogeochem. Cycles.* **2:** 357-370.

Liss, P. S., and P. G. Slater. 1974. Flux of gases across the air-sea interface. *Nature* **247:** 181-184.

Marquardt, D. W. 1963. An algorithm for least-squares estimation of nonlinear parameters. *J. Soc. Indust. Appl. Math.* **11:** 431-441.

Marshall, K. C., R. Stout, and R. Mitchell. 1971. Selective sorption of bacteria from seawater. *Can. J. Microbiol.* **17:** 1413-1416.

Millsap, K., G. Reid, H. C. van der Mei, and H. J. Busscher. 1994. Displacement of *Enterococcus faecalis* from hydrophobic and hydrophilic substrata by *Lactobacillus* and *Streptococcus* spp. as studied in a parallel plate flow chamber. *Appl. Environ. Microbiol.* **60:** 1867-1874.

Miyamoto, S., and H. Seki. 1992. Environmental factors controlling the population growth rate of the bacterial community in Matsumi-ike Bog. *Water Air and Soil Pollut.* **63:** 379-396.

Mizuno, T. 1971. Illustrations of the freshwater plankton of Japan. Hoikusha, Osaka. (in Japanese).

Monod, L. 1949. The growth of bacterial cultures. *Ann. Rev. Microbiol.* **3:** 371-394.

More, J. J. 1978. The Levenberg-Marquardt algorithm: Implementation and theory, p.105-116. *In* Watson, G. A. (ed.), Lecture Note in Mathematics 630 Numerical Analysis. Springer, Berlin.

Mueller, R. F., W. G. Characklis, W. L. Jones, and J. T. Sears. 1992. Characterization of initial events in bacterial surface colonization by two Pseudomonas species using image analysis. *Biotechnol. Bioeng.* **39:** 1161-1170.

Naganuma, T., and H. Seki. 1985. Population growth rate of the bacterioplankton community in a bog, Matsumi-ike, Japan. *Arch. Hydrobiol.* **104:** 543-556.

Naganuma, T., and H. Seki. 1988. Effect of rapid oligotrophication by an aquatic treatment pilot plant on the microbial community of a mesotrophic bog IV. Effect on the bacterioplankton community. *Water Air and Soil Pollut.* **42:** 397-406.

Naganuma, T., A. Otsuki, and H. Seki. 1989. Abundance and growth rate of bacterioplankton community in hydrothermal vent plumes of the North Fiji Basin. *Deep-sea Research* **36:** 1379-1390.

Naganuma, T., and H. Seki. 1993. Abundance and productivity of bacterioplankton in a eutrophication gradient of Shimoda Bay. *J. Oceanogr.* **49:** 657-665.

Nakamura, T., Y. Nojiri, A. Otsuki, and S. Hashimoto. 1994. Methane concentration and its variation in seawater of highly eutrophic Tokyo Bay. *Geochemistry* **28:** 47-57. (in Japanese with English abstract).

Nakamura, T., Y. Nojiri, T. Nozawa, M. Utsumi, and A. Otsuki. Long-term measurement of dissolved methane in eutrophic shallow Lake Kasumigaura, Japan. Global Biogeochem. Cycles (submitted).

Nojiri, Y. 1991. Chemical survey for seafloor hydrothermalism. *Adv. Mar. Tech. Conf.* **4:** 17-24. (in Japanese with English abstract).

Odum, E. P. 1971. Fundamentals of Ecology (3rd ed.). Saunders, Philadelphia. 574pp.

Ohle, W. 1965. Sulfat als "Katalysator" des limnishen Stoffkreislaufes. *Von Wasser.* **21:** 13-32.

Otsuki, A., and T. Hanya. 1967. Some precursors of humic acid in Recent lake sediment suggested by infra-red spectra. *Geochim. Cosmochim. Acta* **31:** 1505-1515.

Otsuki, A., R. H. Goma, M. Aizaki, and Y. Nojiri. 1993. Seasonal and spatial variations of dissolved nitrogenous nutrient concentrations in hypertrophic shallow lake, with special reference to dissolved organic nitrogen. *Verh. Internat. Verein. Limnol.* **25:** 187-192.

Pamatmat, M. M. 1971. Oxygen consumption by the seabed IV. Shipboard and laboratory experiments. *Limnol. Oceanogr.* **16:** 536-550.

Parsons, T. R., Y. Maita, and C. M. Lalli. 1984. A Manual of Chemical and Biological Methods for Seawater Analysis. Pergamon Press, Oxford. 173pp.

Pedros-Alio, C., and T. D. Brock. 1982. Assessing biomass and production of bacteria in eutrophic Lake Mendota, Wisconsin. *Appl. Environ. Microbiol.* **43:** 203-218.

Peyton, B. M., and W. G. Characklis. 1993. A statistical analysis of the effect of substrate utilization and shear stress on the kinetics of biofilm detachment. *Biotechnol. Bioeng.* **41:** 728-735.

Powell, M. J. D. 1970(a). A hybrid method for nonlinear equations, p. 87-114. *In* Rabinowits, P. (ed.), Numerical Methods for Nonlinear Algebraic Equations. Gordon and Breach, London.

Powell, M. J. D. 1970(b). A fortran subroutine for solving systems for nonlinear algebraic equations. p. 115-161. *In* Rabinowits, P. (ed.), Numerical Methods for Nonlinear Algebraic Equations. Gordon and Breach, London.

Prescott, G. W. 1973. Algae of the Western Great Lakes Area. W. C. Brown, Dubuque. 977pp.

Prieur, L., and S. Satyendranath. 1981. An optical classification of coastal and oceanic waters based on the specific spectral absorption curves of phytoplankton pigments, dissolved organic matter, and other particulate material. *Limnol. Oceanogr.* **26:** 671-698.

Rostan, J. C., and B. Cellot. 1995. On the use of UV spectrophotometry to assess dissolved organic carbon origin variation in the Upper Rhone. *Aquatic Sci.* **57:** 70-80.

Rudd, J. W. M., R. D. Hamilton, and N. E. R. Campbell. 1974. Measurement of microbial oxidation of methane in lake water. *Limnol. Oceanogr.* **19:** 519-524.

Rudd, J. W. M., and R. D. Hamilton. 1975. Factors controlling rates of methane oxidation and the distribution of the methane oxidizers in a small stratified lake. *Arch. Hydrobiol.* **75:** 522-538.

Rudd, J. W. M., and R. D. Hamilton. 1978. Methane cycling in a eutrophic shield lake and its effects on whole lake metabolism. *Limnol. Oceanogr.* **23:** 337-348.

Rudd, J. W. M., and R. D. Hamilton. 1979. Methane cycling in Lake 227 in perspective with some components of carbon and oxygen cycles. *Arch. Hydrobiol. Beih. Ergebn. Limnol.* **12:** 115-122.

Rudd, J. W. M., and C. D. Taylor. 1980. Methane cycling in aquatic environments. *Adv. Aquatic. Microbiol.* **2:** 77-150.

Sansone, F. J., and C. S. Martens. 1978. Methane oxidation in Cape Lookout Bight, North Carolina. *Limnol. Oceanogr.* **23:** 349-355.

Sasa, M., S. Ishizaka, T. Asamizu, M. Aoki, Y. Nojiri, Y. Higashi, M. Utsumi, H. Zheng, N. Ytow, and H. Seki. 1996. Ecosystem structure of a boiling spring with high bacterial production on Mt. Tateyama, Japan. *Arch. Hydrobiol.* **136:** 563-574.

SCOR/UNESCO. 1966. Determination of photosynthetic pigments in water. In Monographs on Oceanographic Methodology 1. UNESCO, Paris.

Scranton, M. I., P. Crill, M. deAngelis, P. L. Donaghay, and J. McN. Sieburth. 1993. The importance of episodic events in controlling the flux of methane from an anoxic basin. *Global Biogeochem. Cycles* **7:** 491-507.

Sebacher, D. I., R. C. Harriss, and K. B. Bartlett. 1983. Methane flux across the air-water interface: air velocity effects. *Tellus* **35B:** 103-109.

Seki, H. 1972. The role of microorganisms in the marine food chain with reference to organic aggregates. *Mem. Ist. Ital. Idrobiol.* **29** Suppl.: 245-259.

Seki, H. 1976. "Suikai-Biseibutsu-Seitai-Kenkyuho (Methods for Aquatic Microbial Ecology)", Kyoritsu-Shuppan, Tokyo. 131pp. (in Japanese).

Seki, H. 1982. Organic Materials in Aquatic Ecosystems. CRC Press, Boca Raton. 201pp.

Seki, H., and H. Nakano. 1981. Production of bacterioplankton with special reference to dynamics of dissolved organic matter in a hypereutrophic lake. *Kieler Meeresforsch., Sonderh.* **5:** 408-415.

Seki, H., and E. Takahashi. 1983. Spring bloom in a hypereutrophic lake, Lake Kasumigaura, Japan 1. Succession of phytoplankton with different accessory pigments. *Water Res.* **17:** 441-445.

Seki, H., T. Saido, K. Iseki, F. Whitney, and C. S. Wong. 1984. Uptake kinetics of microorganisms in the sulfuretum of Saanich Inlet. *Arch. Hydrobiol.* **102:** 229-238.

Sebacher, D. I., R. C. Harriss, and K. B. Bartlett. 1983. Methane flux across the air-water interface: air velocity effects. *Tellus* **35B:** 103-109.

Sebacher, D. I., R. C. Harriss, and K. B. Bartlett. 1985. Methane emissions to the atmosphere through aquatic plants. *J. Environ. Qual.* **14:** 40-46.

Shiraishi, K., Y. Uno, Y. Hara, and H. Seki. 1985. Factors controlling phytoplankton population in a bog, Matsumi-ike, Japan. *Arch. Hydrobiol.* **104:** 387-406.

Smith, G. M. 1933. Fresh-water Algae of the United States. McGraw-Hill, New York. 716pp.

Sohngen, N. L. Über Baktevien, welche Methan als Kohlenstoffnahrung und Energiequelle gebrauchen. *Zentralblatt fur Bakteriologie Parasitenkenkunde Infektions Krankheiten*, Abt. *2.* **15:** 513-517.

Stewart, A. J., and R. G. Wetzel. 1981. Asymmetrical relationships between absorbance, fluorescence, and dissolved organic carbon. *Limnol. Oceanogr.* **26:** 590-597.

Strickland, J. D. H., and T. R. Parsons. 1968. A Practical Handbook of Seawater Analysis. *Fish. Res. Bd. Can., Bull.* **167:** 1-311.

Sullivan, C. W., and A. C. Palmisano. 1984. Sea ice microbial communities: Distribution, abundance, and diversity of ice bacteria in McMurdo Sound, Antarctica, in 1980. *Appl. Environ. Microbiol.* **47:** 788-795.

Takamura, N., T. Iwakuma, and M. Yasuno. 1985. Photosynthesis and primary production of *Microcystis aeruginosa* Kutz. in Lake Kasumigaura. *J. Plankton Res.* **7:** 303-312.

Takamura, N., A. Otsuki, M. Aizaki, and Y. Nojiri. 1992. Phytoplankton species shift accompanied by transition from nitrogen dependence to phosphorus dependence of primary production in Lake Kasumigaura, Japan. *Arch. Hydrobiol.* **124:** 129-148.

Utsumi, M., S. Kojima, Y. Nojiri, S. Ohta, and H. Seki. 1994. Biomass and production of bacterioplankton at the hydrothermal vent areas in the rift system of the North Fiji Basin. *J. Oceanog.* **50:** 635-642.

Ward, B. B., K. A. Kilpatrick, P. C. Novelli, and M. I. Scranton. 1987. Methane oxidation and methane fluxes in the ocean surface layer and deep anoxic waters. *Nature* **327:** 226-229.

Wiesenburg, D. A., and N. L. Guinasso. 1979. Equilibrium solubilities of methane, carbon monoxide, and hydrogen in water and sea water. *J. Chem. Eng. Data* **24:** 356-360.

Wilson, C. A., and L. H. Stenvenson. 1980. The dynamics of the bacterial populations associated with a salt marsh. *J. Exp. Mar. Biol. Ecol.* **48:** 123-135.

Woese, C. R. 1987. Bacterial evolution. *Microbiol. Rev.* **51:** 221-271.

Wolfaardt, G. M., J. R. Lawrence, R. D. Robarts, S. J. Caldwell, and D. E. Caldwell. 1994. Multicellular organization in a degradative biofilm community. *Appl. Environ. Microbiol.* **60:** 434-446.

Yamamoto, S., J. B. Alcauskus, and T. E. Crozier. 1976. Solubility of methane in distilled water and seawater. *J. Chem. Eng. Data* **21:** 78-80.

Ytow, N., and H. Seki. 1996. Microcolonization mechanism of attached bacteria in a natural water-column. *J. Oceanog.* **52:** 207-219.

Zimmerman, R., R. Iturriage, and J. Becker-Brick. 1978. Simultaneous determination of the total number of aquatic bacteria and the number thereof involved in respiration. *Appl. Environ. Microbiol.* **36:** 926-935.

ZoBell, C. E. 1940. The effect of oxygen tension on the rate of oxidation of organic matter in sea water by bacteria. *J. Mar. Res.* **3:** 211-213.

ZoBell, C. E. 1946. Marine Microbiology. Chronica Botanica, Waltham, Massachusetts. 240pp.

ZoBell, C. E., and D. Q. Anderson. 1936. Observations on the multiplication of bacteria in different volumes of stored sea water and the influence of oxygen tension and solid surface. *Biol. Bull.* **71:** 324-342.

Zumstein, J., and J. Buffle. 1989. Circulation of epdogenic and aquagenic organic matter in a eutrophic lake. *Wat. Res.* **23:** 229-239.

TABLES AND FIGURES

Table 1. Limnological characteristics of Lake Nojiri.

Surface area [km^2]	4.4
Volume [$10^6 m^3$]	95.7
Maximum depth [m]	38.5
Mean depth [m]	21
Length of shoreline [km]	13.6
Altitude of lake surface [m]	645
Turnover time of water [year]	2.0
Catchment area [km^2]	8.2

Table 2. Limnological characteristics of Lake Kasumigaura.

Surface area [km^2]	168
Volume [$10^6 m^3$]	662
Maximum depth [m]	7.3
Mean depth [m]	4
Length of shoreline [km]	121
Altitude of lake surface [m]	0
Turnover time of water [year]	0.55
Catchment area [km^2]	1,597

Table 3. Analytical parameters for the automatic dissolved methane analyzer.

Gas Chromatograph	
Detector	Flame Ionization Detector
Detector temperature	70°C
Gas chromatograph column	Porapak Q (80/100 mesh), 4 mm o.d., 3 mm i.d. 1 m pre-column, 3 m main-column
Oven temperature	45°C
Carrier gas	30 ml min^{-1}, N_2
Purge and Trap System	
Absorption-desorption column	Unibeads C (80/100 mesh)
Absorption temperature	-40°C
Desorption temperature	120°C
Purge gas	60 ml min^{-1}, He
Purge time	5.5 min

Table 4. Box model used to the whole lake value of methane in Lake Kasumigaura.

box	area (km^2)	volume (km^3)	mean depth (m)
station 1	3.4	0.0050	1.5
station 3	19.1	0.0637	3.3
station 7	19.0	0.0518	2.7
station 9	114.0	0.4952	4.3
station 12	12.0	0.0272	2.3
whole lake	167.6	0.6430	3.8

Table 5. Measurement of specific methane oxidation rate by incubation experiment of lake water taken at Station 9 in Lake Kasumigaura.

Sta. 9 date	incubation time (hr)	specific oxidation rate (hr^{-1})	r^2	
95/04/12	26	0.006	0.922	(n=4)
95/06/07	10	0.089	0.996	(n=3)
95/07/12	10	0.081	0.993	(n=4)
95/08/09	10	0.158	0.996	(n=4)
95/09/06	11	0.109	0.999	(n=3)
95/10/04	9	0.102	0.999	(n=3)
95/11/08	5	0.204	0.997	(n=3)
95/12/06	5	0.073	0.964	(n=3)
96/01/16	9	0.012	0.953	(n=3)
96/02/07	11	0.013	0.946	(n=3)
96/03/06	23	0.007	0.955	(n=3)

Table 6. Comparison of diffusive flux to the atmosphere and CH_4 oxidation as sinks for water column CH_4 during lake overturn period in Lake Nojiri.

date	CH_4 conc[a].	wind velocity[b]	total CH_4	EMISSION		OXIDATION	
	nM	($m\ s^{-1}$)	($kg\ CH_4\ lake^{-1}$)	($kg\ CH_4\ lake^{-1}\ day^{-1}$)	($mg\ CH_4\ m^{-2}\ day^{-1}$)	($kg\ CH_4\ lake^{-1}\ day^{-1}$)	($mg\ CH_4\ m^{-2}\ day^{-1}$)
94/12/10	66.3	3.7	5960	3.30	0.751	1470	334
94/12/20	249	1.1	688	3.56	0.809	273	62.0
94/12/23	329	0.5	648	3.73	0.847	187	42.5
94/12/29	294	2.7	399	7.52	1.71	70.2	16.0
95/01/03	145	2.0	219	3.03	0.689	38.0	8.6
95/01/20	72.6	1.0	116	0.63	0.144	5.4	1.2

[a] Methane concentration data is for 0.5 m depth.

[b] Wind velocity is daily average.

Table 7. Monthly change of water temperature, specific methane oxidation rate and methane consumption rate in Lake Kasumigaura. Values are mean and standard deviation of inter-annual variation.

Sta. 3 month	water temperature (°C)	specific oxidation rate (hr^{-1})	consumption rate (nM CH_4 hr^{-1})	
Jan.	5.8 ± 0.7	0.011 ± 0.005	2.9 ± 1.5	(n=5)
Feb.	4.8 ± 1.2	0.007 ± 0.005	1.0 ± 0.5	(n=6)
Mar.	8.0 ± 0.8	0.005 ± 0.004	0.7 ± 0.6	(n=5)
Apr.	13.6 ± 1.0	0.006 ± 0.008	1.0 ± 1.7	(n=5)
May	18.3 ± 1.1	0.009 ± 0.011	0.8 ± 0.9	(n=4)
Jun.	22.7 ± 1.9	0.033 ± 0.026	5.0 ± 3.8	(n=5)
Jul.	25.5 ± 2.3	0.015 ± 0.012	2.4 ± 1.7	(n=5)
Aug.	27.6 ± 3.1	0.056 ± 0.040	18.1 ± 24.9	(n=5)
Sept.	25.6 ± 1.6	0.126 ± 0.072	45.6 ± 36.5	(n=5)
Oct.	19.9 ± 1.5	0.108 ± 0.045	13.7 ± 8.0	(n=5)
Nov.	14.1 ± 1.1	0.093 ± 0.062	10.4 ± 8.8	(n=5)
Dec.	9.7 ± 1.0	0.045 ± 0.028	7.2 ± 5.5	(n=6)

Sta. 9 month	water temperature (°C)	specific oxidation rate (hr^{-1})	consumption rate (nM CH_4 hr^{-1})	
Jan.	5.6 ± 0.6	0.007 ± 0.005	2.9 ± 3.1	(n=5)
Feb.	4.6 ± 1.2	0.007 ± 0.004	1.1 ± 0.7	(n=5)
Mar.	7.5 ± 0.6	0.005 ± 0.005	0.9 ± 1.0	(n=5)
Apr.	12.5 ± 0.8	0.004 ± 0.002	0.3 ± 0.2	(n=4)
May	17.2 ± 0.8	0.022 ± 0.025	2.5 ± 3.0	(n=4)
Jun.	21.9 ± 1.8	0.032 ± 0.036	2.4 ± 2.0	(n=4)
Jul.	24.5 ± 1.9	0.042 ± 0.024	4.7 ± 1.7	(n=5)
Aug.	27.1 ± 3.0	0.080 ± 0.053	13.8 ± 6.5	(n=6)
Sept.	25.5 ± 1.4	0.071 ± 0.040	14.5 ± 8.3	(n=6)
Oct.	20.0 ± 1.5	0.070 ± 0.021	8.4 ± 6.0	(n=5)
Nov.	14.1 ± 1.0	0.090 ± 0.078	8.5 ± 8.9	(n=5)
Dec.	9.9 ± 0.9	0.033 ± 0.025	3.9 ± 2.1	(n=5)

Table 8. Comparison of methane consumption rate and diffusive flux to the atmosphere as sinks for water column methane, and turnover time of dissolved methane in the water column of Lake Kasumigaura. Values are mean and standard deviation of inter-annual variation.

month	methane consumption rate ($mg\ CH_4\ m^{-2}\ day^{-1}$)	diffusive flux ($mg\ CH_4\ m^{-2}\ day^{-1}$)	turnover time (day)
Jan.	4.4 ± 4.0 (n=5)	2.6 ± 1.5 (n=6)	3.0
Feb.	1.4 ± 0.9 (n=6)	2.1 ± 1.8 (n=6)	3.7
Mar.	1.2 ± 1.5 (n=6)	2.7 ± 1.1 (n=6)	2.9
Apr.	0.6 ± 0.6 (n=5)	1.9 ± 0.8 (n=6)	2.2
May	1.4 ± 1.9 (n=4)	3.1 ± 0.8 (n=6)	1.9
Jun.	4.9 ± 6.2 (n=5)	3.7 ± 1.6 (n=6)	1.0
Jul.	6.2 ± 5.9 (n=5)	4.5 ± 6.4 (n=6)	1.2
Aug.	48.2 ± 51.5 (n=5)	12.0 ± 7.1 (n=6)	0.4
Sept.	37.0 ± 19.6 (n=5)	10.8 ± 4.8 (n=6)	0.4
Oct.	19.0 ± 8.9 (n=5)	4.5 ± 1.6 (n=6)	0.5
Nov.	15.9 ± 14.1 (n=5)	1.1 ± 0.6 (n=6)	0.3
Dec.	7.2 ± 3.1 (n=5)	1.9 ± 1.4 (n=6)	1.3
annual average	12.3 ± 15.5	4.2 ± 3.5	1.6

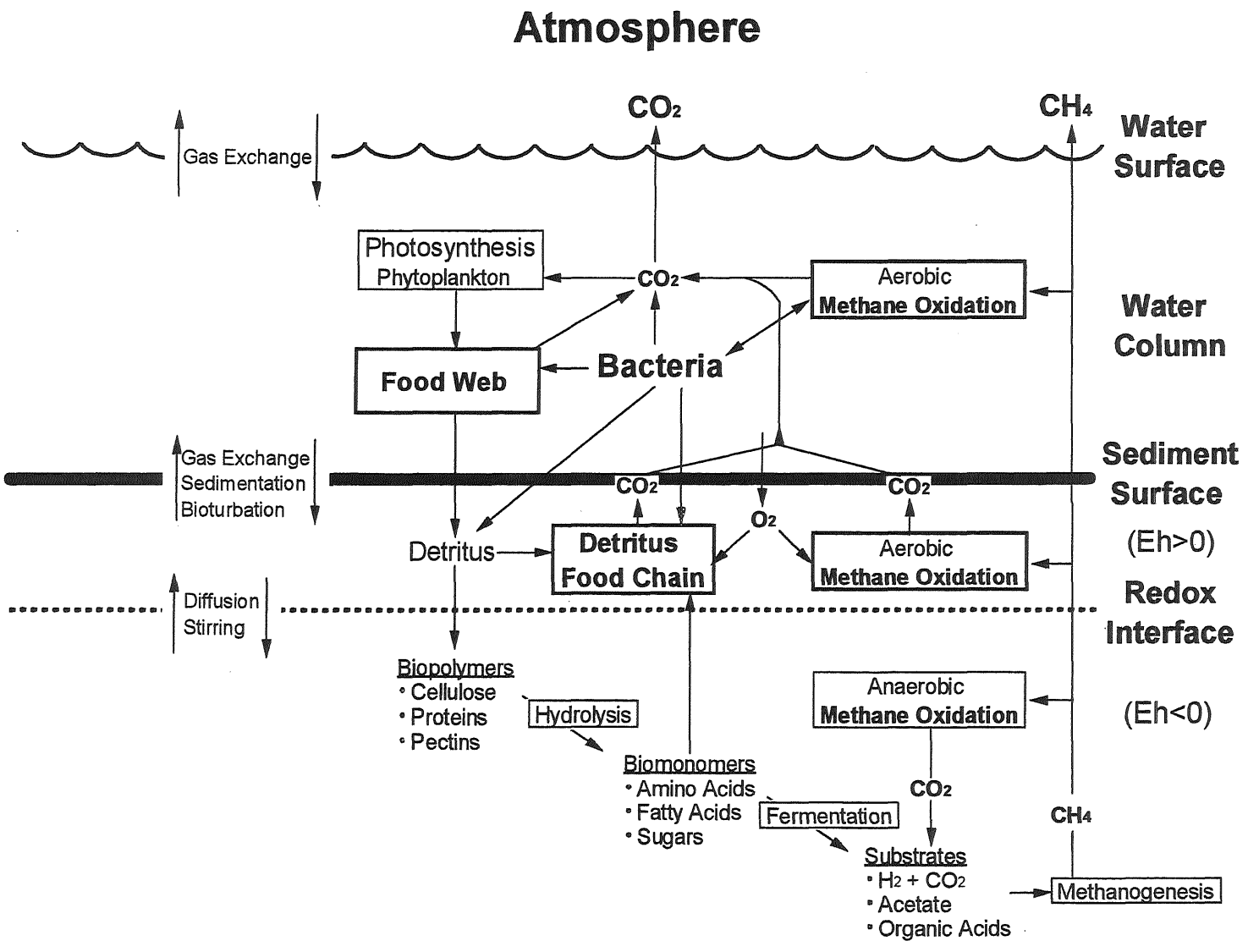

Figure 1. Food web, detritus food chain, production and oxidation of methane in the aquatic environment.

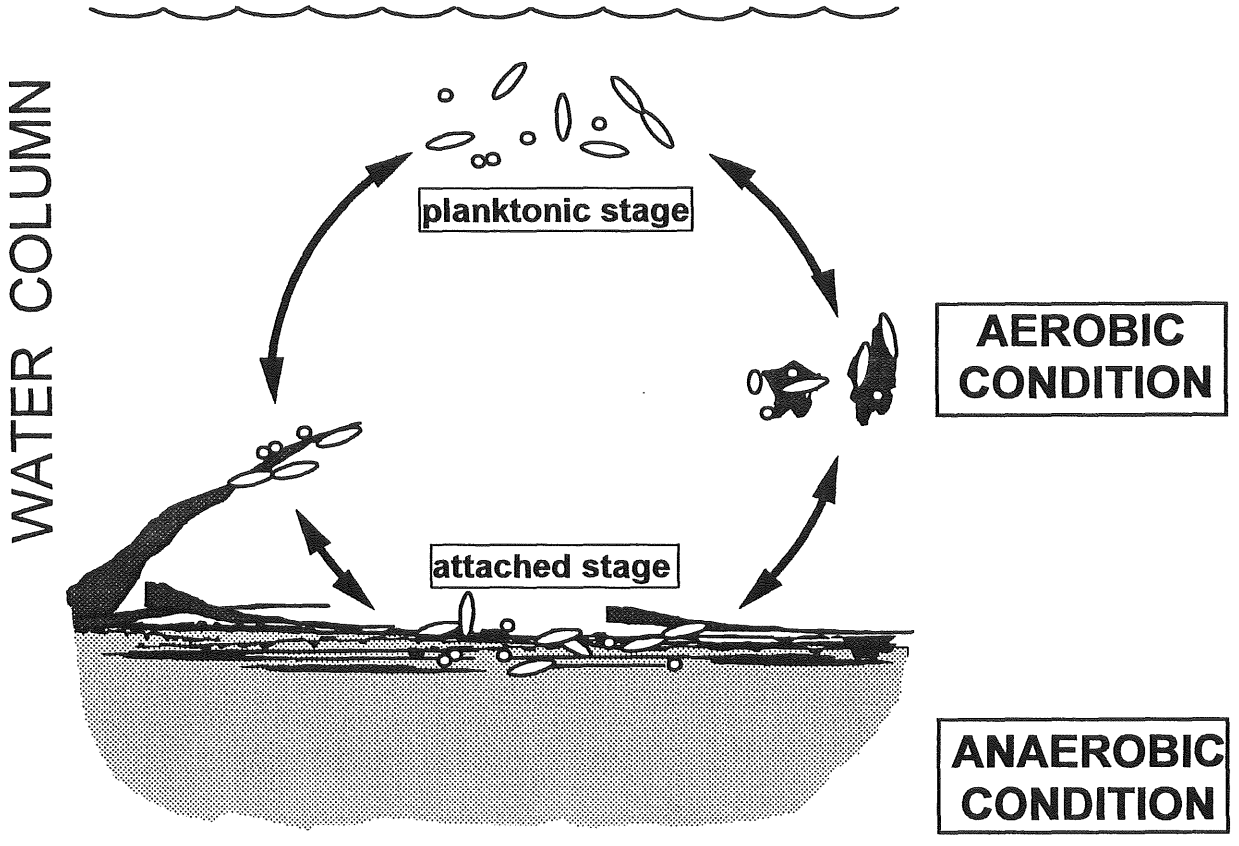

Figure 2. Planktonic and attached stages of the cell cycle in aquatic environments.

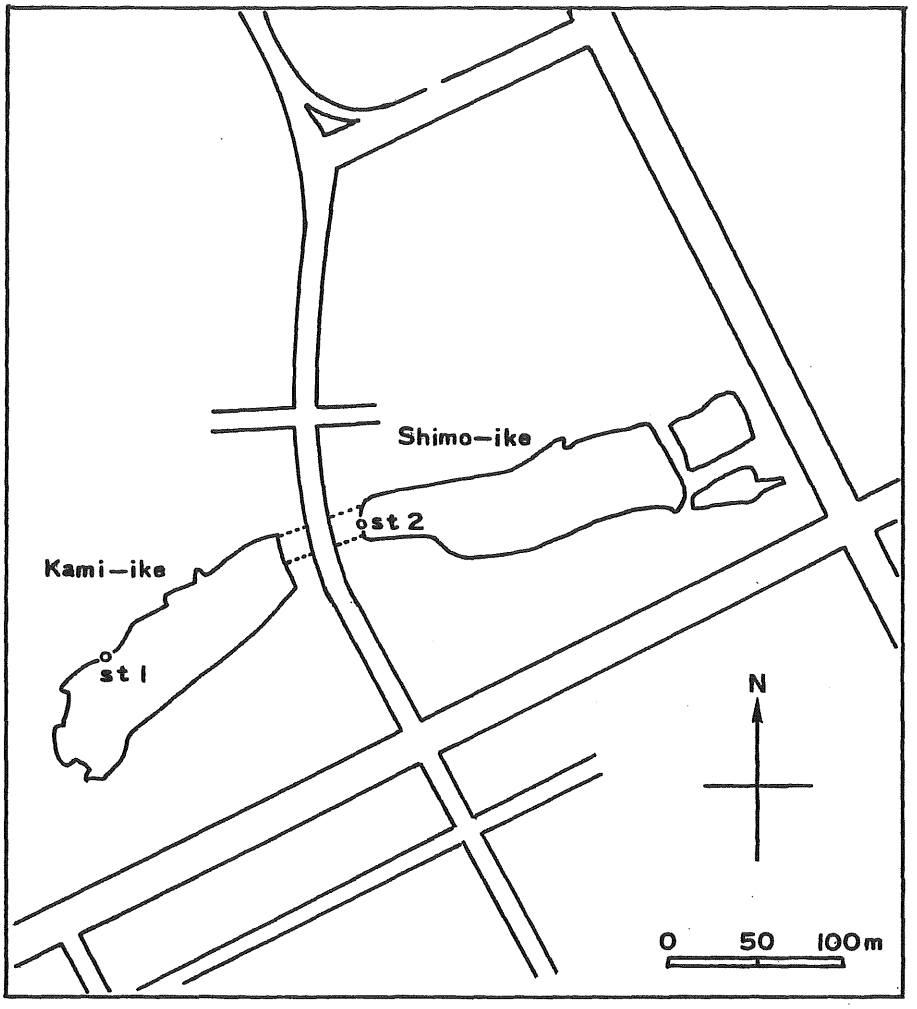

Figure 3. Station locations in the two basins of Matsumi-ike Bog in the campus of the University of Tsukuba.

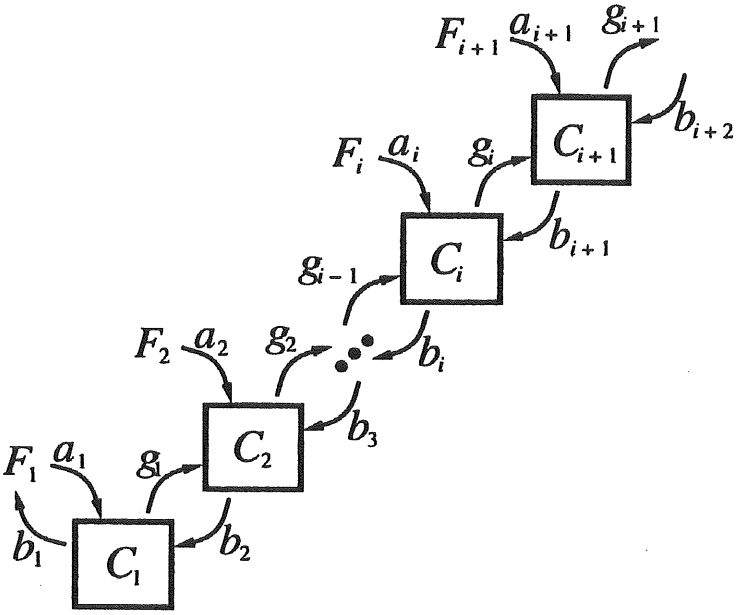

Figure 4. Schematic bacterial processes in the model. C, density of bacterial microcolonies on the substratum; F, density of bacterial particles in water; a, g, b are rate coefficients of attachment, growth and detachment of bacteria, respectively. Suffixes denote the number of bacterial cells in the microcolonies of attached bacteria or bacterial particles in water associating with the substratum. The bacterial microcolonies "step up" to larger colonies by bacterial growth and "step down" to smaller microcolonies by bacterial detachment. These growth, detachment and attachment processes change the microcolony number of each size.

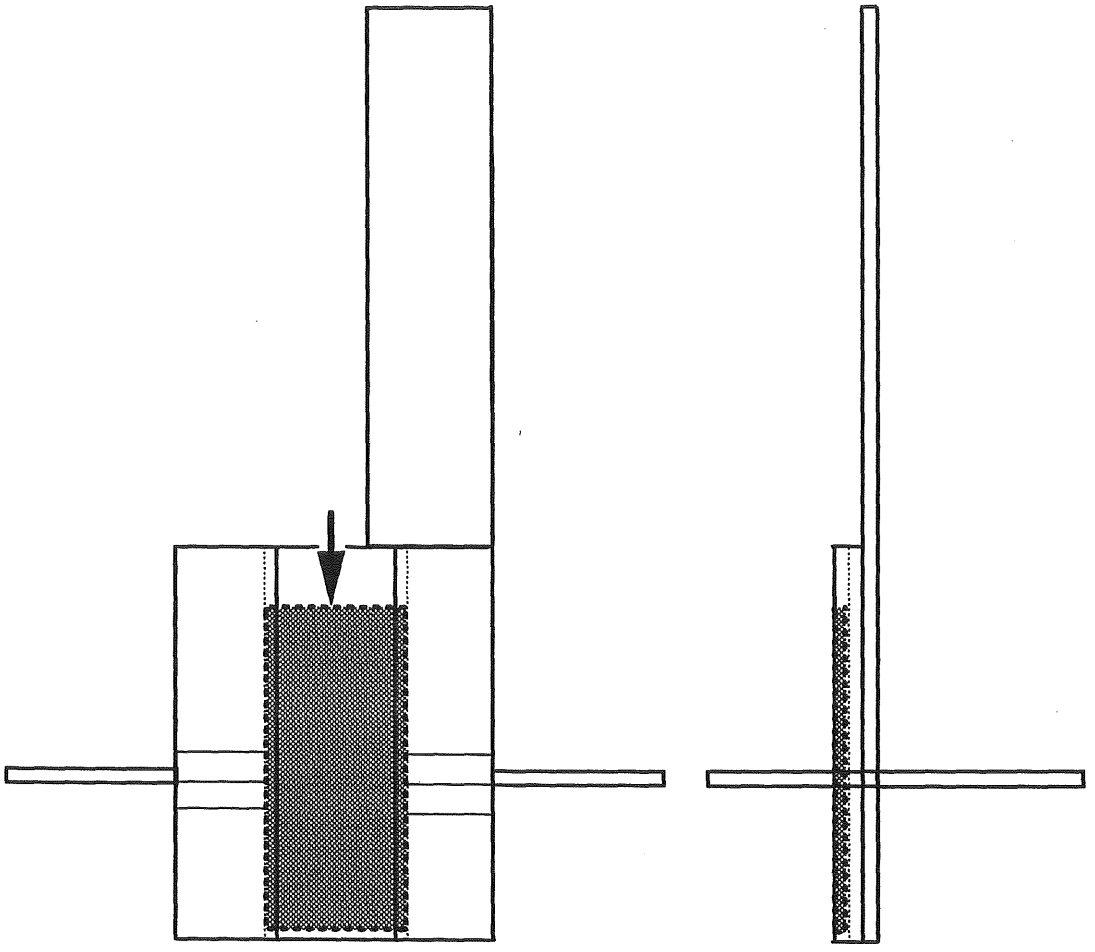

Figure 5. The slide holder for the bacterial attachment at the boundary layer between water column and bottom sediment. A glass slide insert as followed the arrowhead.

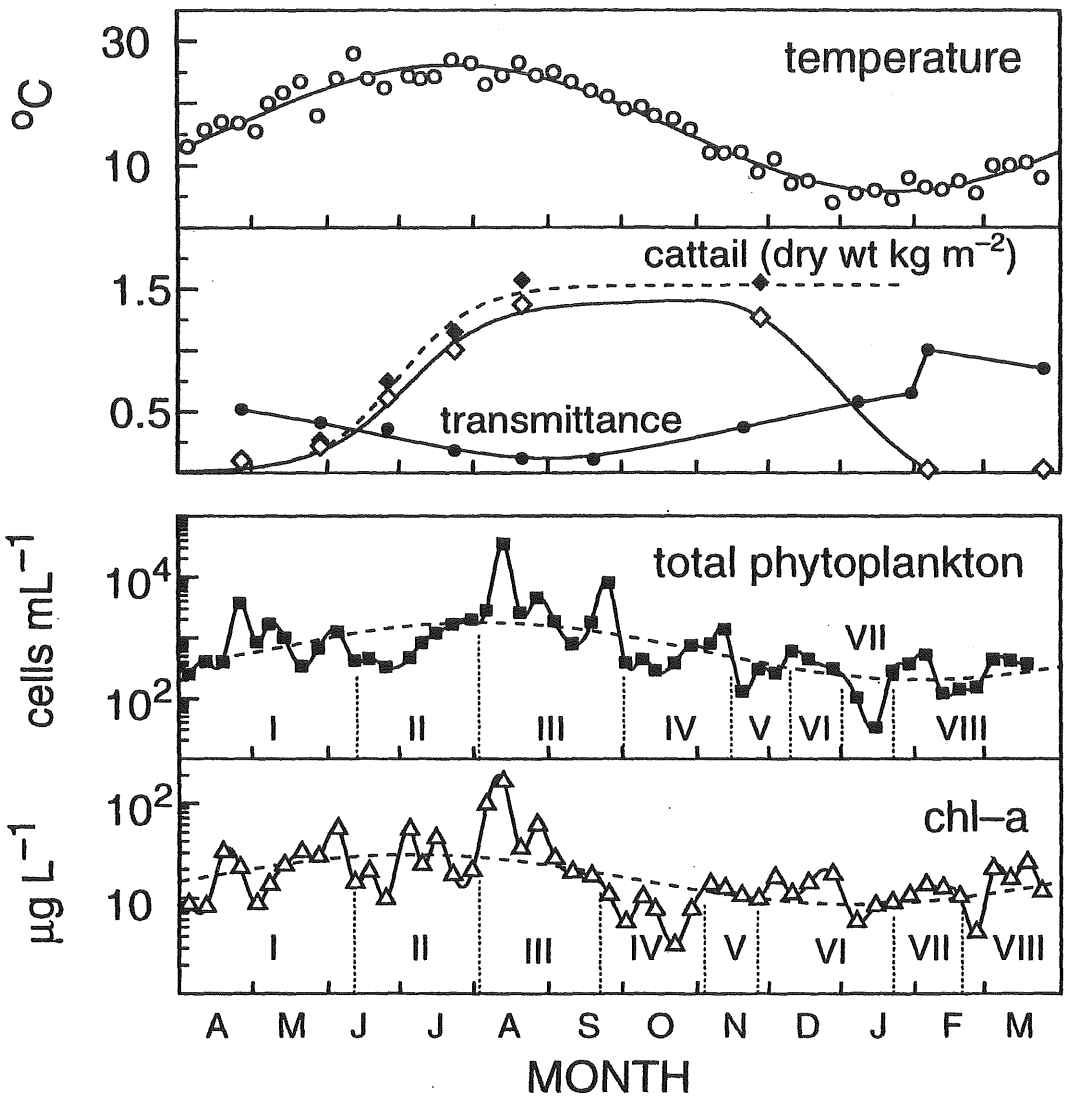

Figure 6. Water temperature, optical transmittance through cattail, biomass of total cattail (closed diamond) and leaves (open diamond), total phytoplankton and chlorophyll-a in Matsumi-ike Bog from 1991 to 1992. I, II, III, IV, V, VI, VII, VIII: inter peak internal of fluctuation (total phytoplankton or chlorophyll-a).

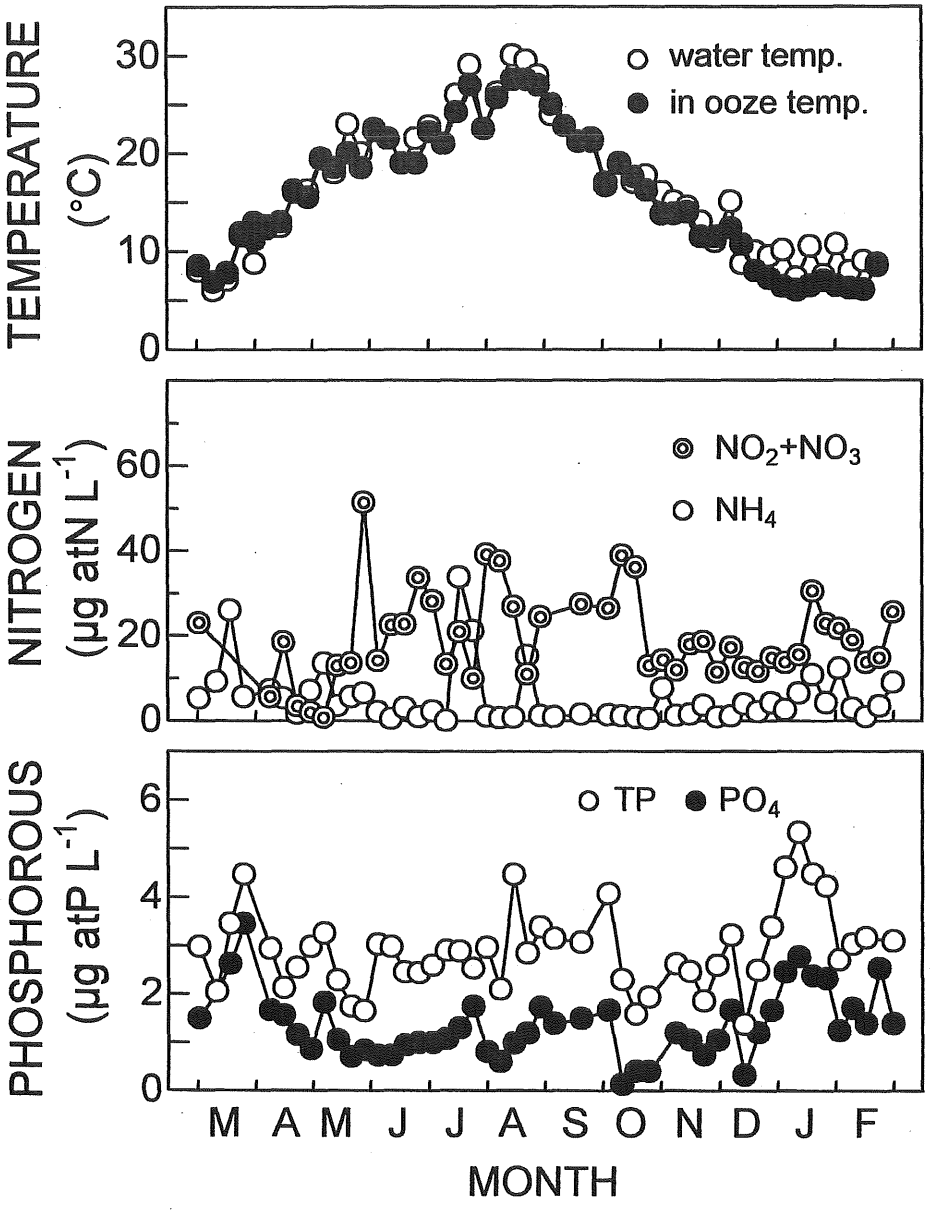

Figure 7. Seasonal fluctuation of the physico-chemical parameters in Matsumi-ike Bog from May 1992 to February 1993.

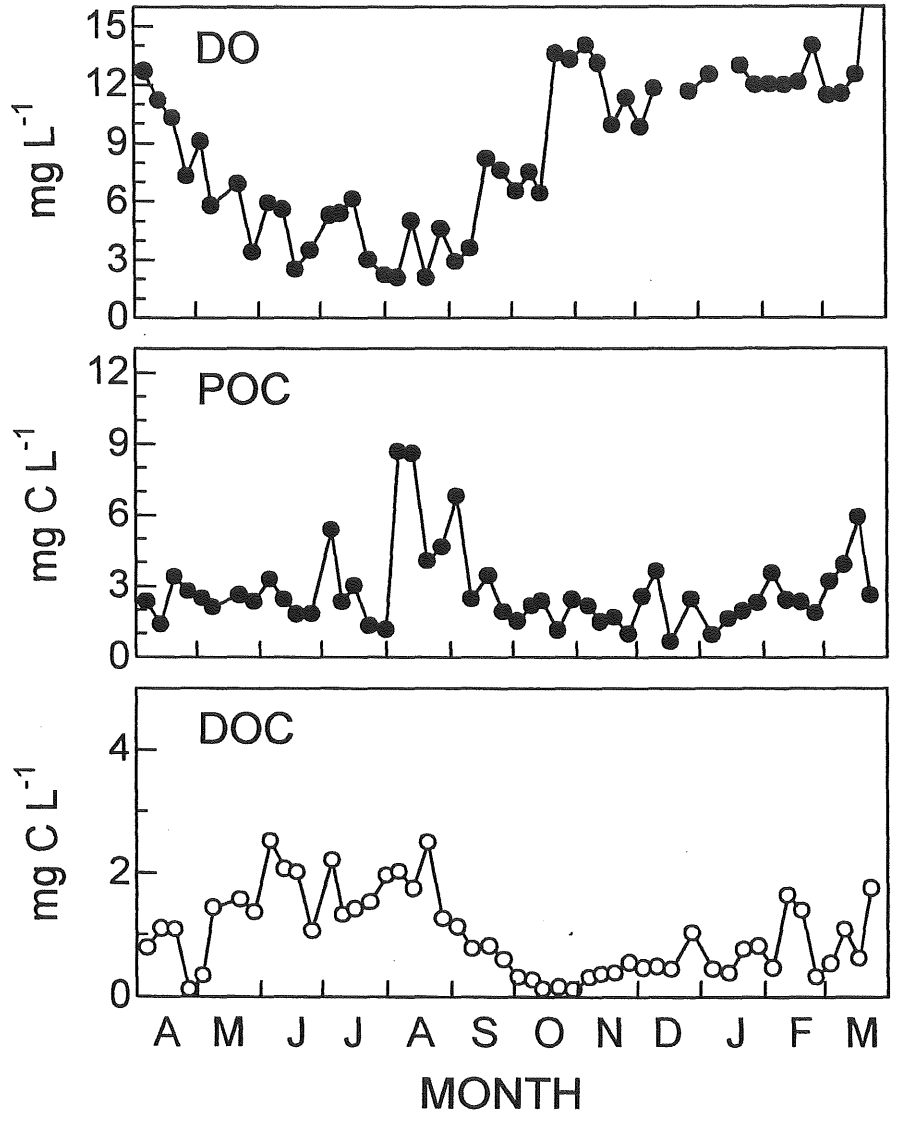

Figure 8. Seasonal fluctuation of the environmental factors (DO, POC and DOC) in Matsumi-ike Bog from April 1991 to March 1992.

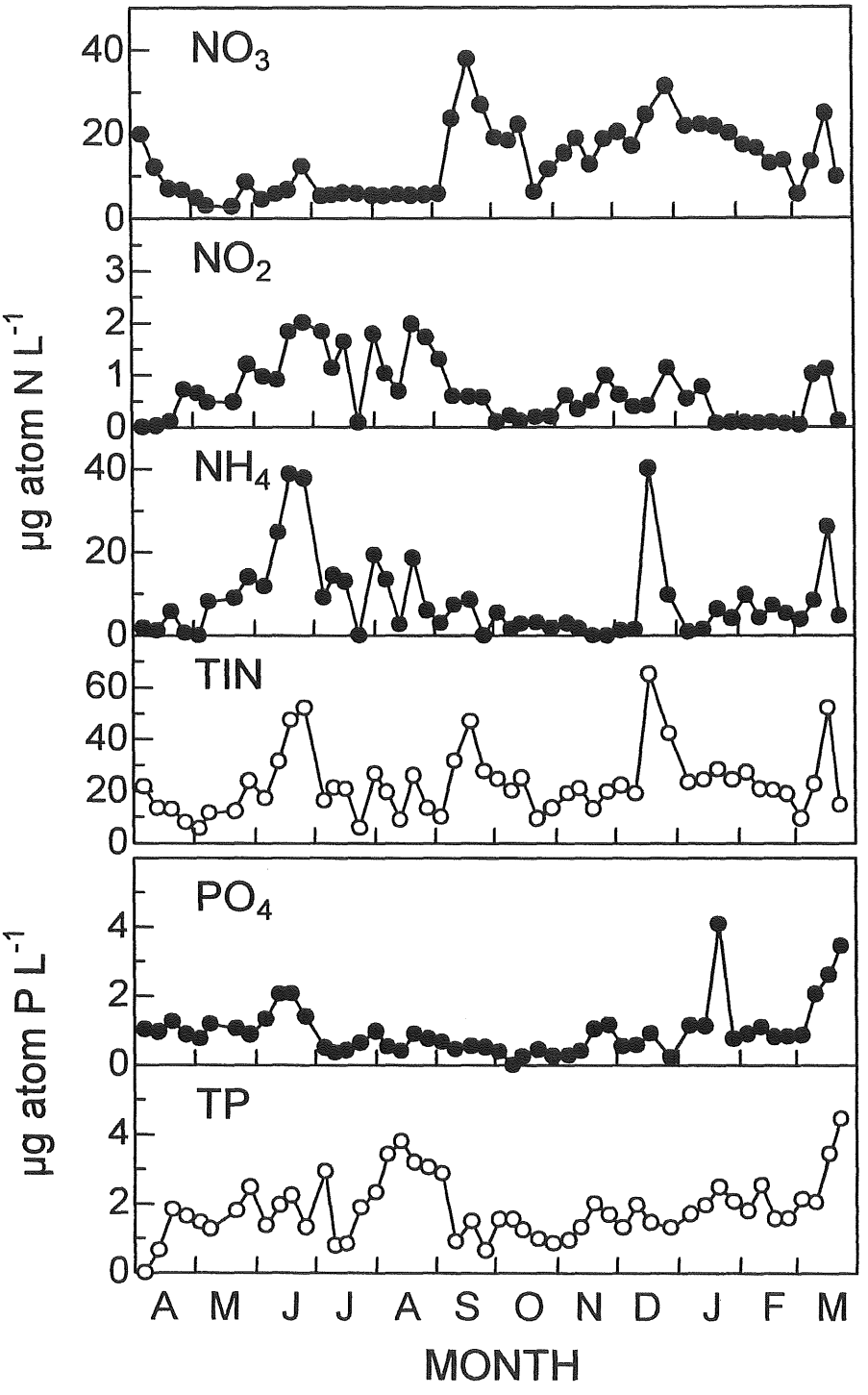

Figure 9. Seasonal fluctuation of the environmental factors (nutrients) in Matsumi-ike Bog from April 1991 to March 1992.

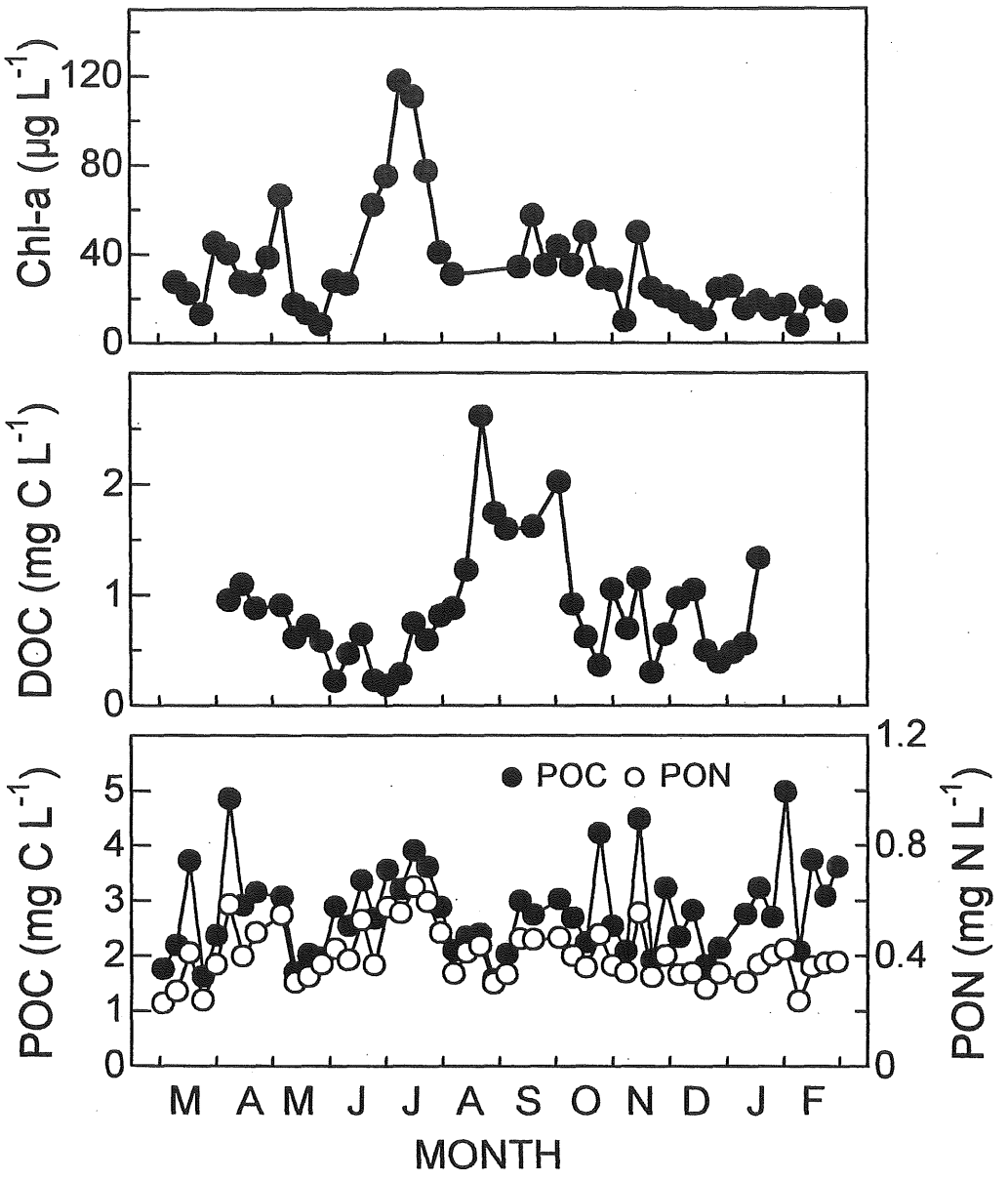

Figure 10. Seasonal fluctuation of chlorophyll-a, DOC, POC and PON in the bog water of Matsumi-ike Bog from May 1992 to February 1993.

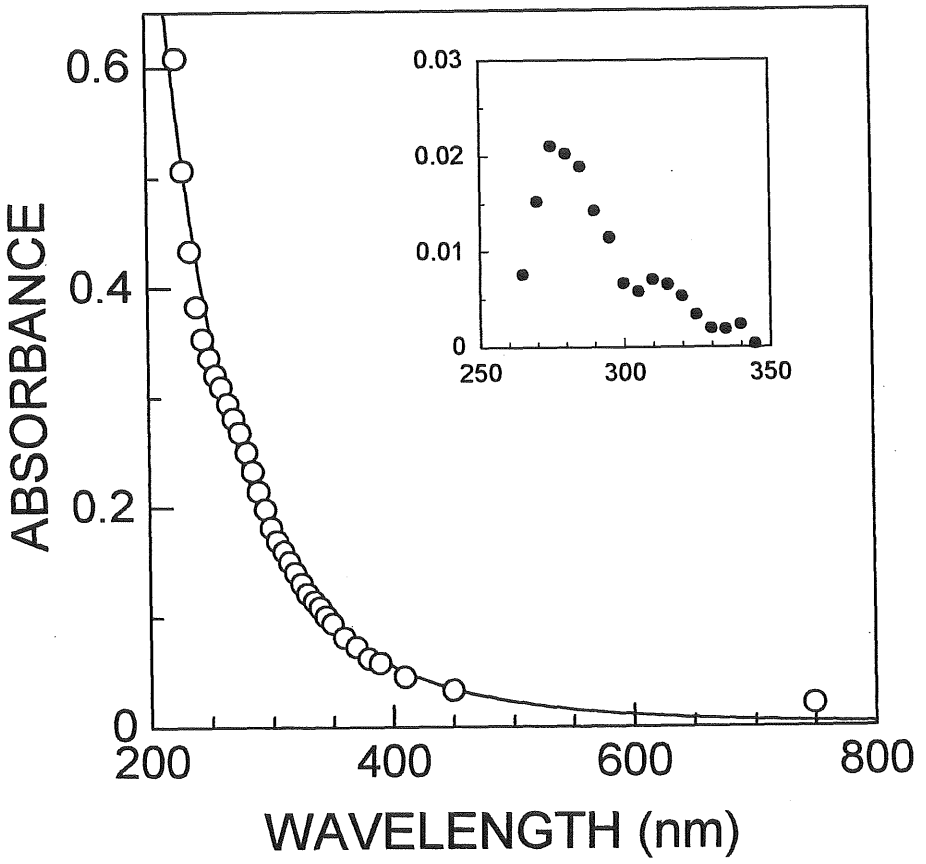

Figure 11. Optical density spectra of DOM. Symbols indicate measured optical density at the corresponding wavelength. The spectrum shows λ^{-4} dependency (solid line). This dependency indicates that molecular scattering is a major contribution to the optical density. The residue to the regression is shown in the insertion. It shows two absorption maxima at 280 nm and 320 nm.

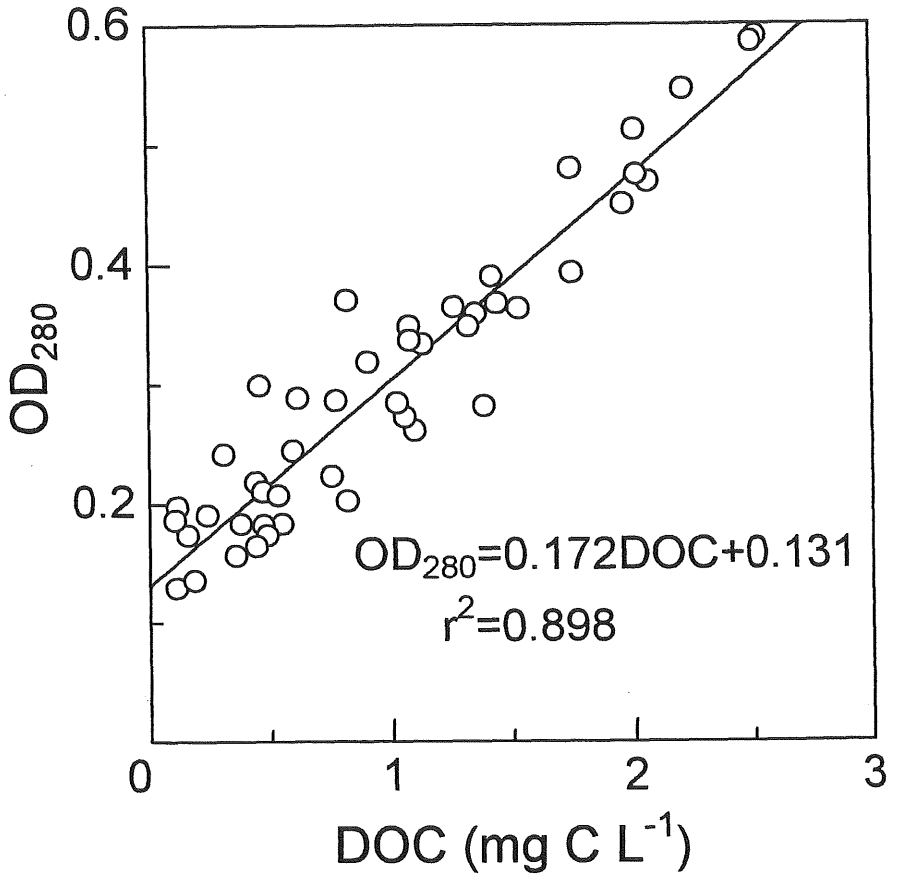

Figure 12. Optical density at the wavelength of 280 nm depends on DOC. The dependency was expressed by a regression of OD_{280} = 0.172 DOC + 0.131 (r^2=0.898), where OD_{280} is optical density at the wavelength of 280 nm and DOC is dissolved organic carbon in mg C l^{-1}, respectively. There was no seasonal variation in the regression.

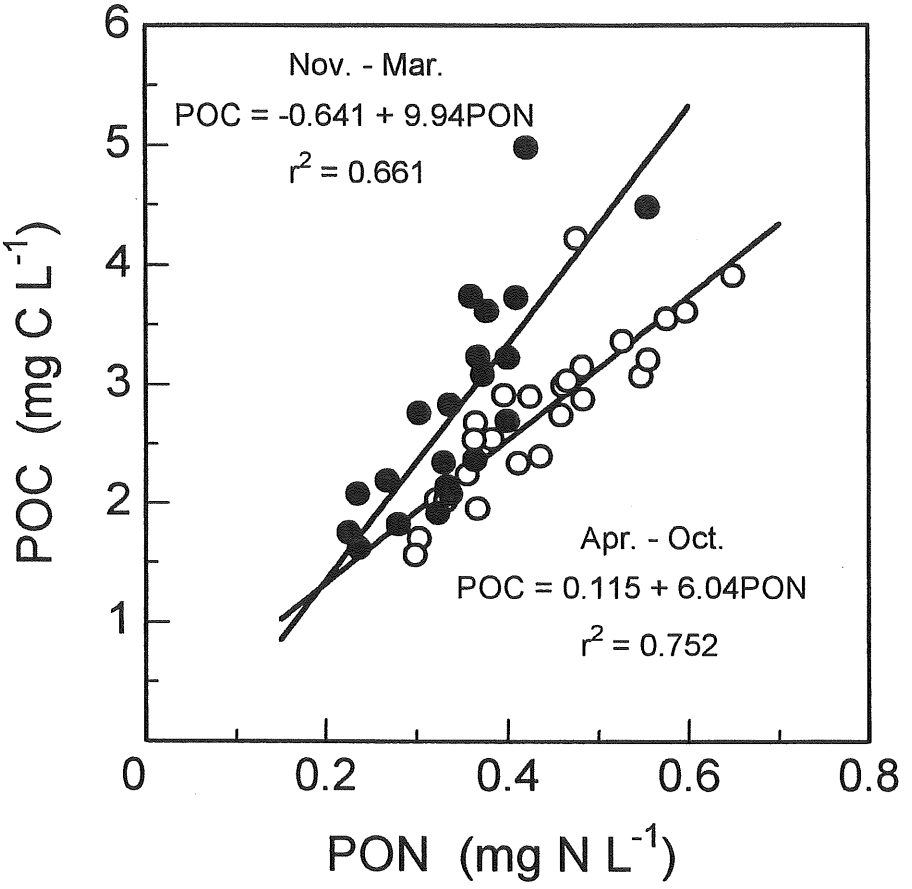

Figure 13. Relationship between the concentration of POC and PON in Matsumi-ike Bog. Open and closed symbols represent data from April to October and those from November to March, respectively.

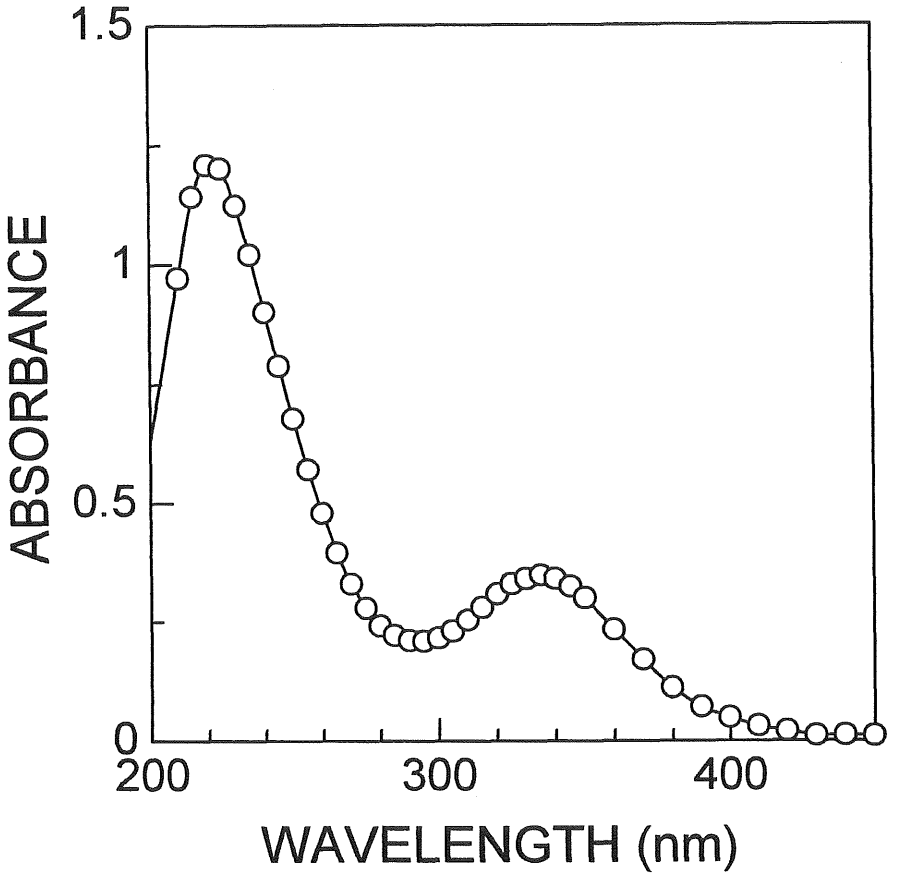

Figure 14. Absorption spectra of the acid extract from POM. Symbols indicate measured optical density at corresponding wavelength. There were two peaks at 220 and 335 nm. The absorption spectra fits the sum of two Lorentz funnctions (solid line).

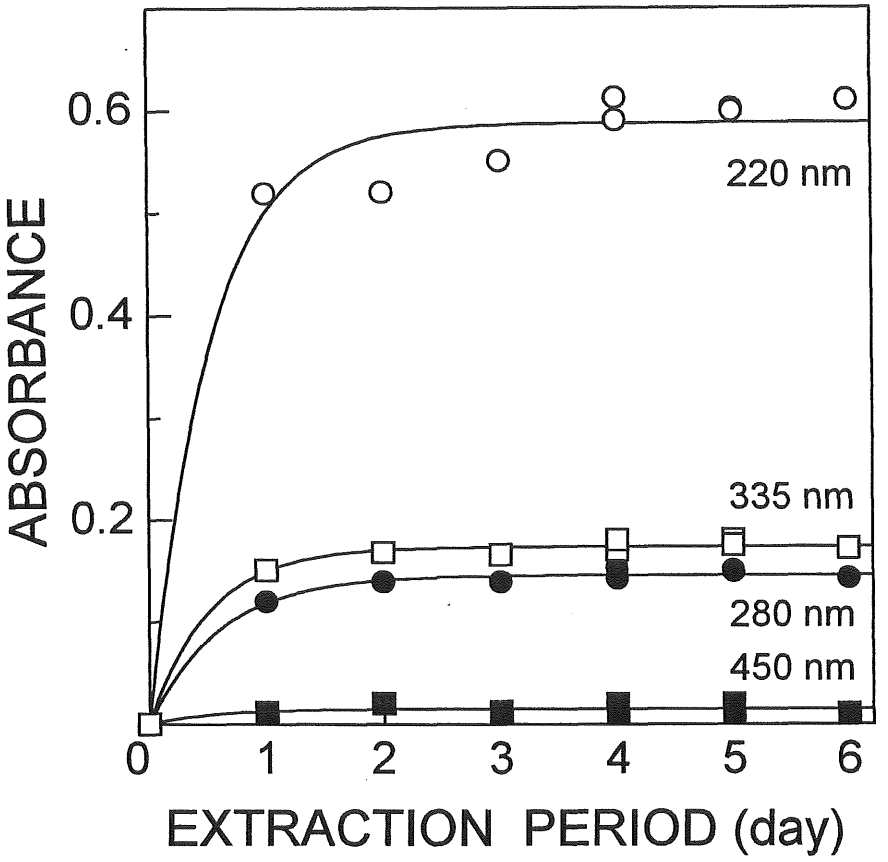

Figure 15. Time course of acid extraction from POM on a glass fiber filter (GF/C) monitored by absorption at several wavelength. The absorption increased exponentially in the initial stage of the extraction. After 3 days extraction, the absorption reached a constant level.

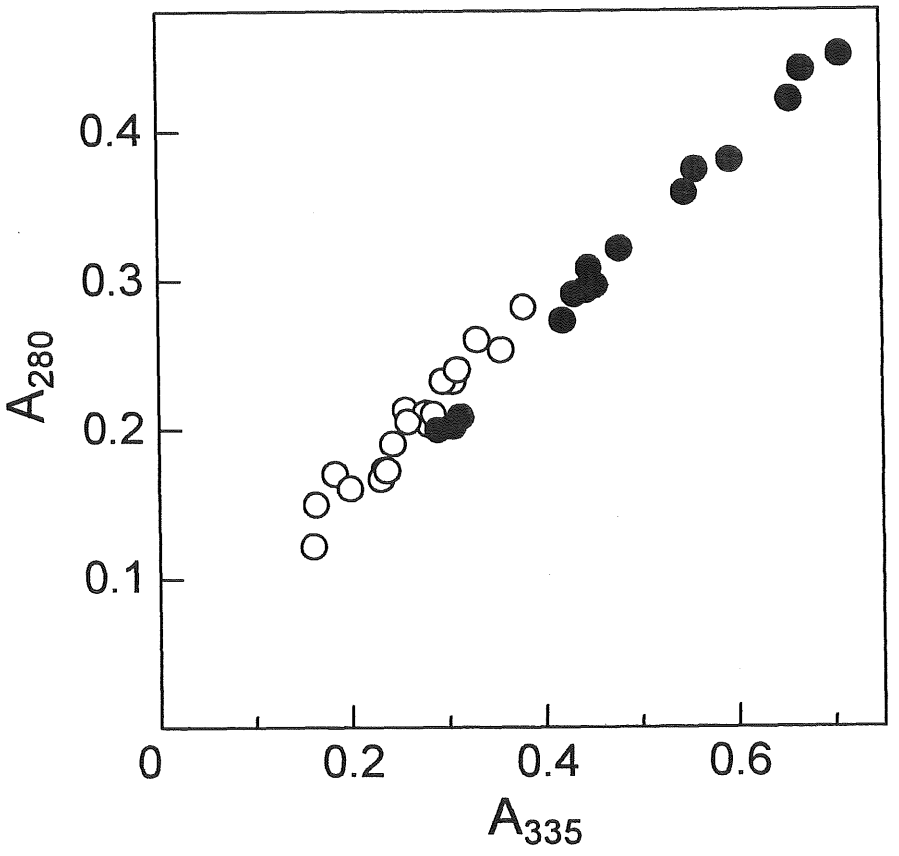

Figure 16. Correlation of absorption maxima of acid extract at wavelength of 280 and 335 nm. Open and closed symbols indicate an absorption ratio A_{280}/A_{335} greater or less than 0.7, respectively. There was tendency that A_{280}/A_{335} were smaller than 0.7 for higher A_{335}.

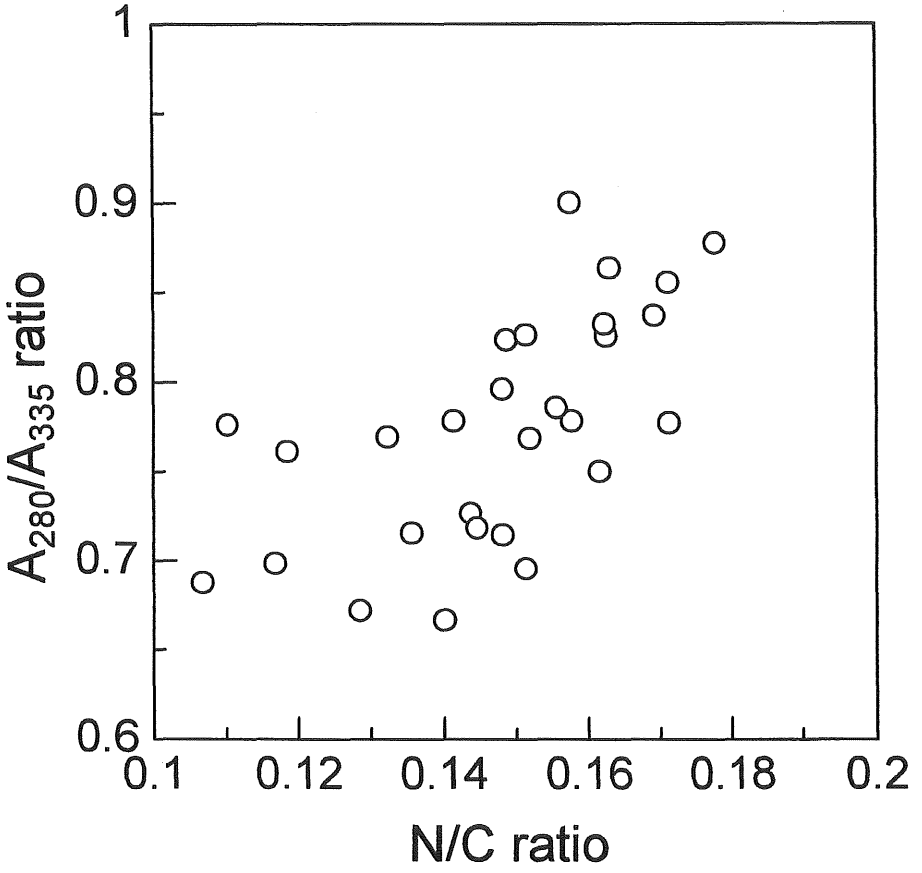

Figure 17. The absorption ratio A_{280}/A_{335} depended on the nitrogen/carbon (N/C) ratio. For N/C ratios less than 0.14 (one nitrogen atom per 7 carbon atoms), the absorption ratio was constant. For N/C ratio greater than 0.14, on the other hand, the ratio increased.

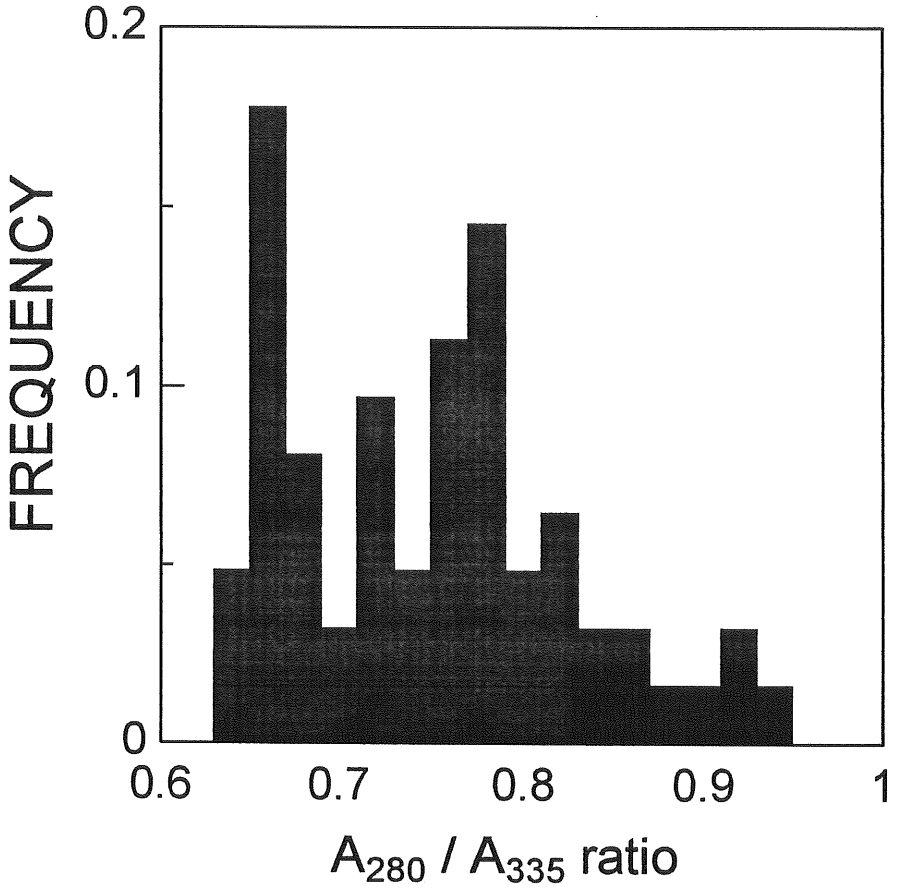

Figure 18. The distribution of the absorption ratio A_{280}/A_{335}. The measurements can be divided into two groups with A_{280}/A_{335} above and below 0.7.

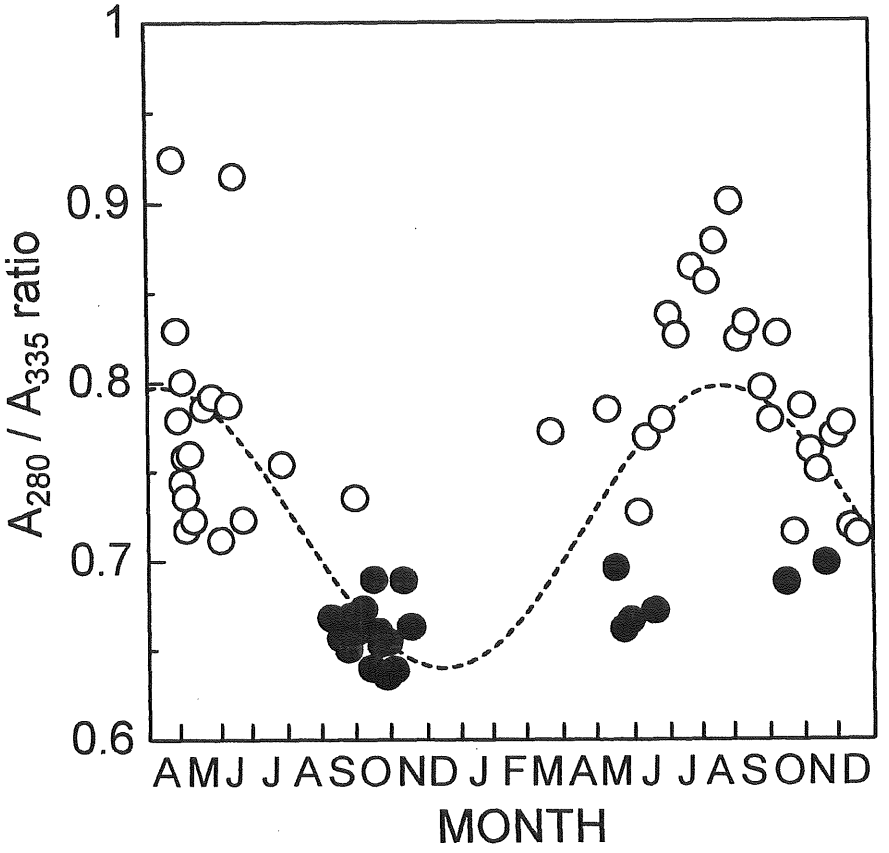

Figure 19. Seasonal fluctuation of the ratio of absorption at wavelengths of 280 nm/335 nm from April 1991 to December 1992. Open and closed symbols indicate a ratio greater or less than 0.7, respectively. The ratio could be expressed as an annual sinusoidal curve with a minimum during autumn. High ratios in April and June corresponded to phytoplankton blooms.

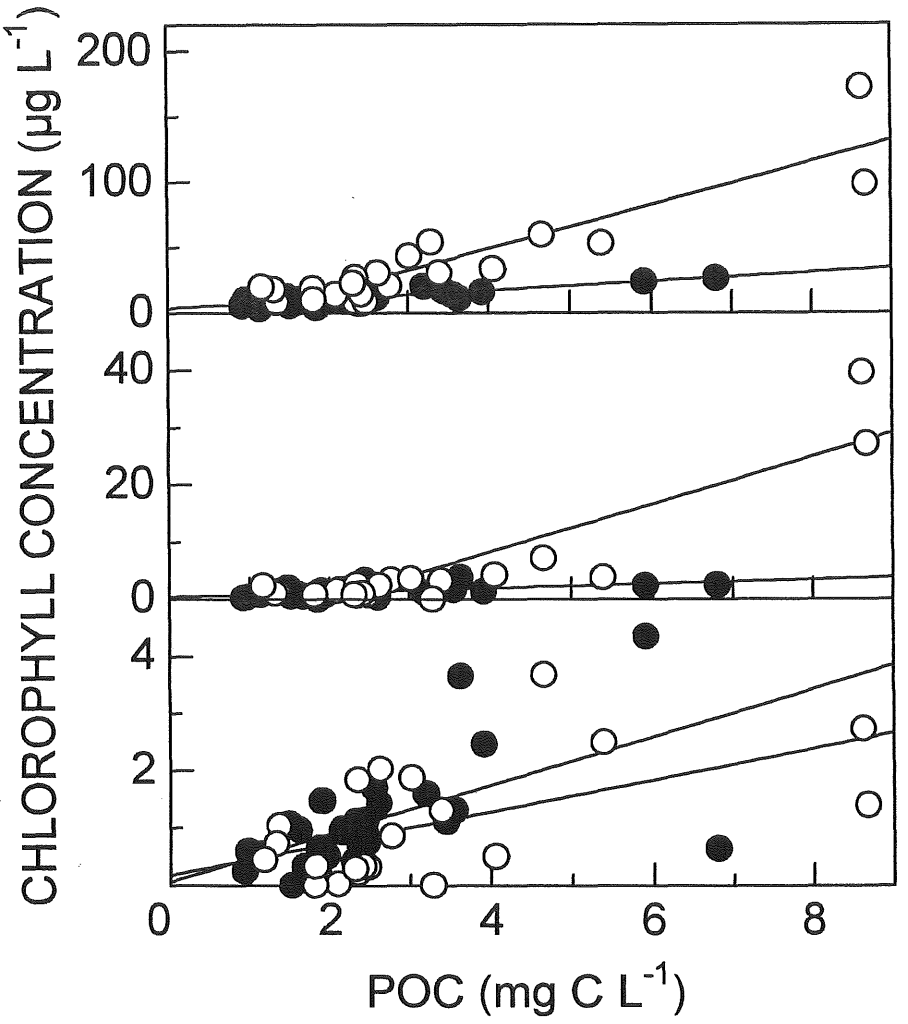

Figure 20. Chlorophyll-a (top), -b (middle) and -c (bottom) dependency on POC. Open and closed symbols indicate the seasons of high and low A_{280}/A_{335}. The dependency of Chlorophyll-a and -b on POC was different according to seasons. The relation between Chlorophyll-c and POC, on the other hand, was independent from the ratio.

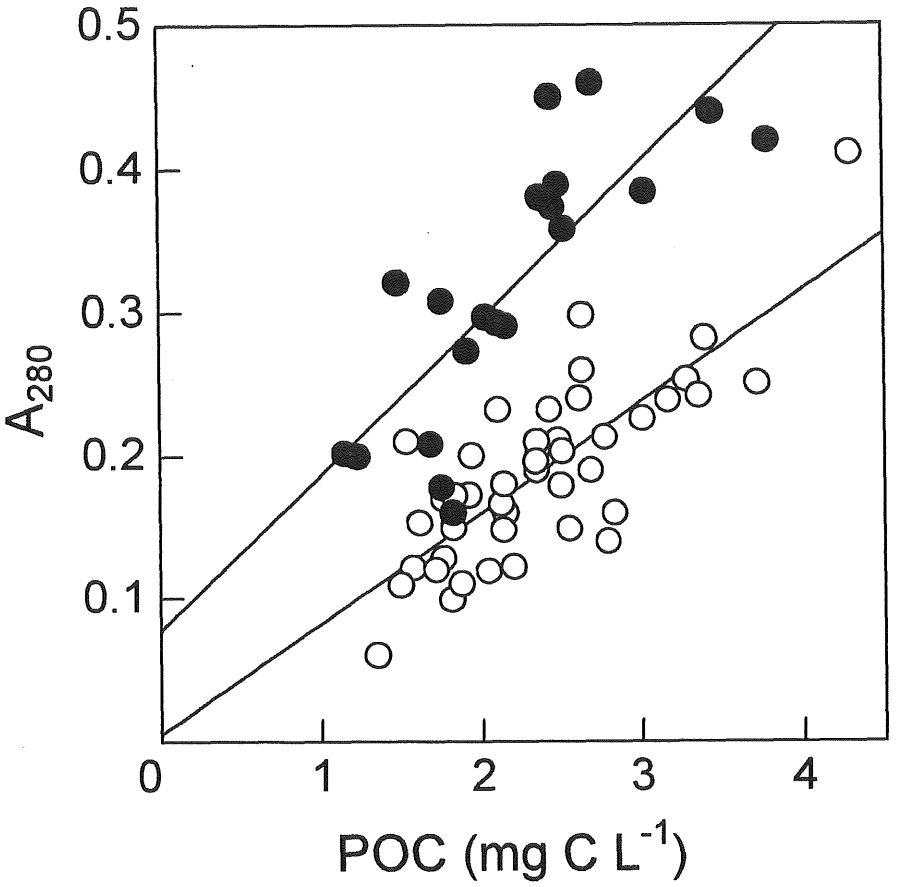

Figure 21. The absorbance of POM acid extraction at wavelength of 280 nm correlated with the POC concentration. Open and closed symbols indicate the absorbance ratio A_{280}/A_{335} greater than 0.7 or less. There was no significant difference in the slopes ($t = 1.671 < t\,(60,0.05) = 2.000$) but in intercept ($t = 11.25 > t\,(60,0.01) = 3.460$).

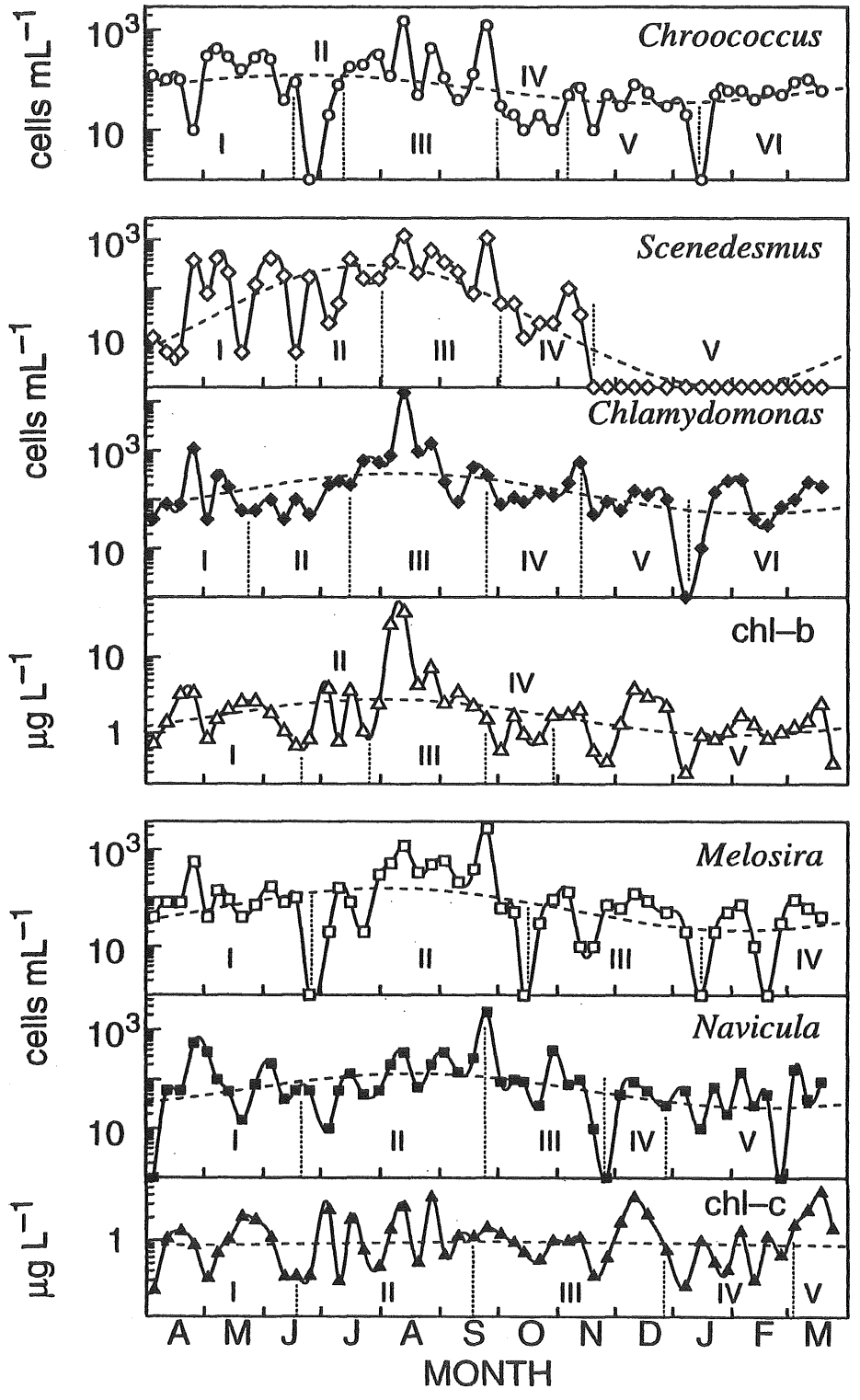

Figure 22. Seasonal fluctuation of dominant phytoplankton and chlorophyll-b and -c in Matsumi-ike Bog from 1991 to 1992. I, II, III, IV, V, VI: inter peak internal of fluctuation (each phytoplankton or chlorophyll).

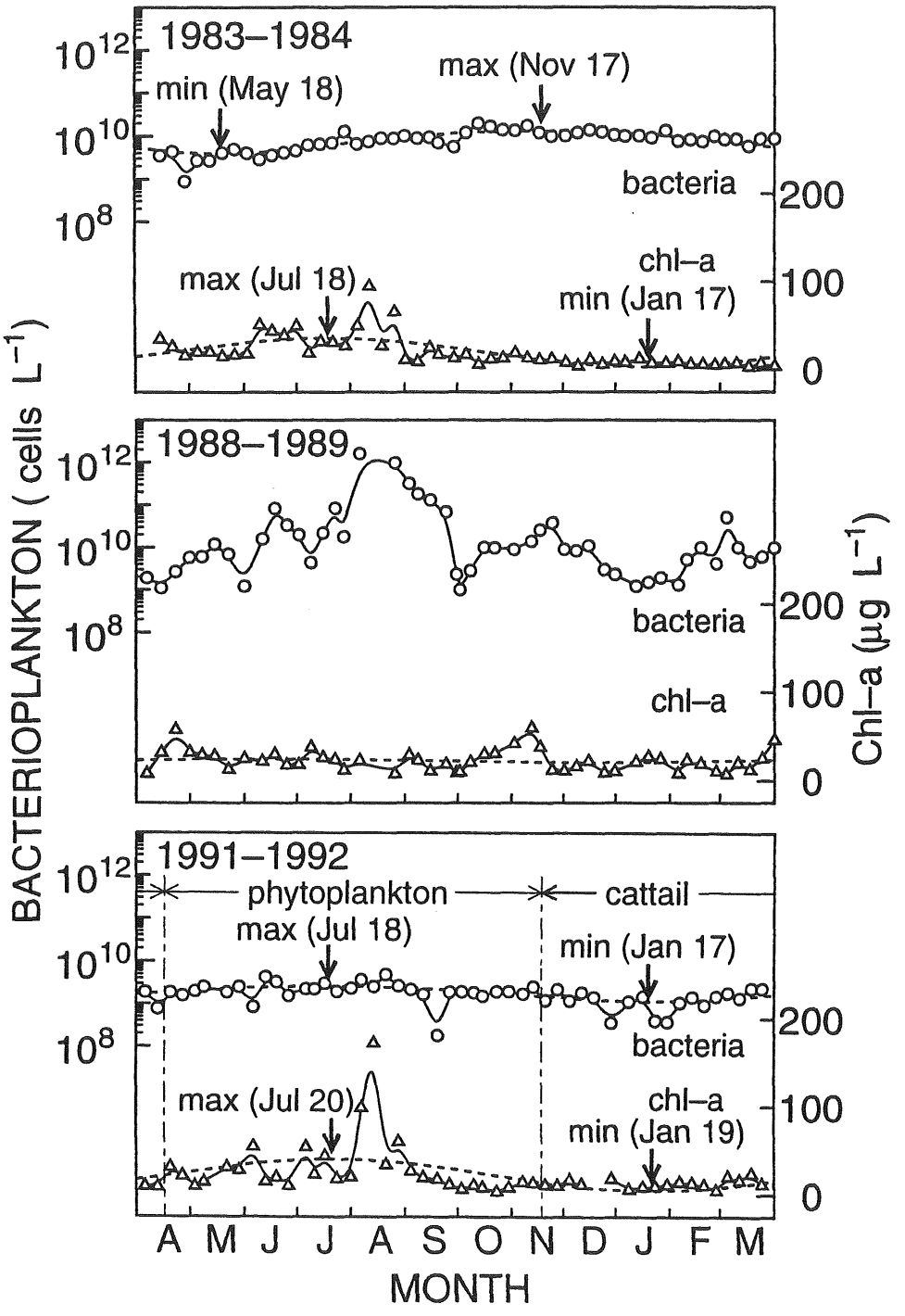

Figure 23. Seasonal fluctuation of the population densities of bacterioplankton and phytoplankton in Matsumi-ike Bog at each stage of limnological succession.

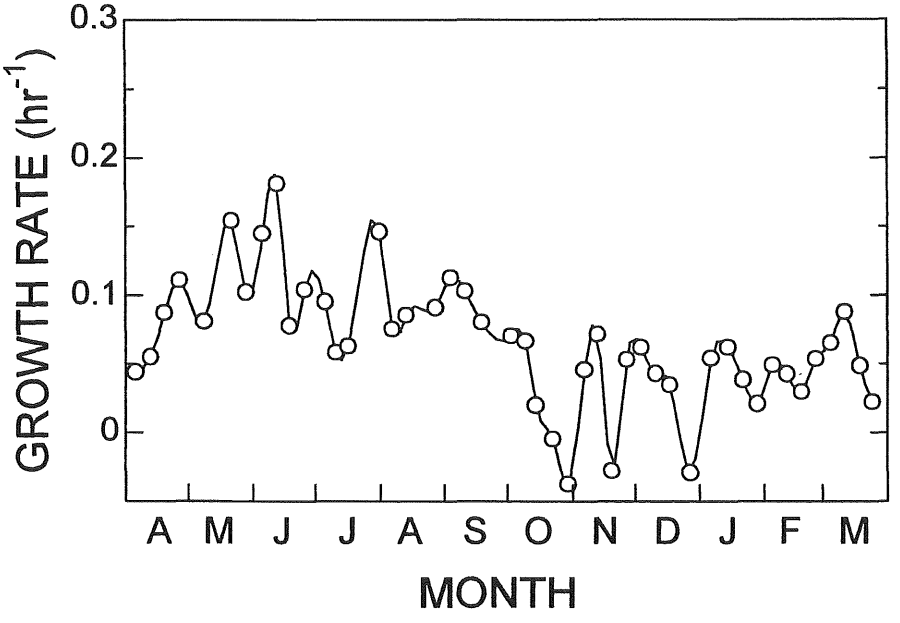

Figure 24. Seasonal fluctuation of the population growth rate of bacterioplankton in Matsumi-ike Bog from April 1991 to March 1992.

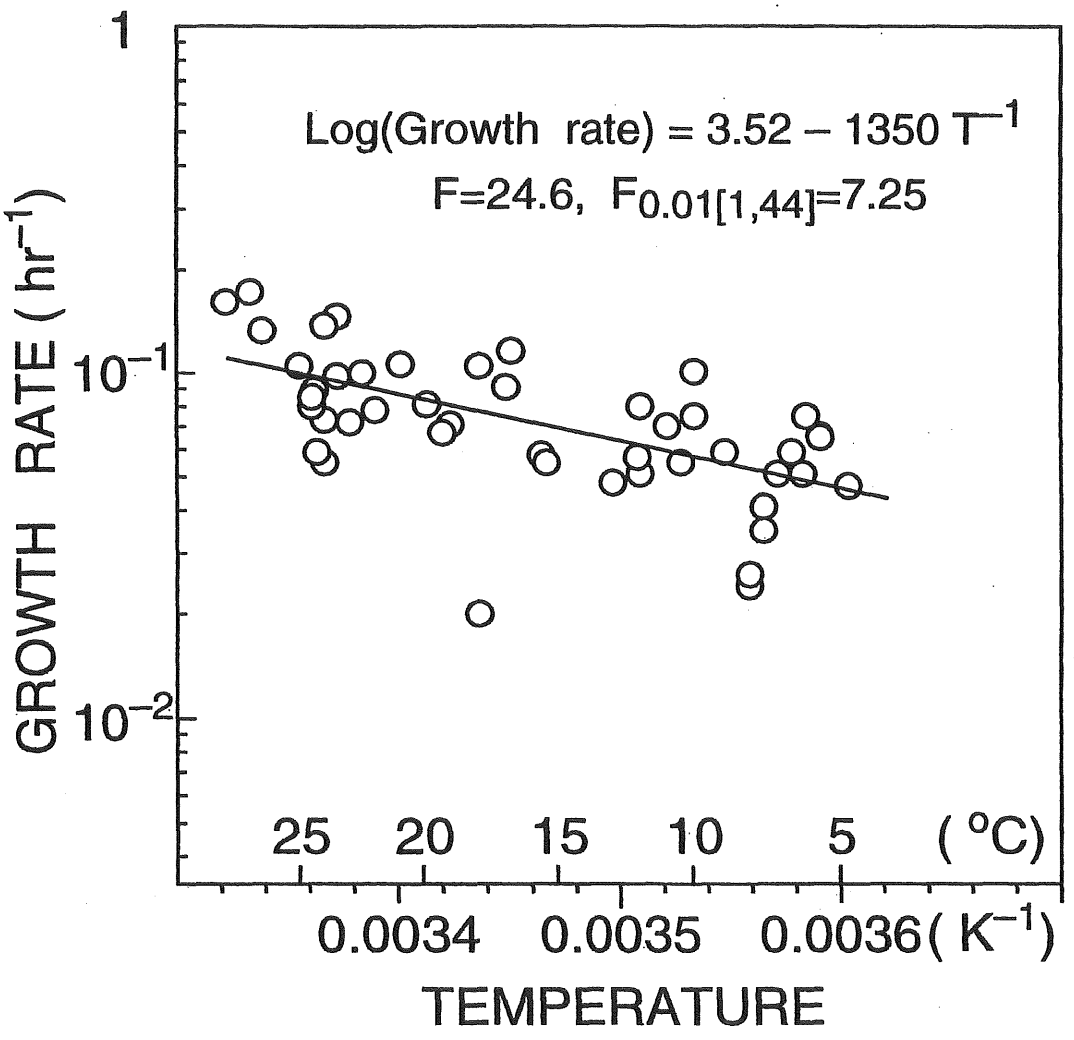

Figure 25. The Arrhenius plot for the growth rate of bacterioplankton in Matsumi-ike Bog. T is absolute temperature.

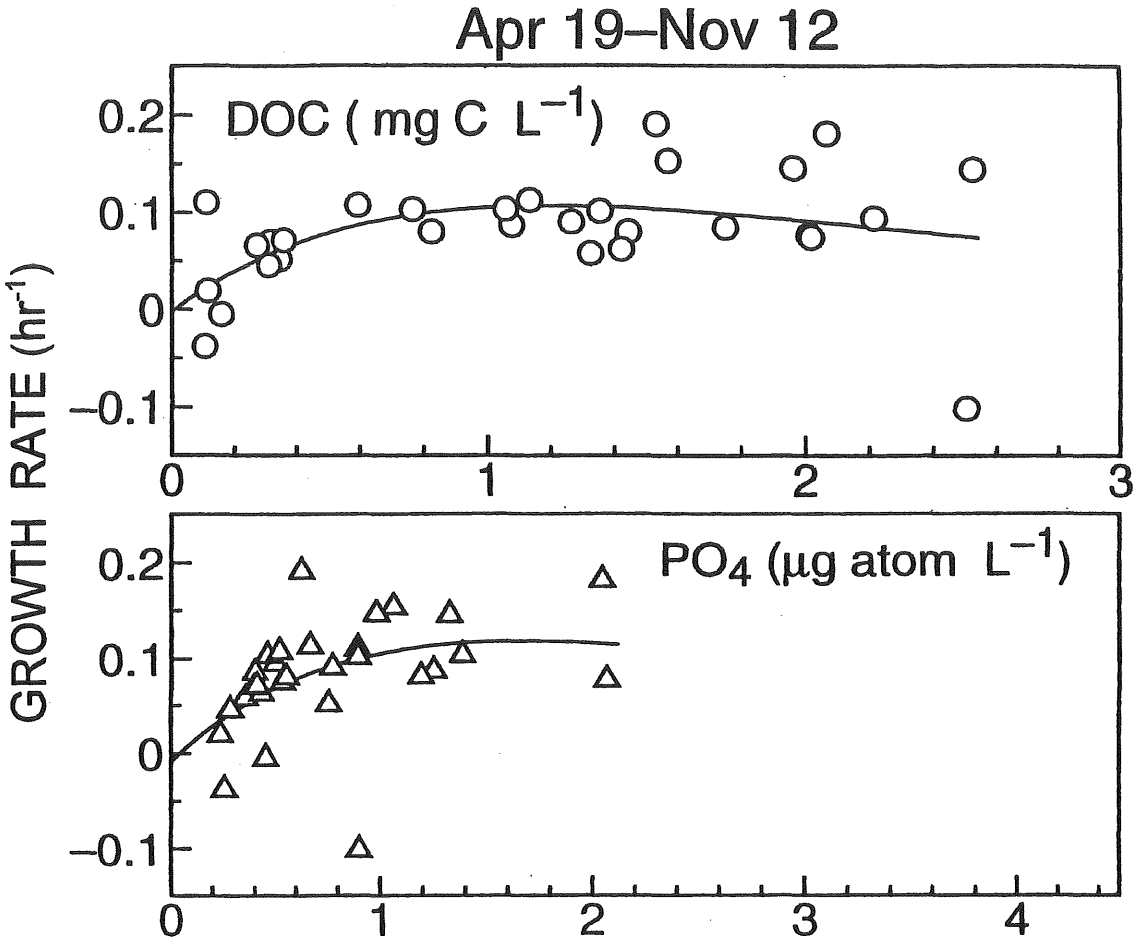

DOC

R'=0.089(d-0.0096)exp(1-0.83(d-0.0096))

F=8.67, $F_{0.01[1,28]}$=7.64

PO_4

R'=0.074(p-0.050)exp(1-0.61(p-0.050))

F=6.20, $F_{0.025[1,27]}$=5.63

Figure 26. Effects of the DOC and phosphate concentrations on the growth rate of bacterioplankton in Matsumi-ike Bog during Period I.

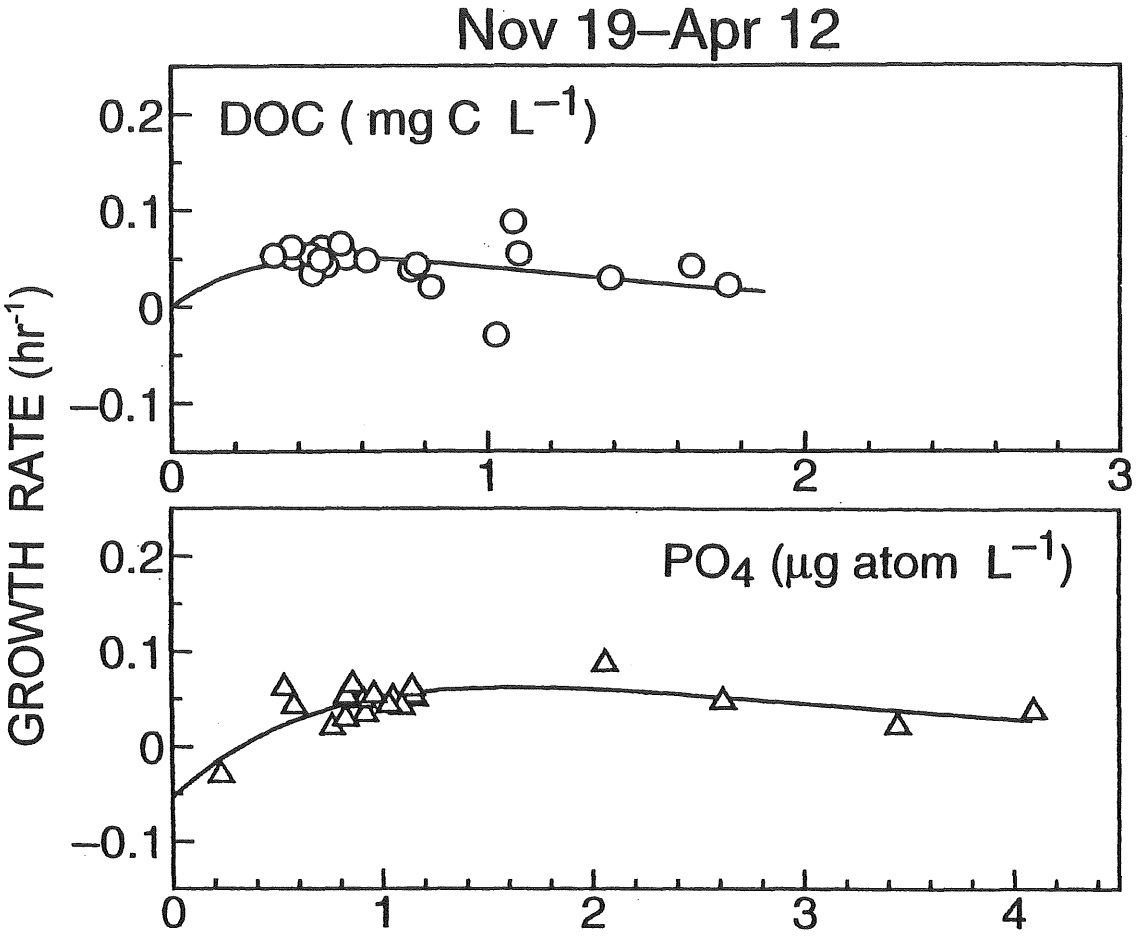

DOC

$R'=0.048d\exp(1-0.83d)$

$F=0.81,\ F_{0.05[1,18]}=4.35$

PO_4

$R'=0.048(p-0.32)\exp(1-0.76(p-0.32))$

$F=20.5,\ F_{0.01[1,18]}=8.29$

Figure 27. Effects of the DOC and phosphate concentrations on the growth rate of bacterioplankton in Matsumi-ike Bog during Period II.

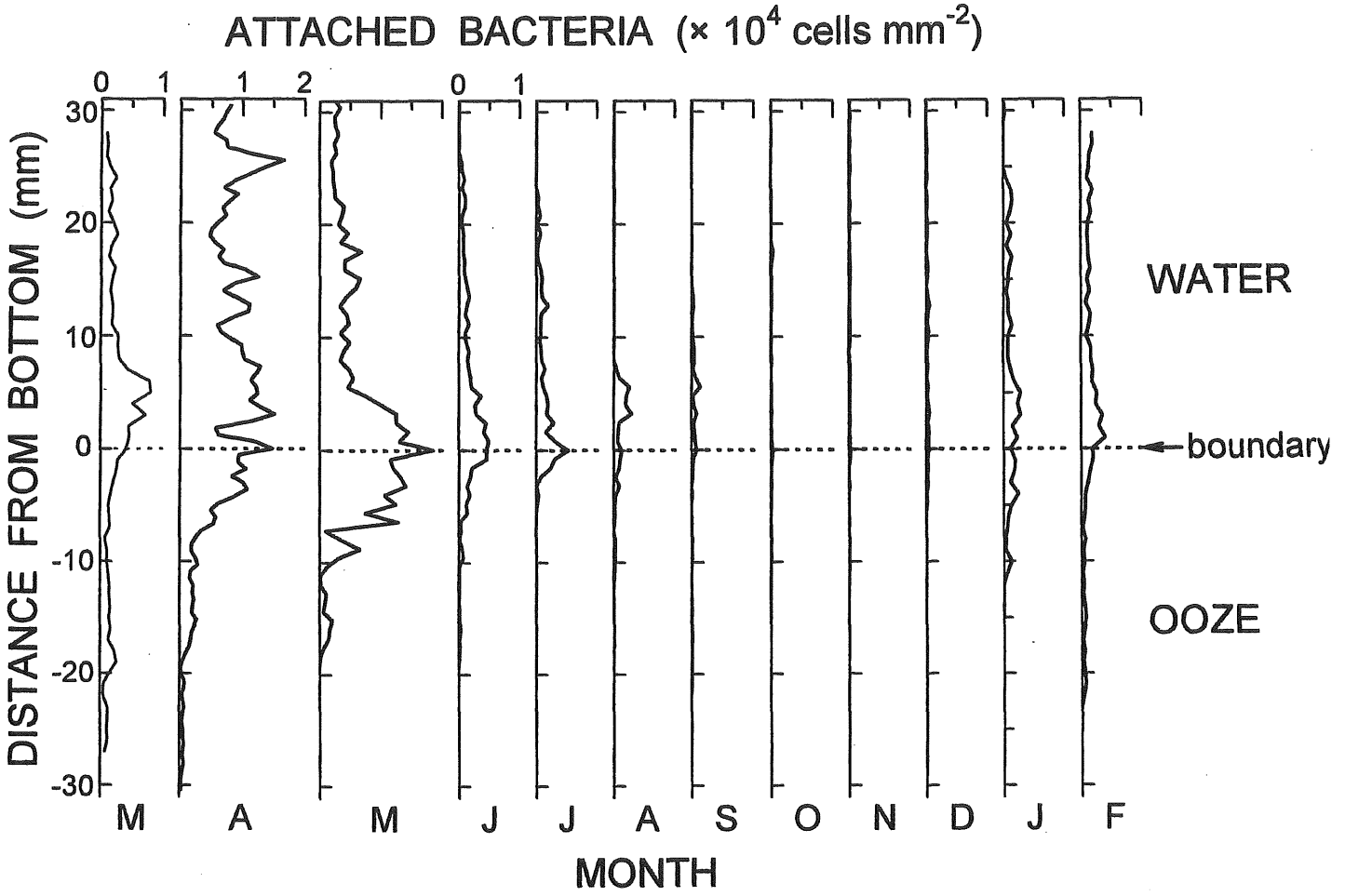

Figure 28. Vertical profile of the epibacterial population in Matsumi-ike Bog.

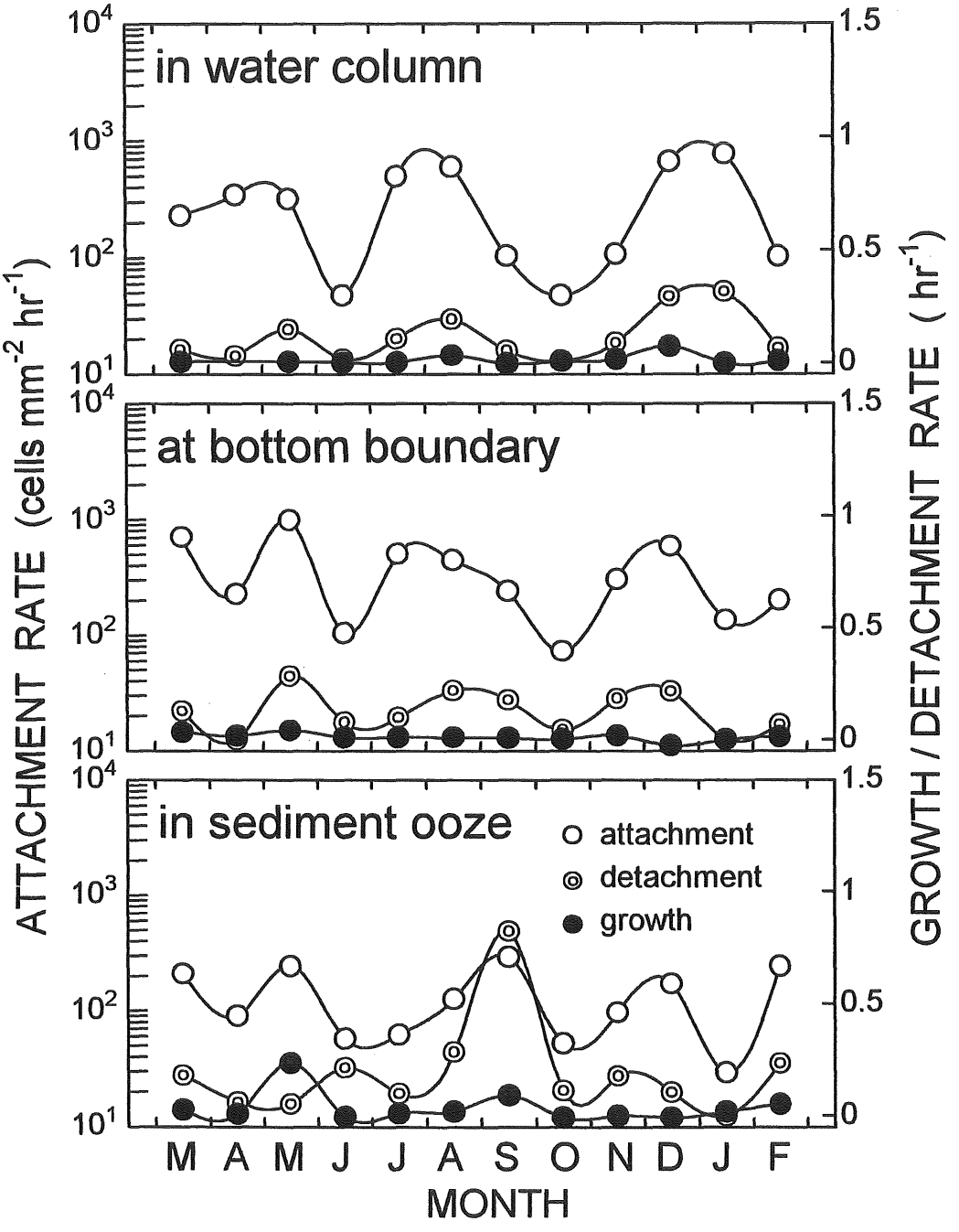

Figure 29. Monthly fluctuation of attachment, detachment and growth rates of epibacterial population in Matsumi-ike Bog. From top to bottom; in water column, at bottom boundary, in sediment ooze.

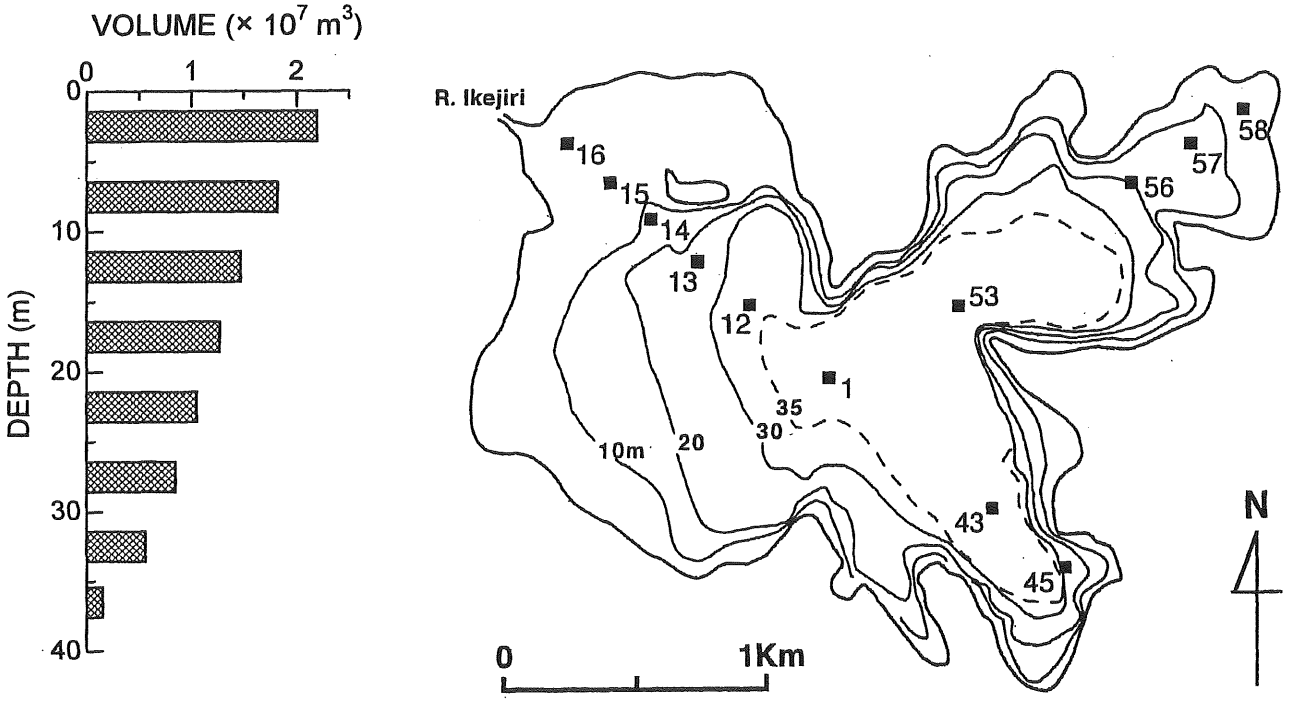

Figure 30. Sampling stations and depth-volume relationship of Lake Nojiri. St. 53 is the deepest point in the lake.

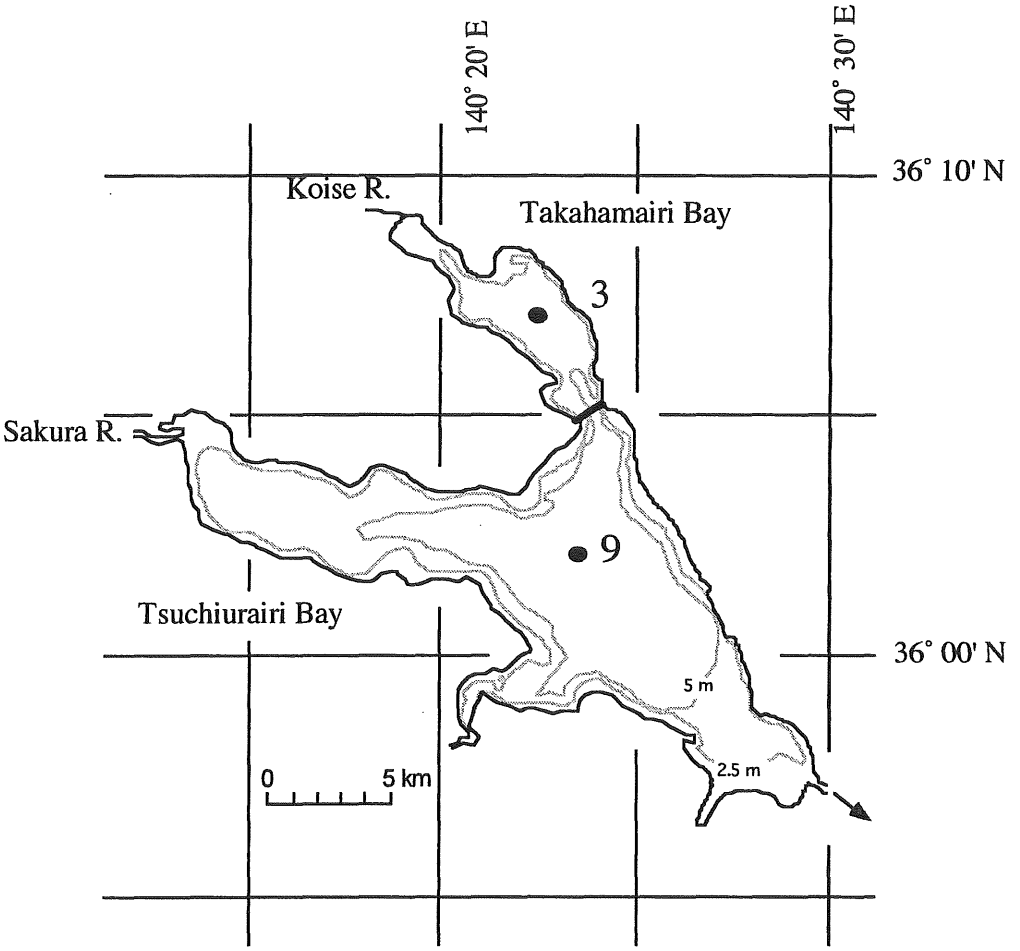

Figure 31. Bathymetric chart of Lake Kasumigaura with station positions noted. Contour intervals are 2.5 and 5 m.

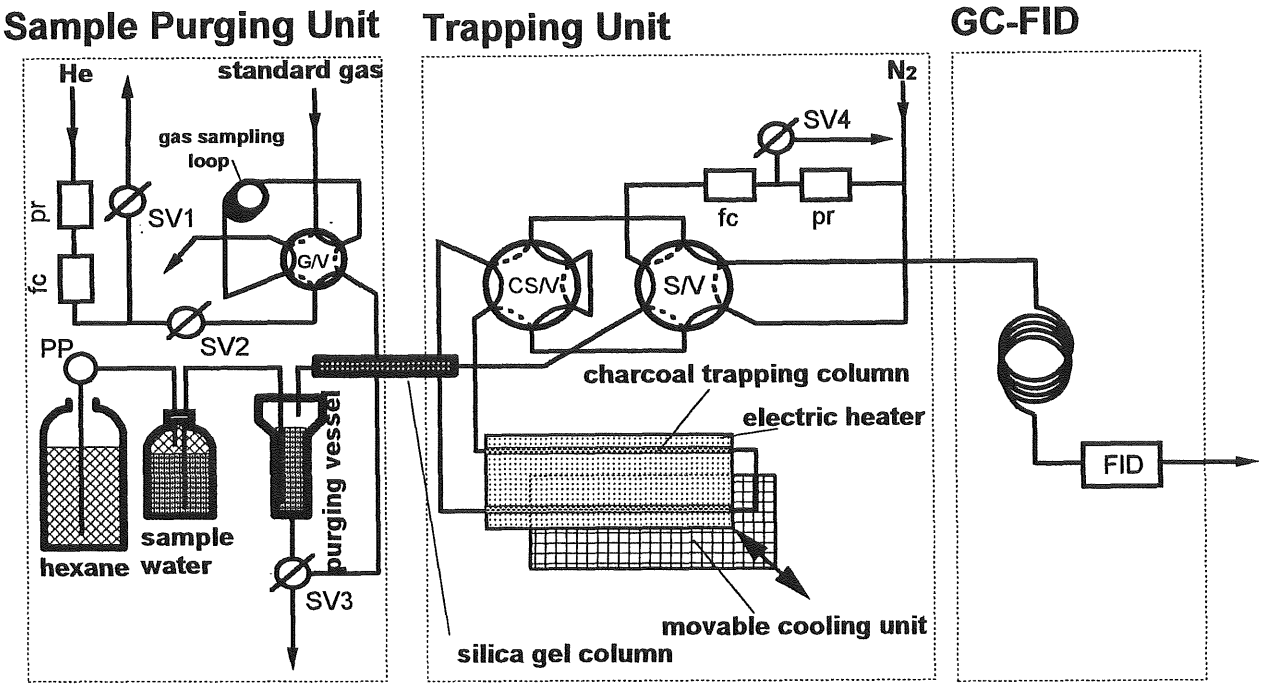

Figure 32. Schematic diagram of the automated system for dissolved methane analysis. SV, solenoid valves; G/V, standard gas sampling valve; S/V, sample injection valve; CS/V, concentrated sample switching valve; PP, plunger pump; pr, pressure regulator; FID, flame ionization detector.

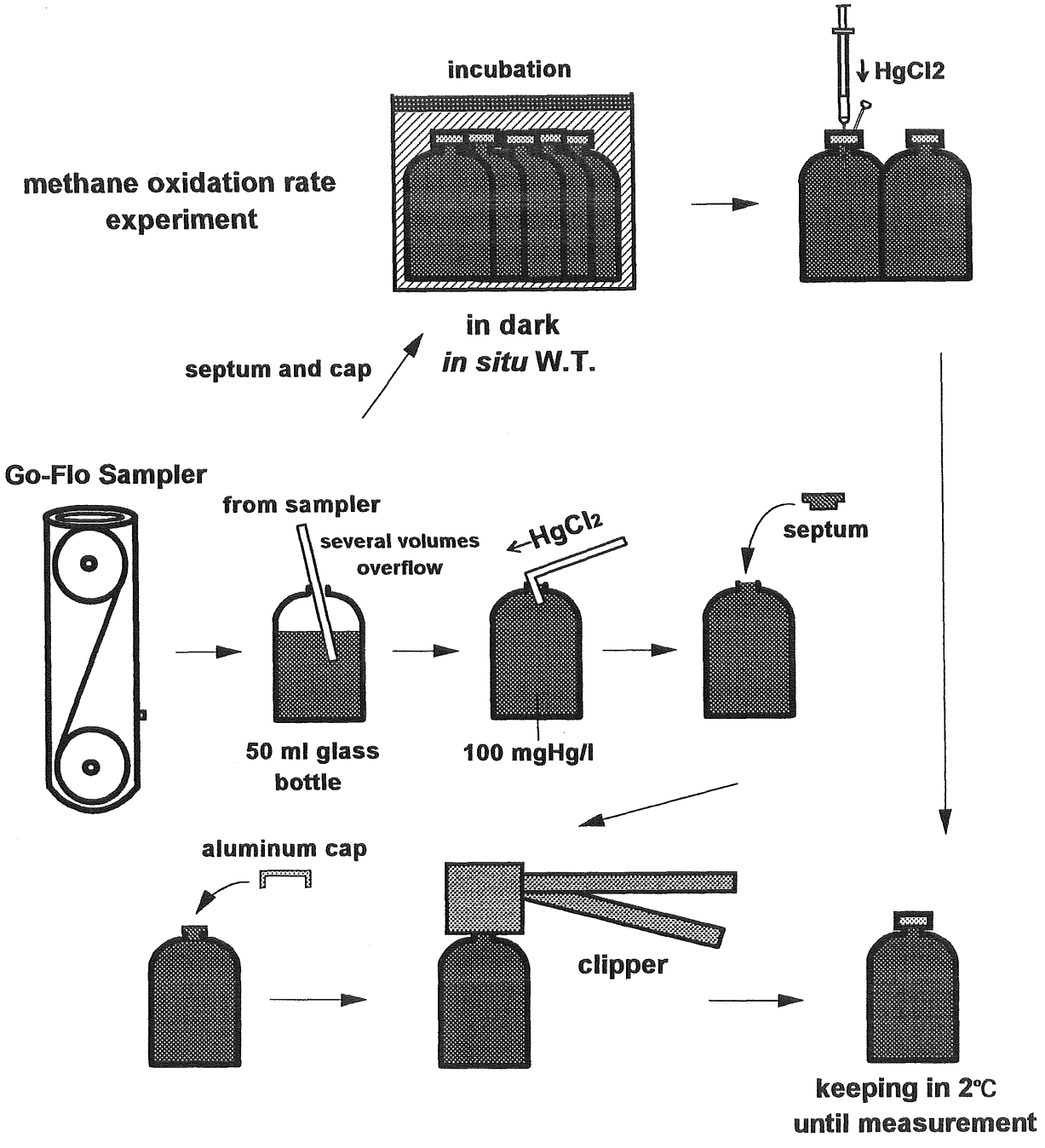

Figure 33. Procedure for experiment of methane oxidation rate and methane concnetration. Bottles for methane oxidation experiment were sterilized.

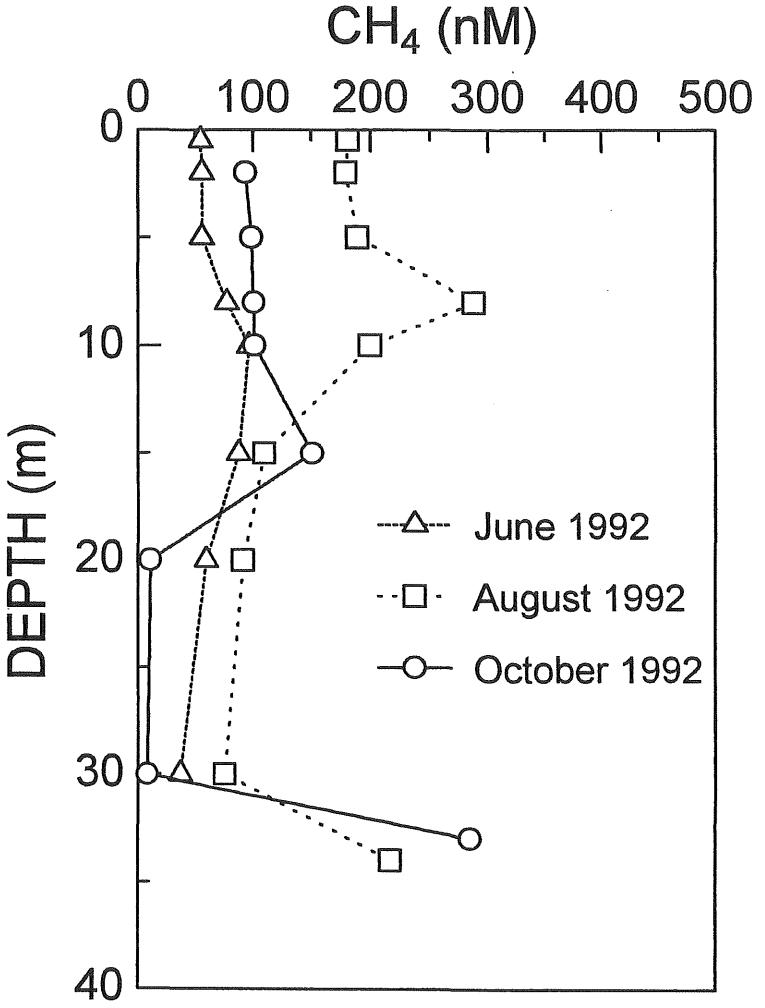

Figure 34. Methane profiles for the water column of Lake Nojiri during 1992. June (△), August (□) and October (○).

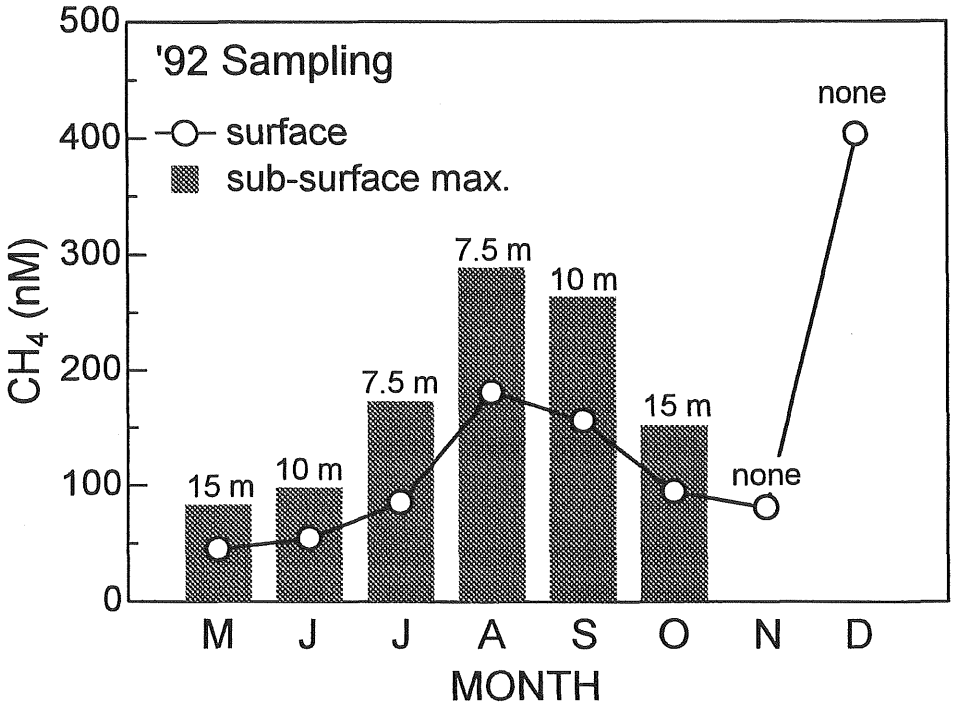

Figure 35. Surface methane concentrations and the depth of the sub-surface maximum in Lake Nojiri in 1992. The numbers indicates the depth of the sub-surface maximum.

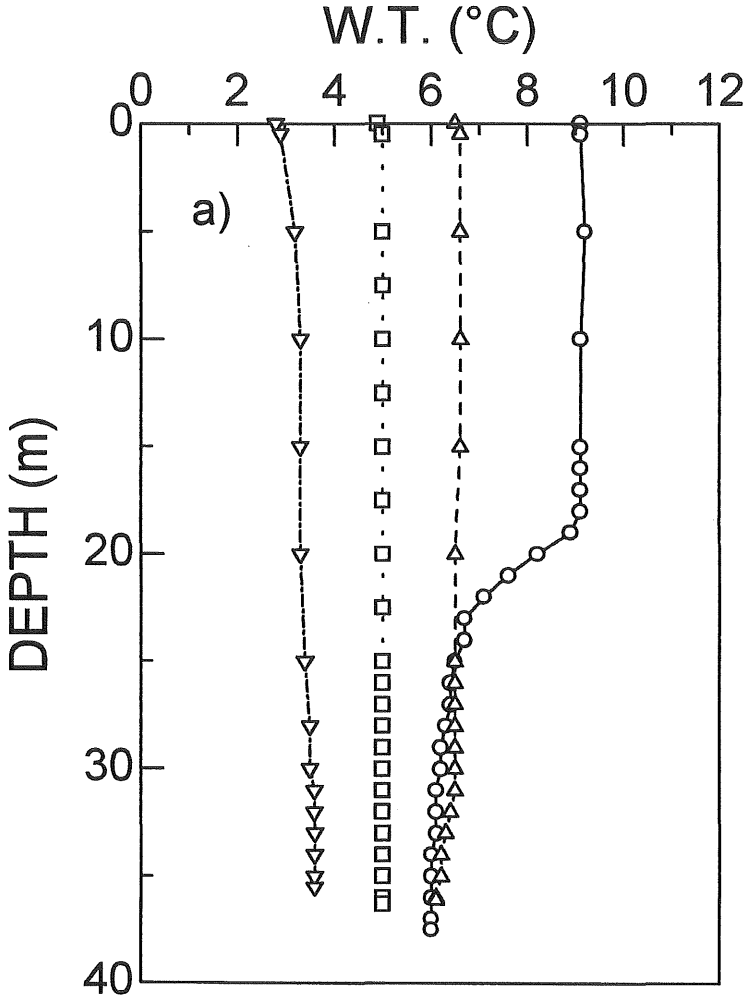

Figure 36a. Vertical profiles of water temperature at Station 53 from 4 December 1993 to 26 January 1994. (○ : 4 December, △ : 22 December, □ : 6 January, ▽ : 26 January).

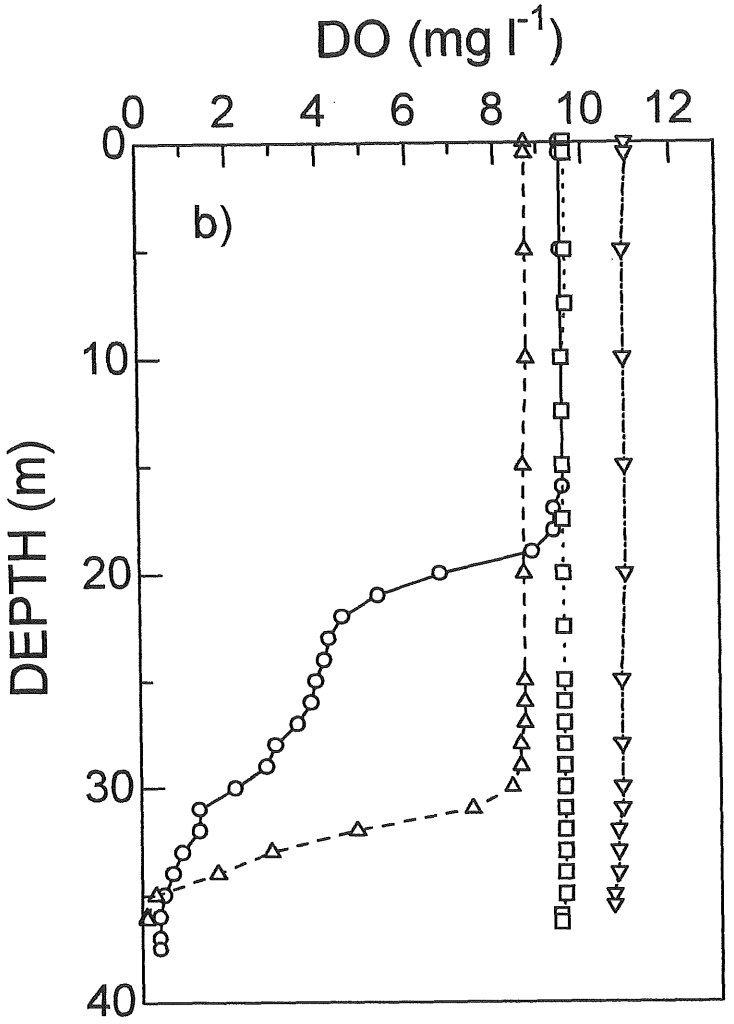

Figure 36b. Vertical profiles of DO at Station 53 from 4 December 1993 to 26 January 1994. (○ : 4 December, △ : 22 December, □ : 6 January, ▽ : 26 January).

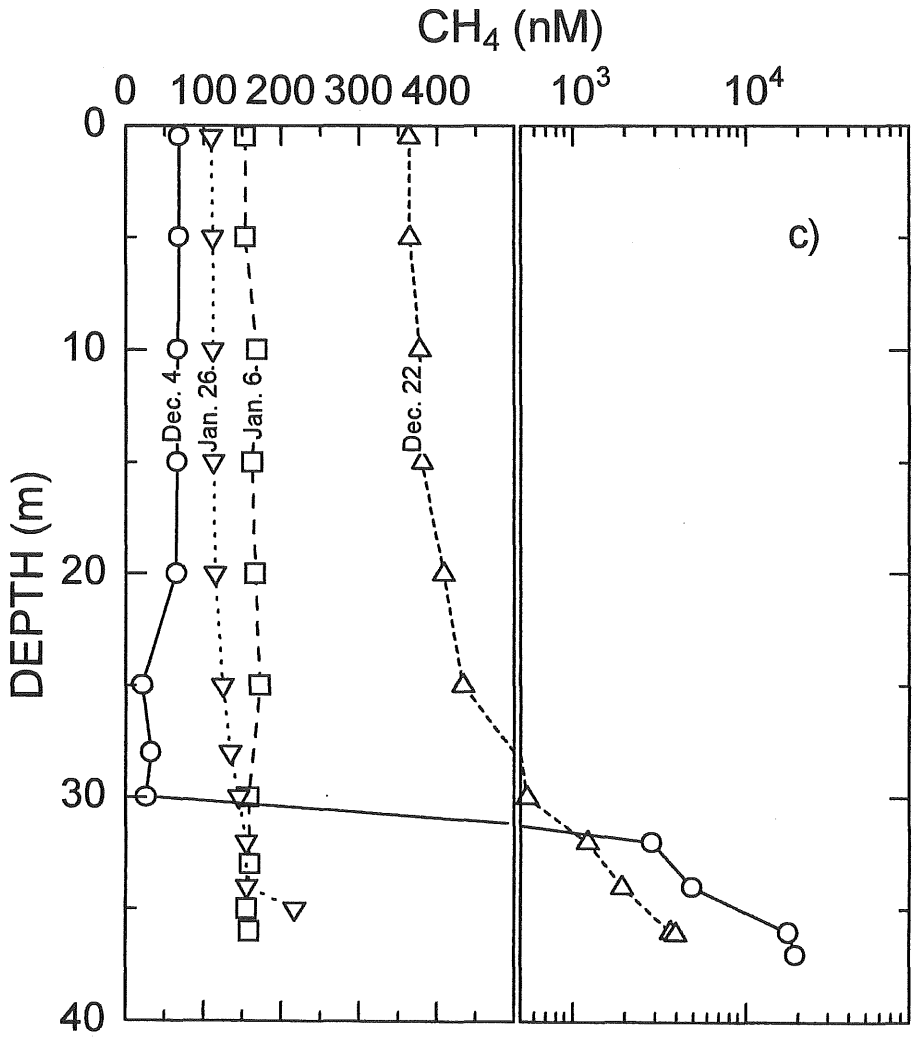

Figure 36c. Vertical profiles of methane at Station 53 from 4 December 1993 to 26 January 1994. (○ : 4 December, △ : 22 December, □ : 6 January, ▽ : 26 January).

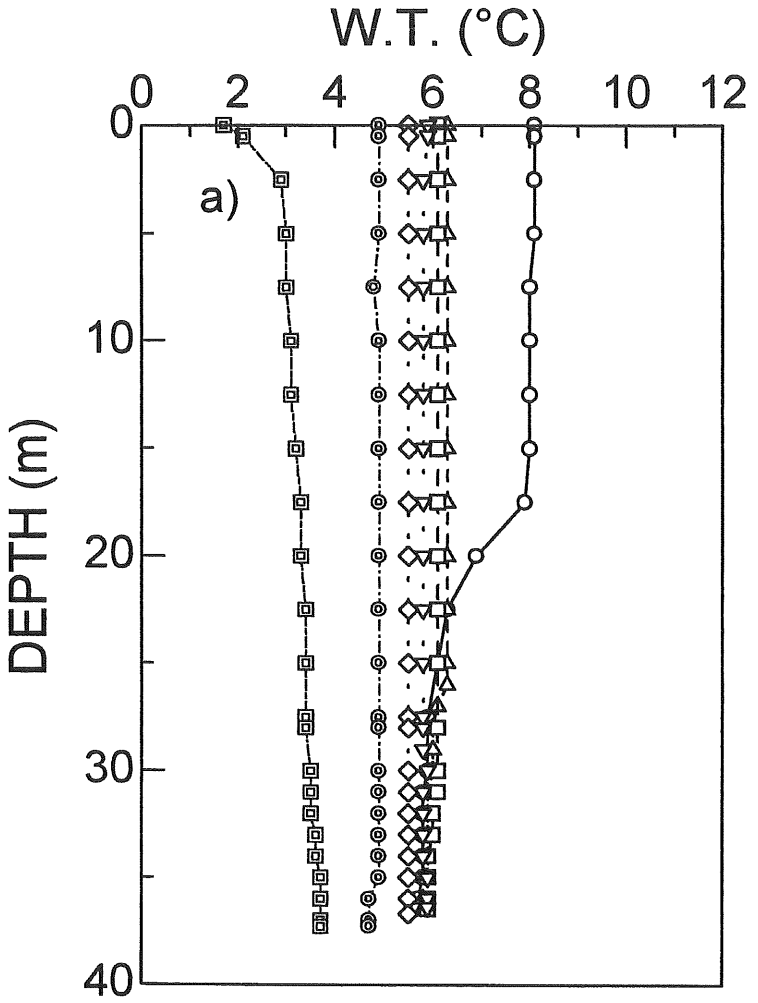

Figure 37a. Vertical profiles of water temperature at Station 53 from 10 December 1994 to 20 January 1995. (○ : 10 December, △ : 19 December, □ : 20 December, ▽ : 23 December, ◇ : 29 December, ◎ : 3 January, ▣ : 20 January).

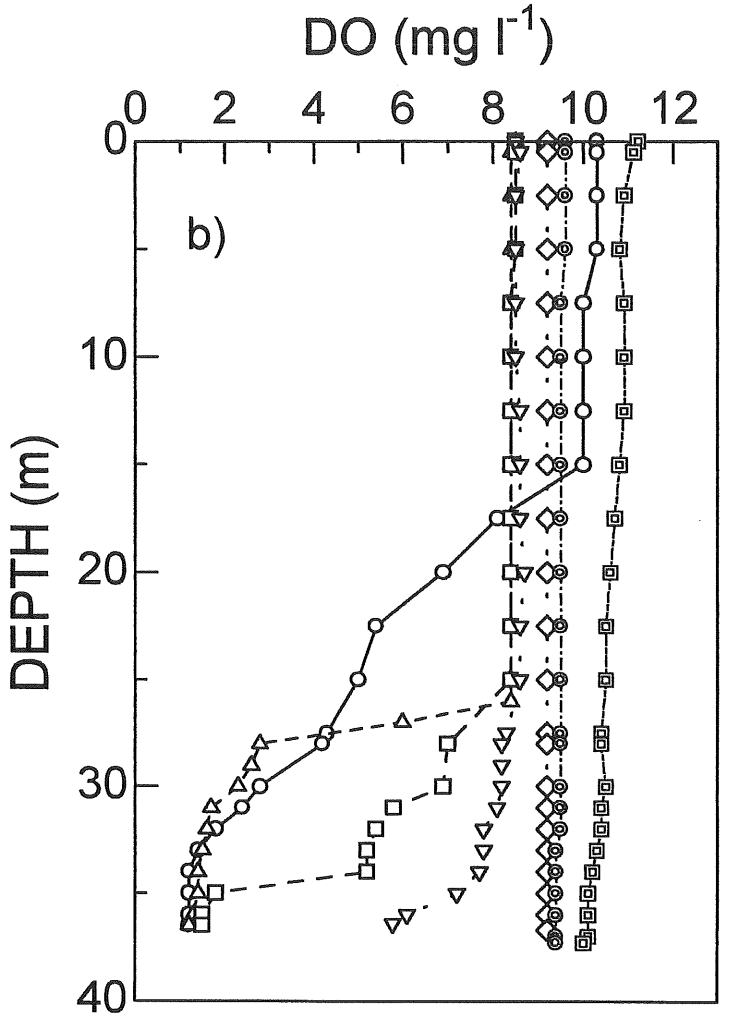

Figure 37b. Vertical profiles of DO at Station 53 from 10 December 1994 to 20 January 1995. (○ : 10 December, △ : 19 December, □ : 20 December, ▽ : 23 December, ◇ : 29 December, ◎ : 3 January, ⧈ : 20 January).

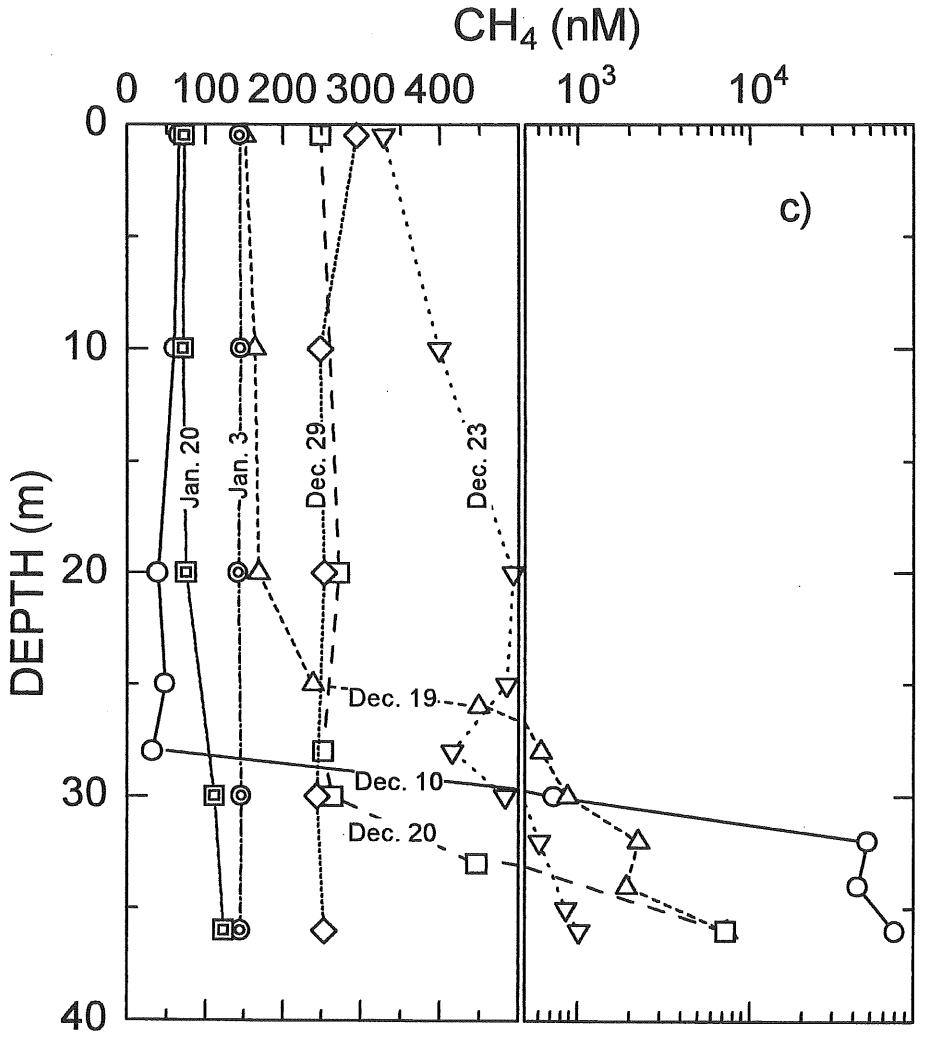

Figure 37c. Vertical profiles of methane at Station 53 from 10 December 1994 to 20 January 1995. (○ : 10 December, △ : 19 December, □ : 20 December, ▽ : 23 December, ◇ : 29 December, ◎ : 3 January, ▣ : 20 January).

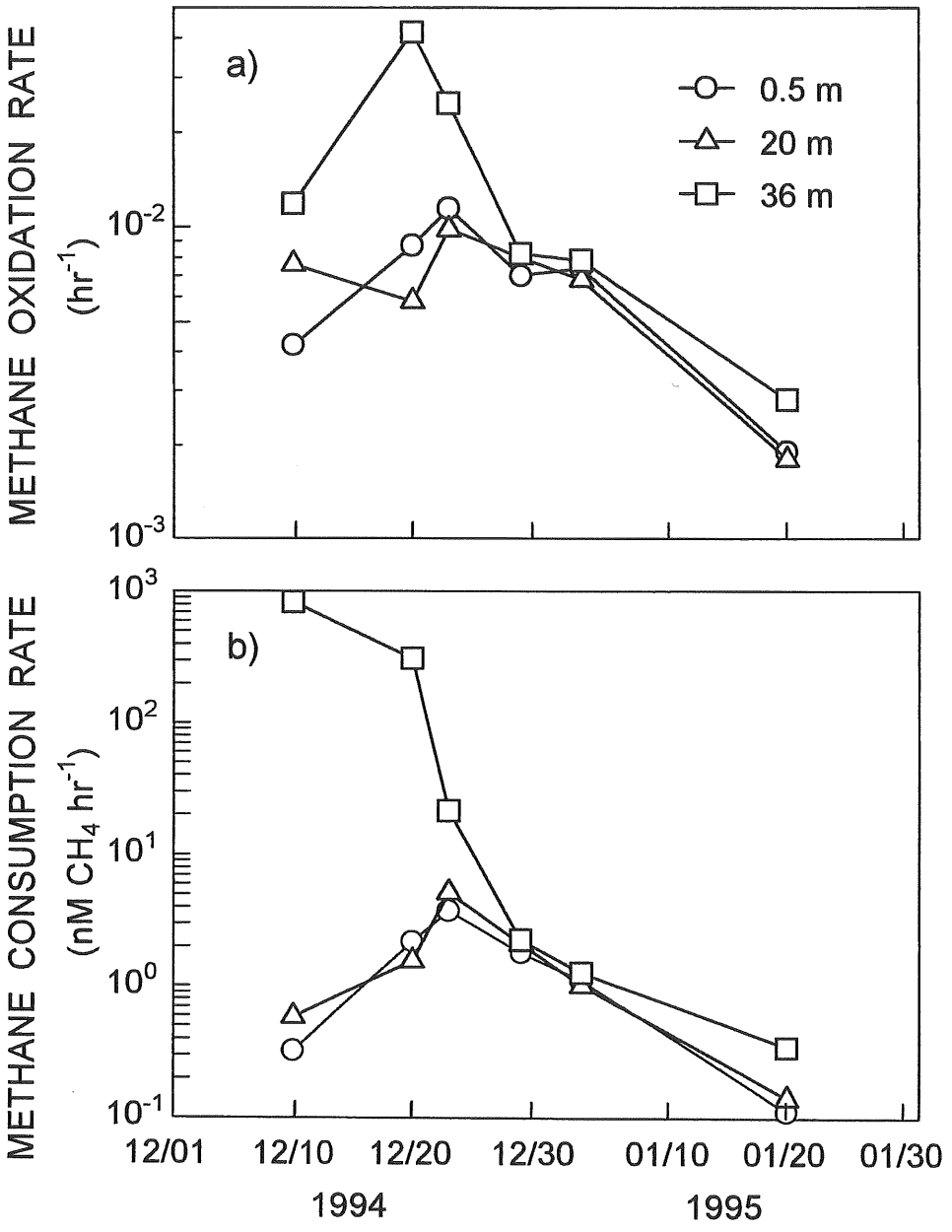

Figure 38. Specific (a) and absolute (b) methane oxidation rates from 10 December 1994 to 20 January 1995 at Lake Nojiri. Open circle (0.5 m depth), open triangle (20 m depth), and open square (36 m depth).

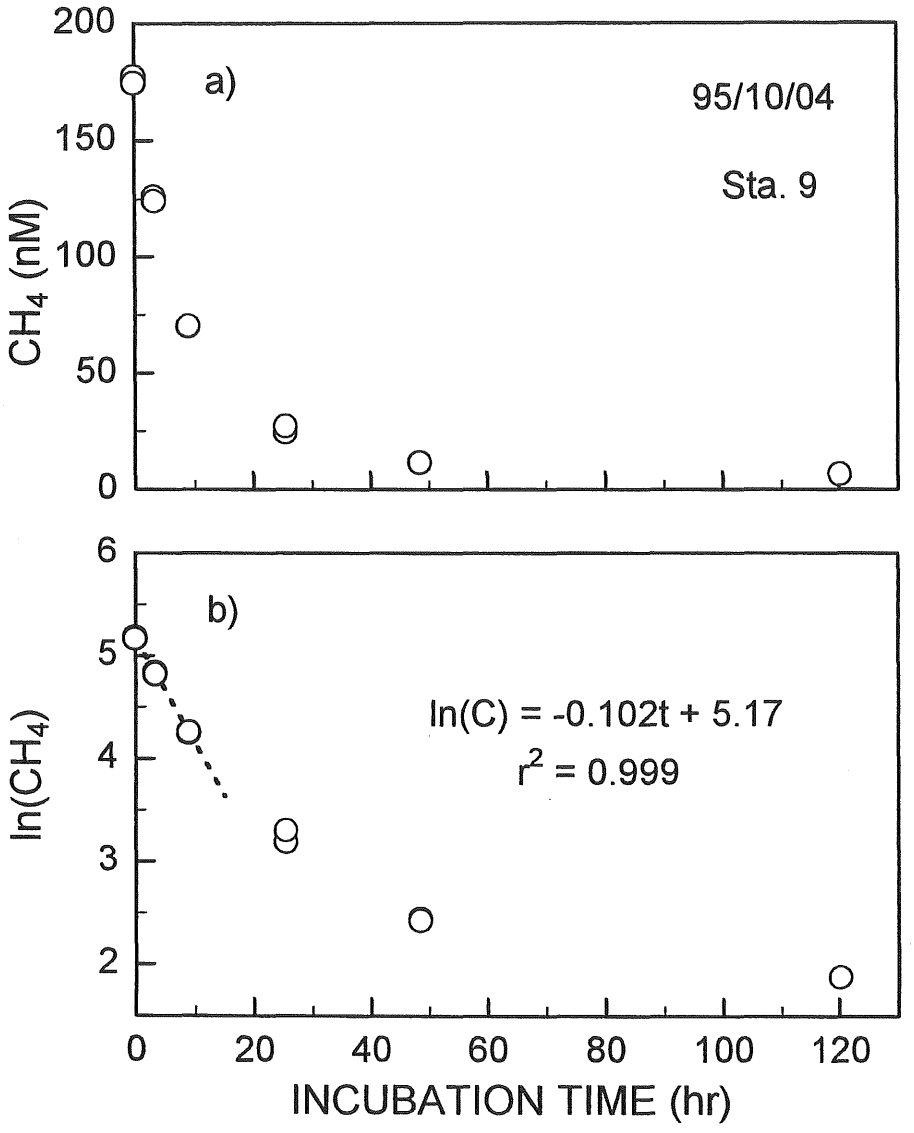

Figure 39. Decrease in methane concentration during an incubation of a Lake Kasumigaura water sample. (a): linear ordinate, (b): logarithmic ordinate. The regression for the initial 3 time points can be expressed as $\ln(C) = -0.102t + 5.17$ ($r^2 = 0.999$), where C is concentration of methane (nM) and t is the time (hours) elapsed after starting the incubation.

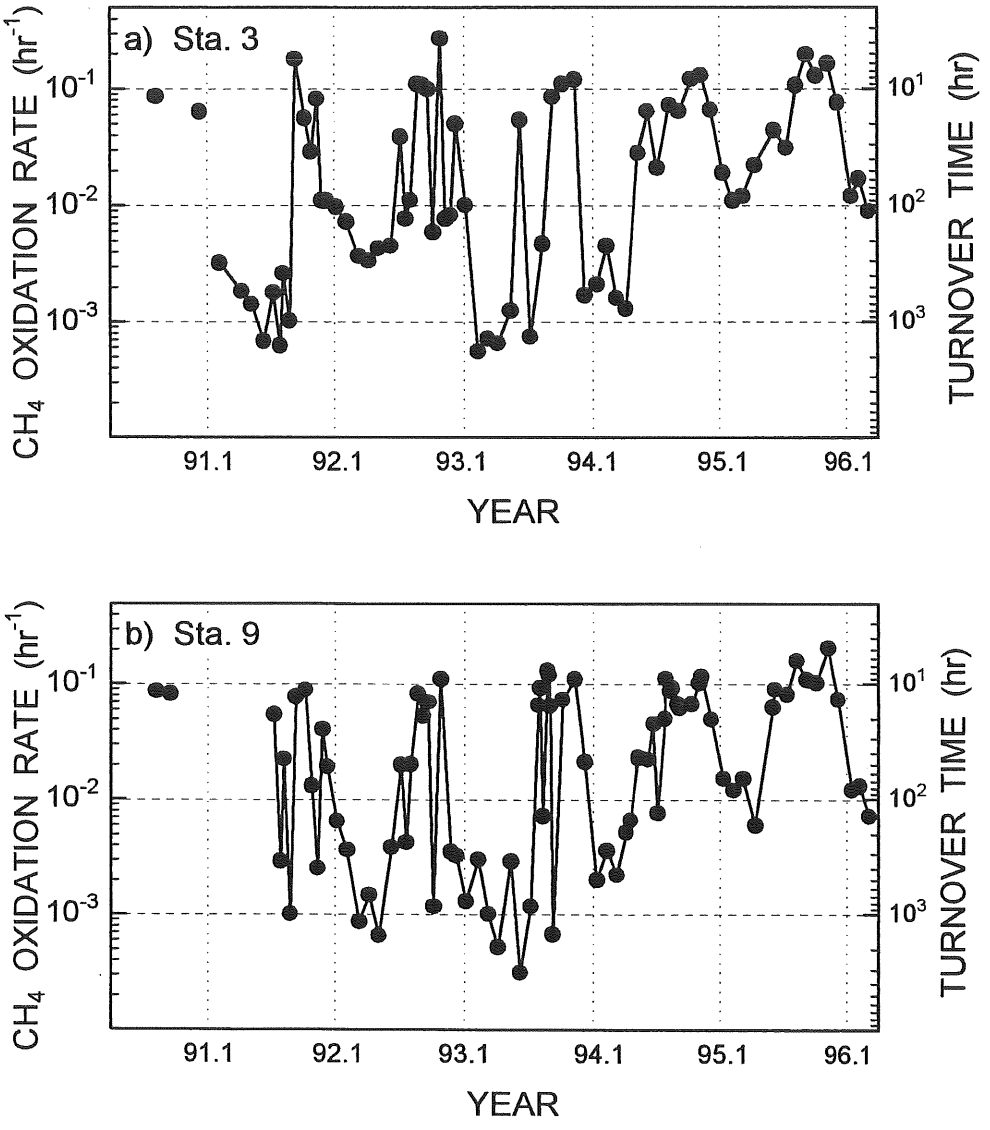

Figure 40. Changes in specific methane oxidation rate and turnover time with respect to in situ oxidation for dissolved methane in Lake Kasumigaura. (a): Station 3. (b): Station 9.

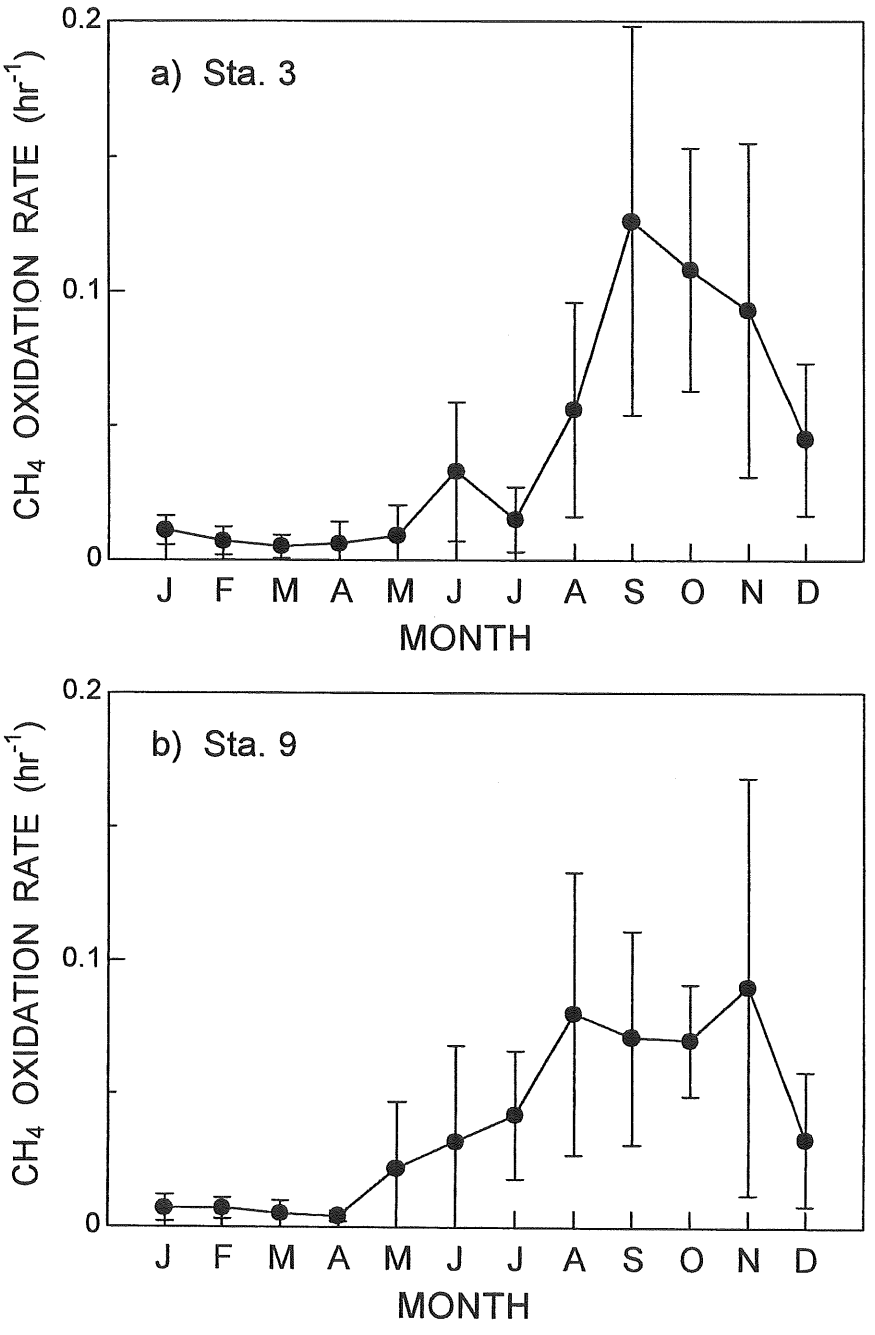

Figure 41. Monthly average specific methane oxidation rates (a: Sta. 3, b: Sta. 9), methane consumption rates and methane concentrations (c: Sta. 3, d: Sta. 9) in Lake Kasumigaura. Results represent the monthly averages for the observed years, 1990-1996, with bars indicating standard deviation (representing inter-annual variability).

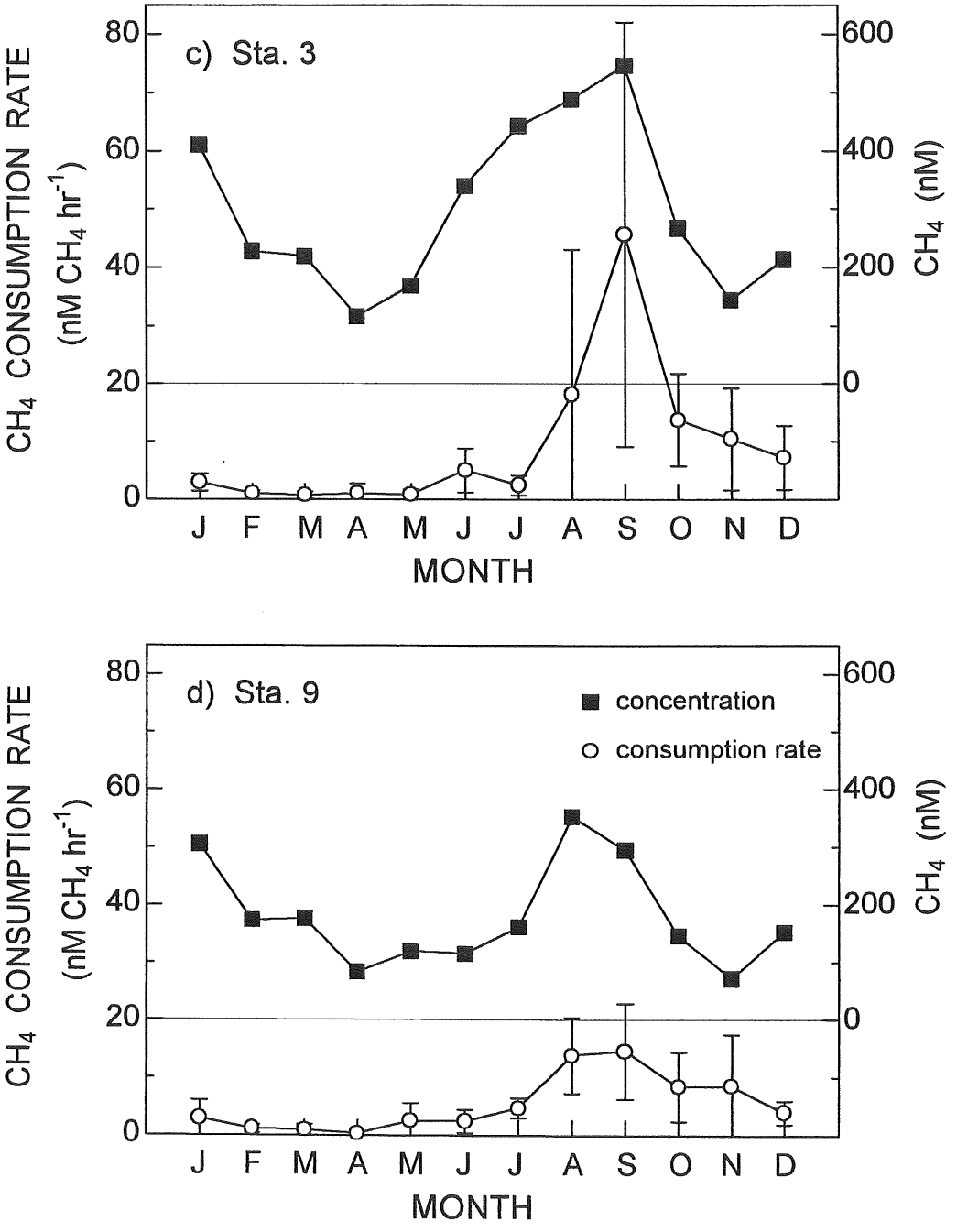

Figure 41. Monthly average specific methane oxidation rates (a: Sta. 3, b: Sta. 9), methane consumption rates and methane concentrations (c: Sta. 3, d: Sta. 9) in Lake Kasumigaura. Results represent the monthly averages for the observed years, 1990-1996, with bars indicating standard deviation (representing inter-annual variability).

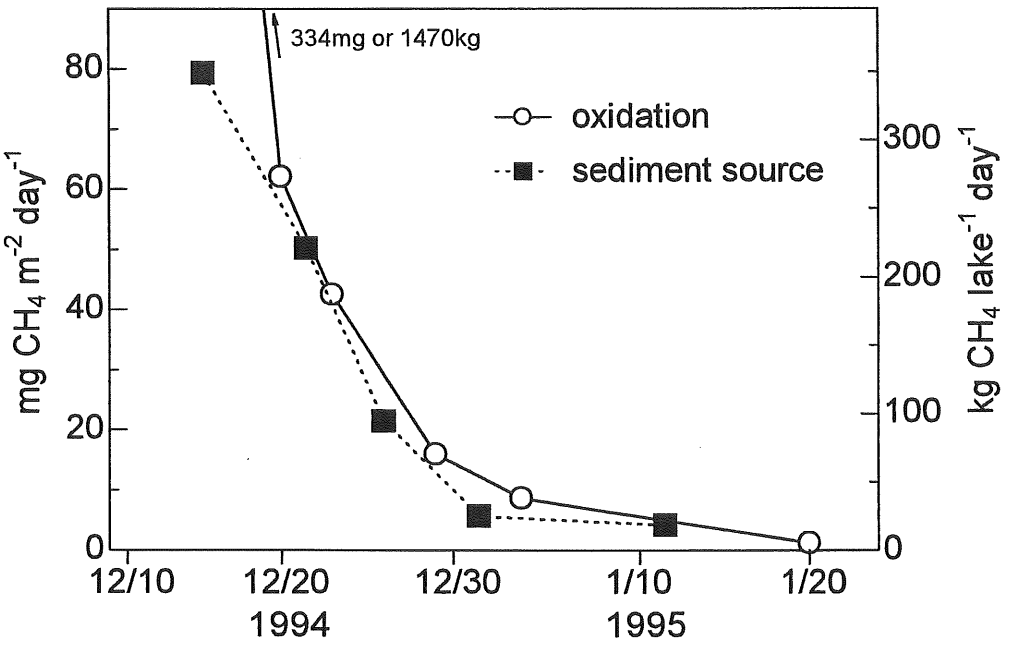

Figure 42. Methane oxidation rates and calculated methane fluxes from the bottom sediments from 10 December 1994 to 20 January 1995 in Lake Nojiri.

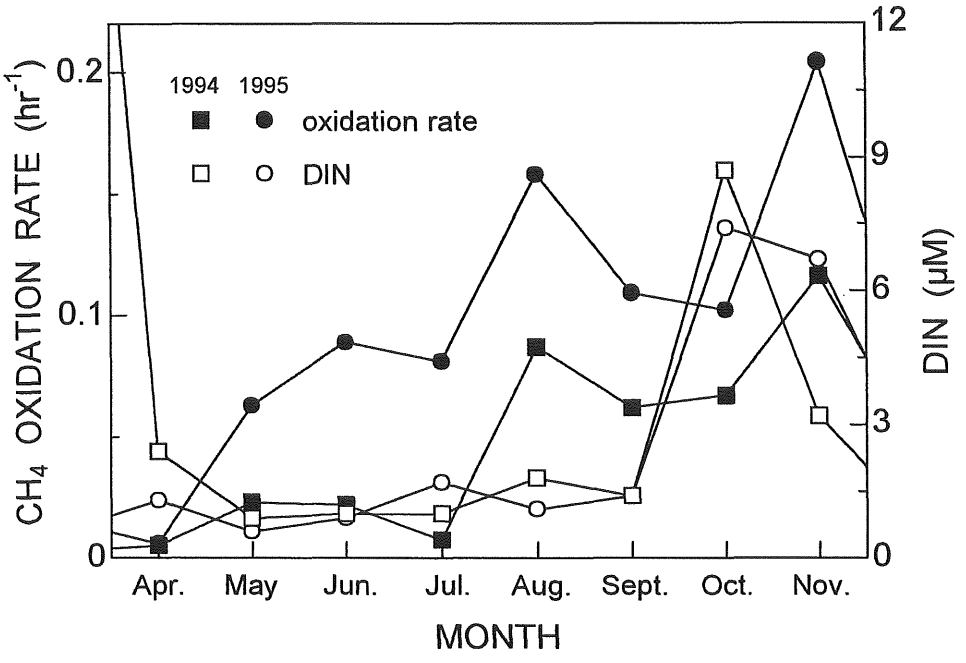

Figure 43. Changes in specific methane oxidation rate and dissolved inorganic nitrogen (DIN) concentration at Station 9 in 1994 and 1995. ■ : oxidation rate of 1994, □ : DIN for 1994, ● : oxidation rate of 1995, ○ : DIN for 1995.

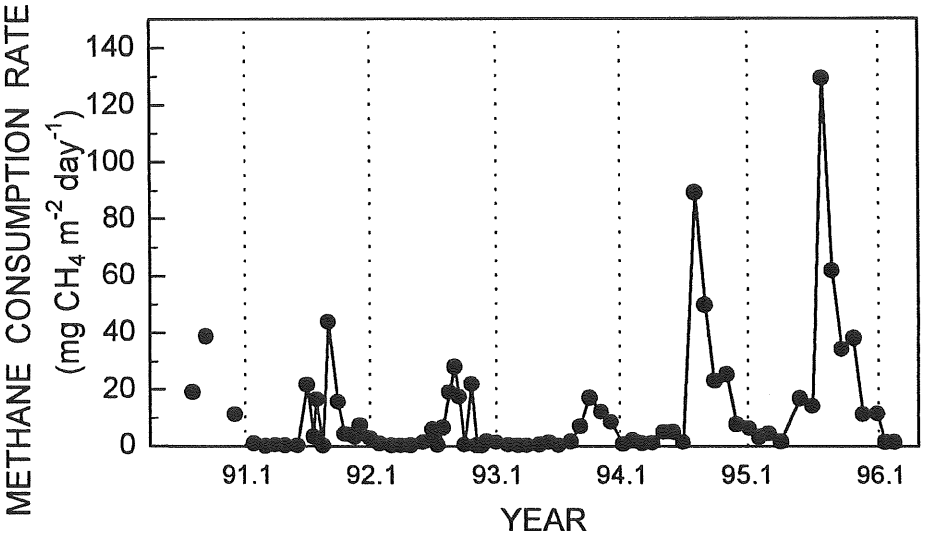

Figure 44. Methane consumption rate in Lake Kasumigaura over 5 years.

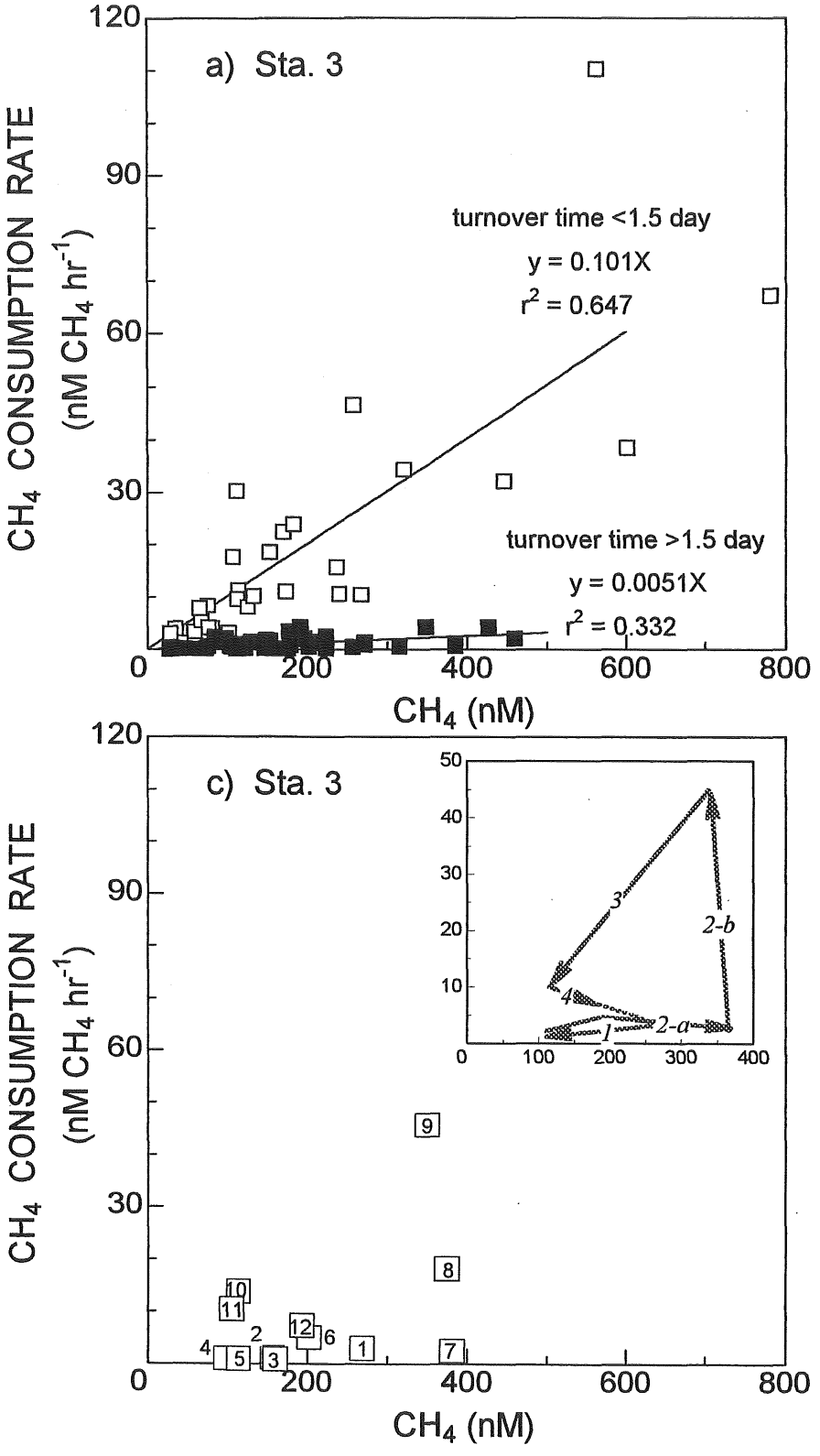

Figure 45. Relationship between the concentration of dissolved methane and methane consumption rate at Station 3 (a) and Station 9 (b) (open symbols: turnover time <1.5 day, filled symbols: turnover time >1.5 day), and monthly averages at Station 3 (c) and Station 9 (d) in Lake Kasumigaura. Numbers in the symbols indicate month. The typical trends with time are shown in the insertion. *1*: January to April, *2*: April to September (*2-a*: April to July and *2-b*: July to September in Sta. 3), *3*: September to November, *4*: November to December.

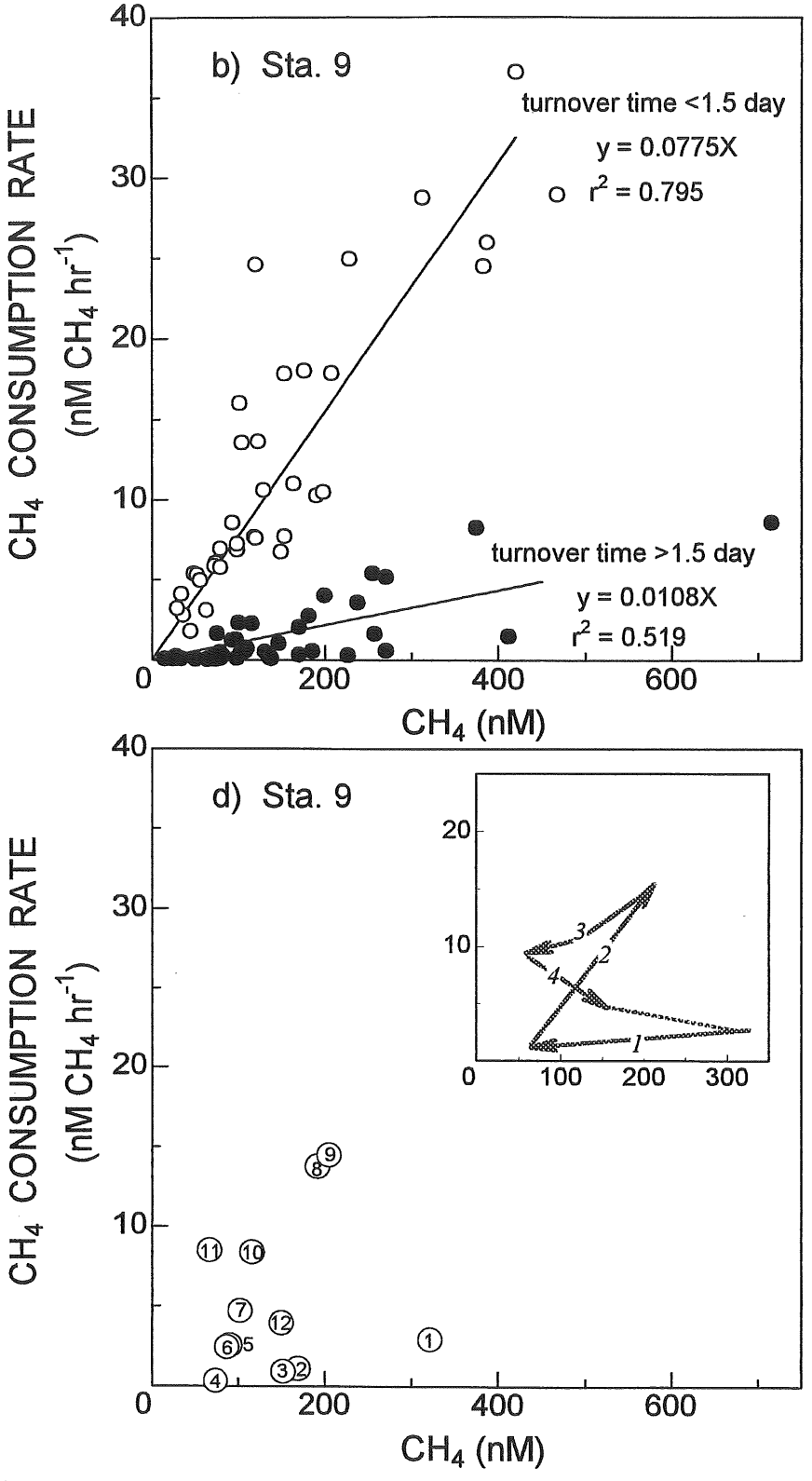

Figure 45. Relationship between the concentration of dissolved methane and methane consumption rate at Station 3 (a) and Station 9 (b) (open symbols: turnover time <1.5 day, filled symbols: turnover time >1.5 day), and monthly averages at Station 3 (c) and Station 9 (d) in Lake Kasumigaura. Numbers in the symbols indicate month. The typical trends with time are shown in the insertion. *1*: January to April, *2*: April to September (*2-a*: April to July and *2-b*: July to September in Sta. 3), *3*: September to November, *4*: November to December.